



Norwegian University of
Science and Technology

Experimental investigation of a heat pump assisted drum drying system using propane (R290) as working fluid

Espen Storslett

Master of Energy Use and Energy Planning

Submission date: June 2018

Supervisor: Trygve Magne Eikevik, EPT

Norwegian University of Science and Technology
Department of Energy and Process Engineering

Project description

Project description, page 1 of 2



Norwegian University
of Science and Technology

Department of Energy
and Process Engineering

EPT-M-2018-89

MASTER THESIS

for

Student Espen Storslett

Spring 2018

Experimental investigation of a heat pump assisted drum drying systems using propane (R290) as working fluid

Eksperimentelle undersøkelser av et varmepumpe assistert tørkesystem som bruker propan (R290) som arbeidsmedium

Background and objective

Drum dryers have been used for a long time in homes for drying of laundries. These dryers have been developed over years from the simple type with direct electric heaters and rejection of the humid air to the ambient. The next generation included a heat exchanger between the inlet air and the exit air from the drum (condensation units). In this case it is possible to reduce the electric consumption. More modern system have been developed with a heat pump for cooling of the air to a temperature below the dew point (condensation and removal of water) and then reheating of the inlet air to the drum dryer. In this case there is a closed loop of the air in the dryer. Typical working fluid in this type of dryer is R134a. This refrigerant has a GWP factor of 1300. The industry of these type of dryers like to reduce the environmental impact factor of their systems and have looked into using propane (R290) as the working fluids in the heat pump system.

In this master thesis we will finalize test of the existing system with R134a to compare with the results after rebuilding. The system have to be rebuild to be able to operate with R290, especially the compressor.

The following tasks are to be considered:

1. Literature study of the heat pump drum dryer system
2. Plan and perform tests of the R134a system to be compare with the
3. Rebuild the system for R290 and reinstall the instrumentation of temperature, humidity, air flow and energy consumption
4. Plan and perform the test with the R290 heat pump
5. Make a simulation tool to predict the drying program and compare with measurements
6. Make a draft paper of the main results from the master thesis
7. Make proposal for further improvement of the process

-- " --

Project description, page 2 of 2

Within 14 days of receiving the written text on the master thesis, the candidate shall submit a research plan for his project to the department.

When the thesis is evaluated, emphasis is put on processing of the results, and that they are presented in tabular and/or graphic form in a clear manner, and that they are analyzed carefully.

The thesis should be formulated as a research report with summary both in English and Norwegian, conclusion, literature references, table of contents etc. During the preparation of the text, the candidate should make an effort to produce a well-structured and easily readable report. In order to ease the evaluation of the thesis, it is important that the cross-references are correct. In the making of the report, strong emphasis should be placed on both a thorough discussion of the results and an orderly presentation.

The candidate is requested to initiate and keep close contact with his/her academic supervisor(s) throughout the working period. The candidate must follow the rules and regulations of NTNU as well as passive directions given by the Department of Energy and Process Engineering.

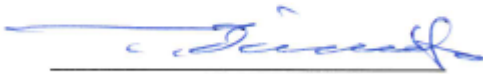
Risk assessment of the candidate's work shall be carried out according to the department's procedures. The risk assessment must be documented and included as part of the final report. Events related to the candidate's work adversely affecting the health, safety or security, must be documented and included as part of the final report. If the documentation on risk assessment represents a large number of pages, the full version is to be submitted electronically to the supervisor and an excerpt is included in the report.

Pursuant to "Regulations concerning the supplementary provisions to the technology study program/Master of Science" at NTNU §20, the Department reserves the permission to utilize all the results and data for teaching and research purposes as well as in future publications.

The final report is to be submitted digitally in DAIM. An executive summary of the thesis including title, student's name, supervisor's name, year, department name, and NTNU's logo and name, shall be submitted to the department as a separate pdf file. Based on an agreement with the supervisor, the final report and other material and documents may be given to the supervisor in digital format.

- Work to be done in lab (Water power lab, Fluids engineering lab, Thermal engineering lab)
 Field work

Department of Energy and Process Engineering, January 15th 2018



Trygve M. Eikevik, Professor
Academic Supervisor

Research Advisor:
Dr. Ignat Tolstorebrov, NTNU, ignat.tolstorebrov@ntnu.no

Preface

This master thesis comprising 30 ECT credits is done in the final semester of the two-year Master of Science engineering program at the Norwegian University of Science and Technology (NTNU) in Trondheim. The project goal is to experimentally investigate the suitability of utilizing R290 (propane) as working fluid in replacement of R134a in a heat pump assisted drum dryer. This is done by extensive theoretical research, laboratory experiments and rebuilding of a mass-produced drum dryer. In preparation for this master thesis, a specialization project on the same subject comprising 15 ECT credits, has been completed during the preceding semester.

I would like to thank my supervisors Prof. Trygve Magne Eikevik and Dr. Ignat Tolstorebrov for teaching and guidance throughout the project. Also, I would like to thank Inge Håvard Rekstad for help with administrative tasks in cohesion with the NTNU Thermal Engineering Laboratory, as well as Helge Laukholm and Reidar Tellebon for technical support regarding the test rig and instrumentation. Finally, I wish to thank my co-students for the past five years for making my time at the university a time to remember.



Espen Storslett

Abstract

Drum dryers has been used for drying fabric for a long time. Drying is performed by heating air causing the relative humidity to fall before blowing the heated air through wet fabric in a rotating drum. The moisture removed from the fabric can be rejected to the ambient along with the heated air or condensed to be collected or drained. Conventional drum dryer's heats air using an electric heater or combustion. This means of heating is energy consuming and requires relatively high temperatures for efficient drying.

Heat pump assisted drum dryers utilizes heat pump technology to condense the removed moisture and reheat the air in a closed loop. This technology provides higher energy efficiency and the possibility of drying at lower temperatures. Heat pump assisted drum dryers has mainly used environmental unfriendly refrigerants, such as CFC and HFC gases. The use of CFC gases has already been banned by the European Union as well as all other countries ratifying the Montreal Protocol. As HFC gases have high GWP-values they are to be banned by the EU shortly in new systems.

Due to the fact that hydrocarbons such as propane feature excellent properties as refrigerants, offer zero ODP and very low GWP they appear to be the ideal substitute for HFCs.

This thesis describes the rebuild and experimental investigation of a mass-produced heat pump assisted drum dryer utilizing the HFC gas R134a as refrigerant to utilizing propane (R290) as refrigerant. Instrumentation and sensors has been adapted to the system, and a series of experiments performed before and after the rebuild, providing an extensive documentation of system performance.

The results show that providing installation of commercially available compressors for propane, the use of propane in heat pump assisted drum dryers does not deteriorate system performance and can be implemented without excessive changes in system design. By redesigning the capillary tube, the COP of the heat pump were found to increase by 6%.

Sammendrag

Tørketromler har blitt brukt til å tørke tøy i lang tid. Tørking gjennomføres ved at luft varmes opp slik at relativ fuktighet i luften faller, for så å blåses gjennom vått tøy i en roterende trommel. Fuktigheten som fjernes fra tøyen kan avgis til omgivelsene sammen med avkastluften, eller kondenseres for å samles i en beholder eller føres til avløp. Konvensjonelle tørketromler varmer luften ved bruk av et elektrisk varmeelement eller ved forbrenning. Slik oppvarming er lite energieffektiv, og krever relativt høy temperatur for effektiv tørking.

Varmepumpeassisterte tørketromler benytter varmepumpeteknologi til å kondensere fuktigheten som er fjernet fra klærne og å gjenoppvarme luften i en lukket syklus. Denne teknologien gir høyere energieffektivitet og mulighet for effektiv tørking ved lavere temperaturer. Varmepumpeassisterte tørketromler har i hovedsak benyttet miljøskadelige KFK og HFK gasser som arbeidsmedier. Bruk av KFK gasser er allerede forbudt i EU og alle andre land som har signert Montreal-protokollen. På grunn av den sterke klimapåvirkningen fra HFK gasser vil det innen kort tid bli forbud mot bruk av disse i nye systemer i EU.

Ettersom enkelte hydrokarboner slik som propan har utmerkede egenskaper som arbeidsmedier, ingen ozon-ødeleggende effekt og svært lavt potensiale som klimagasser fremstår de som ideelle alternativer for HFK gasser.

Denne rapporten beskriver ombygning og eksperimentelle undersøkelser av en masseprodusert varmepumpeassistert tørketrommel som fra fabrikk benytter HFK gassen R134a som arbeidsmedie til å benytte propan (R290) som arbeidsmedie. Systemet har blitt instrumentert og en serie eksperimenter har blitt gjennomført på systemet før og etter ombygning. Gjennom eksperimentene har systemets ytelser blitt utførlig dokumentert.

Resultatene viser at ved å installere en kommersielt tilgjengelig kompressor utviklet for propan, opprettholdes systemets ytelser og energieffektivitet. Dermed kan propan implementeres som arbeidsmedie med kun små endringer i utførelsen av systemet. Ved å tilpasse kapillarrøret til propan ble det funnet økning i varmepumpens COP på 6%.

Contents

Project description	ii
Preface.....	iv
Abstract	v
Sammendrag	vi
List of symbols	ix
List of terms.....	xi
1 Introduction	1
1.1 Limitations and premises.....	1
2 Theory	3
2.1 Drum dryers.....	3
2.1.1 Conventional air vented dryers.....	6
2.1.2 Conventional condensing dryers	6
2.1.3 Thermoelectric dryers.....	7
2.1.4 Air cycle heat pump dryers.....	7
2.1.5 Heat pump assisted dryers	8
2.2 The heat pump cycle for drum dryers.....	9
2.3 Refrigerants	13
2.4 Comparison of properties of R134a and R290	14
2.5 Publications on propane in HPDD	17
2.6 Safety regulations	19
2.7 Consequences on system design.....	19
2.8 Important equipment for propane.....	20
2.9 Drying and dehumidification.....	21
2.9.1 Operating schemes and control parameters	24
3 Materials and method	25
3.1 Overview of the drum dryer	25
3.2 Equipment	28
3.2.1 Compressor.....	29
3.2.2 Heat exchangers.....	30
3.2.3 Refrigerant charge	30
3.3 Experimental setup and procedure	31
3.3.1 Standardized procedure	33
3.4 Rebuild	34
3.5 Instrumentation.....	35

3.5.1	Calibration	41
3.6	Data processing	42
3.6.1	Calculation of absolute humidity and mixing ratio	42
3.6.2	Other calculations.....	44
4	Experiments.....	48
4.1	Overview	48
4.2	Results and discussion.....	50
4.2.1	Drying process.....	50
4.2.2	Heat exchange and temperature development	54
4.2.3	System performance	63
4.2.4	Drying kinetics	68
4.2.5	Charge optimization	70
4.2.6	Capillary tube accommodation.....	73
4.2.7	Overall performance.....	79
4.3	Reliability and assumptions.....	80
4.3.1	COP calculation.....	81
4.3.2	SMER calculation.....	82
4.4	Comparison between R134a and R290	82
5	Further work and improvements	83
6	Conclusion.....	85
	References.....	86
	List of figures	89
	List of tables	91
	Appendix.....	1
	APPENDIX A: MATERIALS COMPATIBILITY OF PROPANE	A1
	APPENDIX B: LIST OF EXPERIMENTS	B1
	APPENDIX C: DATA SHEET: RECHI 39E073B.....	C1
	APPENDIX D: DATA SHEET: TECUMSEH AE4430U-FZ1A	D1
	APPENDIX E: RISK ASSESSMENT	E1

List of symbols

Symbol	Explanation	Unit
Q_C	Condenser heat flow	W
Q_e	Evaporator heat flow	W
h_{fg}	Latent heat of evaporation	kJ/kg
c_p	Specific heat	kJ/kg K
T	Temperature	°C
t	Temperature	Kelvin
ER	Evaporation Rate	kg/h
RH	Relative humidity	%
AH	Absolute humidity	g/m ³
X	Mixing ratio	g/kg
P_w	Water vapor pressure	Pa
P_{ws}	Water vapor saturation pressure	Pa
P_{tot}	Total pressure	Pa
G	Constant (temperature dependent)	-
A	Constant (temperature dependent)	-
T_n	Constant (temperature dependent)	-
B	Constant (dependent on gas)	g/kg
C	Constant, $C = 2.16679$	gK/J
$\eta_{compressor}$	Overall compressor efficiency	[-]
W_{is}	Compressor work assuming isentropic compression	kWh
E_{el}	Electric energy consumption	kWh

$h_{2, \text{isentropic}}$	Enthalpy at compressor outlet, assuming isentropic compression	kJ/kg
$h_{2, \text{adiabatic}}$	Enthalpy at compressor outlet, assuming adiabatic compression	kJ/kg
$h_{2, \text{real}}$	Real enthalpy at compressor outlet	kJ/kg
$h_{1, \text{real}}$	Real enthalpy at compressor inlet	kJ/kg
$h_{4, \text{real}}$	Real enthalpy at condenser outlet	kJ/kg
$\dot{m}_{\text{refrigerant}}$	Mass flow of refrigerant	kg
$P_{\text{el, compressor}}$	Compressor electric power input	W
$P_{\text{el, motor}}$	Electric power input of the drum and drum fan motor	W
$E_{\text{el, compressor}}$	Compressor electric energy consumption	kWh
$E_{\text{el, motor}}$	Drum and drum fan energy consumption	kWh
ΔT	Temperature difference	K
$\Delta T_A, \Delta T_B$	Temperature difference between flows in heat exchangers at end A and end B respectively	K
$\Delta m_{\text{water, weighed, fabric}}$	Difference in the amount of water in fabric, measured by weighing	g
AH_9	Absolute humidity at hygrometer H9	g/m^3
AH_{10}	Absolute humidity at hygrometer H10	g/m^3
AH_{11}	Absolute humidity at hygrometer H11	g/m^3
ΔAH	Difference in absolute humidity	g/m^3
MR	Moisture ratio	-
ω_t	Mass ratio of water vs dry fabric at time = t	-
ω_0	Mass ratio of water vs dry fabric at start of experiments	-
ω_{end}	Mass ratio of water vs dry fabric at end of experiments	-

List of terms

Term	Explanation
atm	Atmospheric pressure at sea level
Capillary tube	A small internal diameter tube used for throttling/pressure reduction in a heat pump circuits
CD	Cool Down
CFC	Chlorofluorocarbons – ozone depleting synthetic refrigerants, e.g. R12
Condenser	A heat exchanger where condensation of the refrigerant in a refrigeration or heat pump circuit takes place
Condensing unit	A unit cooling moist air in a condensing drum dryer. The condensing unit may be the evaporator in heat pump circuit
CoolPack	EES based collection of simulation models for refrigeration systems
COP	Coefficient of Performance
COP _H	COP relative to heating duty
CRDP	Constant Rate Drying Process
DC-COP	Average SMER throughout a defined drying cycle
DC-MER	Average MER throughout a defined drying cycle
DC-SMER	Average SMER throughout a defined drying cycle
Evaporator	A heat exchanger where evaporation of the refrigerant in a refrigeration or heat pump circuit takes place
FRDP	Falling Rate Drying Process
Freon	Trade name (registered DuPont trademark) for CFC's
GWP	Global Warming Potential
HBP	High Back Pressure
HC	Hydrocarbons, e.g. Methane, Butane and Propane

HCFC	Hydrochlorofluorocarbons – Environmental unfriendly synthetic refrigerants
HFC	Hydrofluorocarbons – High GWP synthetic refrigerants, e.g. R134a and R410a
HFO	Hydrofluoro-olefins – Low GWP synthetic refrigerants, e.g. R1234yf
HP	Heat pump
HPDD	Heat Pump Drum Dryer
HST	High starting torque
HX	Heat Exchanger
Hygrometer	Instrument measuring the humidity of air
I-X diagram	Also called <i>Psychrometric chart</i> . Diagram expressing relative humidity, enthalpy, temperature and mixing ratio of humid air.
LabVIEW	Laboratory Virtual Instrument Engineering Workbench - Computer program for hardware integration and visual programming
LBP	Low Back Pressure
LMTD	Log mean temperature difference
LST	Low starting torque
MBP	Medium Back Pressure
MER	Moisture extraction rate [kg h^{-1}]
Mollier diagram	Term used about several enthalpy related diagrams named after Richard Mollier
NTP	Normal Temperature and Pressure, Defined at 20 °C and 1 atm
ODP	Ozone Depletion Potential
P-h diagram	Pressure – enthalpy diagram
R134a	Common synthetic HFC refrigerant
R290	Refrigerant grade Propane

SMER	Specific Moisture Extraction Rate [kg kWh^{-1}]
TEWI	Total Equivalent Warming Impact
Thermistor	Temperature dependent resistor used for temperature measurement
Thermocouple	Temperature sensor consisting of two dissimilar electrical conductors, producing temperature dependent voltage
VI	Virtual Instrument

1 Introduction

First patented in 1986[1] as “*heat pump closed loop drying*”, heat pump assisted dryers has been researched for more than 30 years. Unfortunately, the heat pump cycle has mainly featured environmental unfriendly HFC and CFC gasses. With questions being raised concerning both the environmental and human health impact of HFO’s[2], propane, along with other natural refrigerants, seems promising as an environmental friendly substitute for HFC’s and CFC’s.

By 2006, about 2% of the Norwegian households total energy consume were consumed by drying of clothes in drum dryers. 46% of the Norwegian households stated that they did have drum dryer or drying cabinet, an increase by 15% since 1990 [3]. As the European electricity mix by 2014 still cause 276 grams of CO₂ emissions per kWh, reduced energy consumes by drum dryers pose a large potential for reduction in climate gas emissions.

1.1 Limitations and premises

This project is based on rebuilding an existing heat pump assisted drum dryer, currently placed in the laboratory at the Department of Energy and Process Engineering at NTNU Gløshaugen in Trondheim, Norway. The drum dryer is acquired ahead of this project; thus, the choice of drum dryer cannot be influenced by findings during the project.

The facilities used for this study is connected to a large laboratory used for several other experiments. Therefore, there is no possibility of ambient air temperature and humidity control specific to this study. Heating, cooling and air exchange rates in the laboratory are controlled by building management without consideration to this specific study.

Although there are several other refrigerants that pose interesting as alternatives to R134a, this project is limited to investigation of R290(propane) as working fluid.

There will be made no attempt of reprogramming the factory set user programs. Drum, fans and compressor will be controlled by manual switches.

The drum dryer selected for this study is a Bosch Serie 4 WTW86298SN. It is a heat pump assisted condensation dryer charged with 220g R134a refrigerant. Maximum capacity is 8 kg dry weigh fabric.

2 Theory

This chapter briefly explains the theoretical background for this study, and provides an update on the current development regarding heat pump assisted drum dryers using R290.

2.1 Drum dryers

The principle operation of drum dryers is a three-step process. First air is heated, causing the relative humidity of the heated air to fall. Then the heated air is blown across the wet fabrics, absorbing moisture. Thirdly the moist air is removed from the drum. Difference in partial vapor pressure between the initially saturated air near the wet fabrics and the relatively dry heated air provides a driving force for drying[4]. Throughout this process, the drum is rotated to allow air to come into contact with the wet fabrics.

There is a wide range of different drum dryer designs commercially and technologically available. There is a trade-off between investment cost and energy efficiency, as well as drying time and degradation of the dried fabric. Though this study will investigate properties of only heat pump assisted drum dryers, a brief overview of other designs will be given, in order to provide better understanding of the energy efficiency challenges.

From a consumer standpoint, the energy efficiency of drum dryers may be compared by checking the product data sheet for the drum dryer. It is important to compare energy consume obtained by the same test standard. There are two relevant standards of test procedures for drum dryers in affect today. The United States Department of Energy (US DOE) D1/D2 test procedure [5], and The Association of Home Appliance Manufacturers (AHAM) test procedure[6].

One of the earliest articles found on using heat pumps to assist drum dryers offers a list of design constraints and expectations[4]. This article has been used as reference for several later studies. As design temperatures for the original dryer is unknown, design temperatures from this article is included as a reference. Table 1 shows the mentioned values.

Table 1- Overview of relevant design parameters derived from literature [4]

Parameter	Value	Unit
Maximal temperature of air entering the drum	130	°C
Maximal temperature of air leaving the drum	80	°C
Minimum temperature anywhere in the cycle	0	°C
Air pressure inside the drum, approx.	1	atm
Expected rate of moisture evaporation	3.5	kg/h
Maximal airflow rate entering the drum	200	kg/h
Design room air temperature	20	°C
Design room relative humidity	60	%

The drying process may be divided into four phases. Respectively Warm up, Constant Rate Drying Process (CRDP), Falling Rate Drying Process (FRDP) and Cool Down (CD). During warm up, energy is added to the process to heat the drying fabric, as well as components of the dryer. As temperature rises the drying rate increases throughout this period, though most of the added energy is used for sensible heating. When the fabric has reached a temperature where the energy needed to maintain the current drying rate equals energy added to the system, the process enters CRDP. Most of the energy added is used to evaporate water, without producing sensible heat. Throughout CRDP the dryer may run at full capacity, maintaining constant drying rate, without increase in temperature. CRDP continues as long as there is enough moisture available at the surface of the drying fabric to maintain constant drying rate at the given temperature. As the fabric dries, less moisture is available for evaporation, and the temperature of the fabric increases when the available moisture becomes insufficient. This happens when entering FRDP. As long as the same amount of energy is added to the dryer, the temperature increases and the drying rate declines. At the end of the drying process no heat is added to the system, and the fabric cools down towards ambient temperature during CD.

Figure 1 provides an illustration of the drying cycle of a conventional air vented dryer divided into the explained four phases. The red line indicates power consumption and the blue line drum exhaust temperature. The red and blue arrows may be ignored. It illustrates that throughout CRDP there is a high rate of evaporation from the fabric, allowing the heater to run at full capacity without overheating the drum. As moisture rate in the fabrics decline at the end of CRDP, the evaporation rate declines and drum exhaust temperature increase as the cycle enters FRDP. To avoid overheating, heating power is reduced when sensors indicate setpoint temperature. At the end, there is a cooldown period allowing the fabrics and drum to cool down to unharmed temperatures before the drum door is released. In modern dryers, the CD is initiated by sensors indicating a residual moisture in fabrics of 2-5 % [7]. Over-drying caused by inaccurate sensors or inferior algorithms significantly affect efficiency.

The principal shape of the figure is relevant also for heat pump assisted drum dryers, though the power consumption may be prone to increased variation as compressor power consumption will depend on cycle temperature.

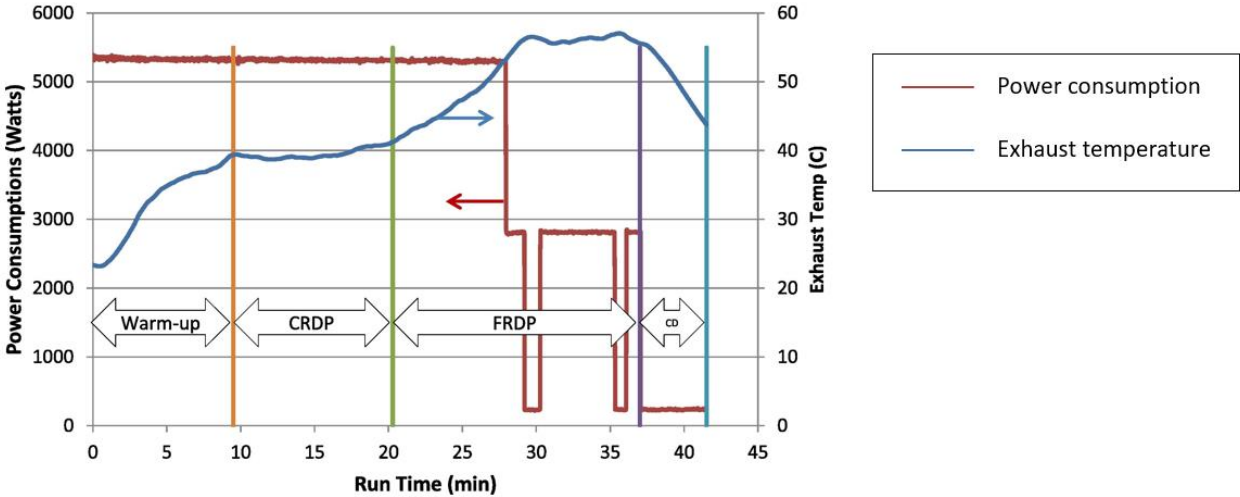


Figure 1 - Illustration of a conventional electric drum drying cycle. Figure created by TeGrotenhuis et.al. [8]

2.1.1 Conventional air vented dryers

The conventional air vented dryer heats ambient air using an electric heater, and exhausts moist air from the drum to the outside. This process is highly energy demanding, as electric energy needs to be added both for heating air and evaporating water. Another drawback with this design is the need for ducts leading moist air to the outside. Figure 2 shows a schematic overview.

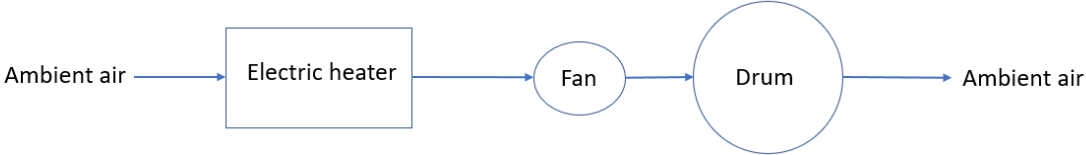


Figure 2 - Conventional air vented dryer

2.1.2 Conventional condensing dryers

A condensing dryer condenses water from the moist exhaust air using a heat exchanger cooled by ambient air. This allows the water to either be collected in a container, or to be drained through a sink. This design can be improved by using a heat recovery heat exchanger to preheat ambient air going to the drum. Further improvement is possible by closing the loop, reusing air that comes from the drum. This requires adding an additional heat exchanger in order to both heat air going to the drum and to be able to cool moist air sufficiently to archive satisfying condensation of water. This dryer design is found to give about 14% improvement in energy efficiency compared to air vented dryers[4]. Conventional condensing drum dryers that are condensing water by exchanging heat with the ambient air in the room where the dryer is placed, rejects a significant amount of often undesirable heat to the laundry room. This may result in thermal discomfort and increased cooling demand for the building. Figure 3 shows an conventional condensing dryer without heat recovery.

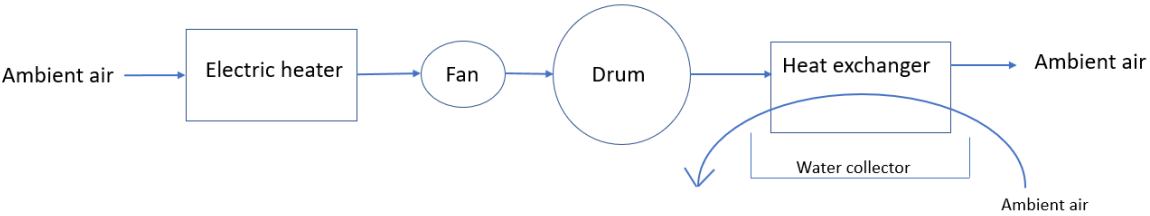


Figure 3 - Conventional condensing dryer

2.1.3 Thermoelectric dryers

Thermoelectric drum dryers are investigated experimentally and may offer lower investment costs than air cycle and vapor compression heat pump dryers. Thermoelectric elements are used to collect heat from drum exhaust air and reject heat to air going to the drum. This design offers the possibility of obtaining drying in a closed air loop. Only heat caused by heat generation in the thermoelectric element as well as heat added by drum engine and fans needs to be rejected to the ambient[9, 10]. Figure 4 shows a schematic of the process.

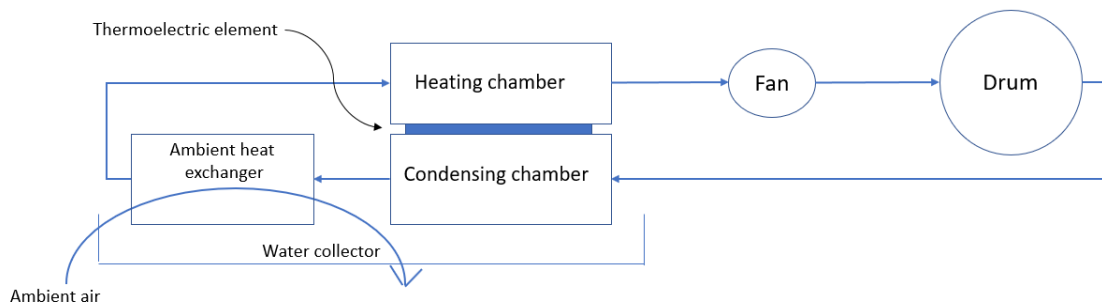


Figure 4 - Thermoelectric dryer

2.1.4 Air cycle heat pump dryers

Air cycle heat pump dryers compresses exhaust air from the drum in order to increase temperature and pressure. This enables improved heat recovery, and only requires heat added by the compressor, drum engine and fans to be rejected. This dryer design is investigated experimentally, and offers up to 40% improvement in energy efficiency compared to air vented dryers[4]. Figure 5 shows a schematic of the process

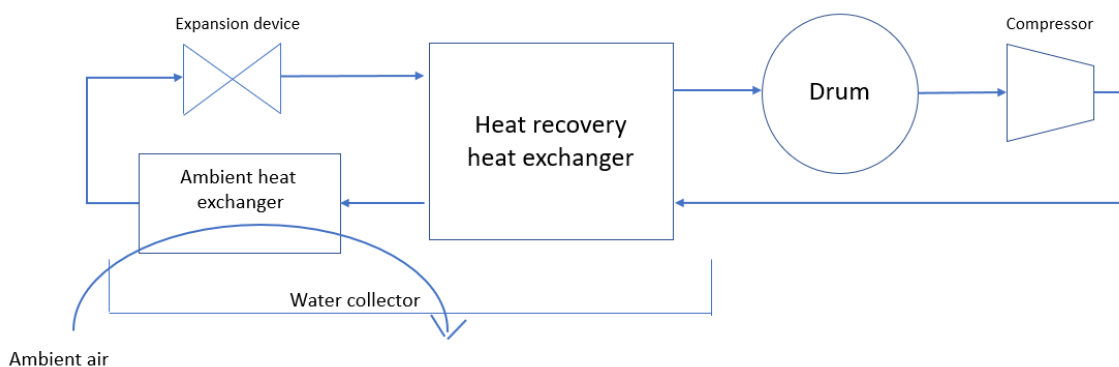


Figure 5 - Air cycle heat pump dryer

2.1.5 Heat pump assisted dryers

The term heat pump normally refers to vapor compression heat pumps. This term is used this way in this report as well. They offer the most energy efficient dryer design commercially available. Heat pump dryers are found to theoretically offer energy savings up to 69%, compared to air vented dryers[11]. This design uses a heat pump collecting heat from drum exhaust air adding heat to air going to the drum. This also demands the highest investment costs, due to the need for a heat pump in addition to other components. Figure 6 shows the process, with the air cycle in blue and the heat pump cycle in red.

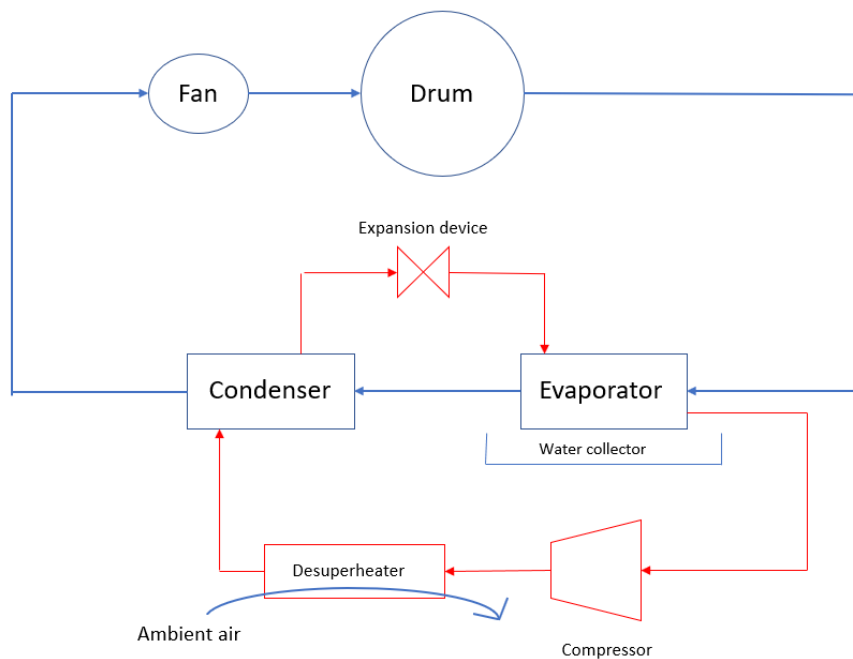


Figure 6 - Heat pump drum dryer

The heat pump exploits the relationship between pressure and temperature found in gases. By compressing a gas initially at relatively low temperature, a significant temperature rise in the gas may be obtained by adding a relatively low amount of energy to compress the gas. This allows the gas to collect heat at a low temperature and reject heat at a higher temperature. It is often desirable to use a gas that can collect heat by evaporation and reject heat by condensation, thus collect and reject heat at constant temperature. When used in refrigeration systems and heat pumps, the gases are referred to as refrigerants or occasionally working fluids.

As this heat pump design is the subject for this study, due to its high efficiency and possibility of upgrading, it will be thoroughly explained over the following pages.

2.2 The heat pump cycle for drum dryers

Heat pumps used in drum dryers normally consists of five main components, referring to the schematic overview of a heat pump assisted drum dryer system in Figure 7.

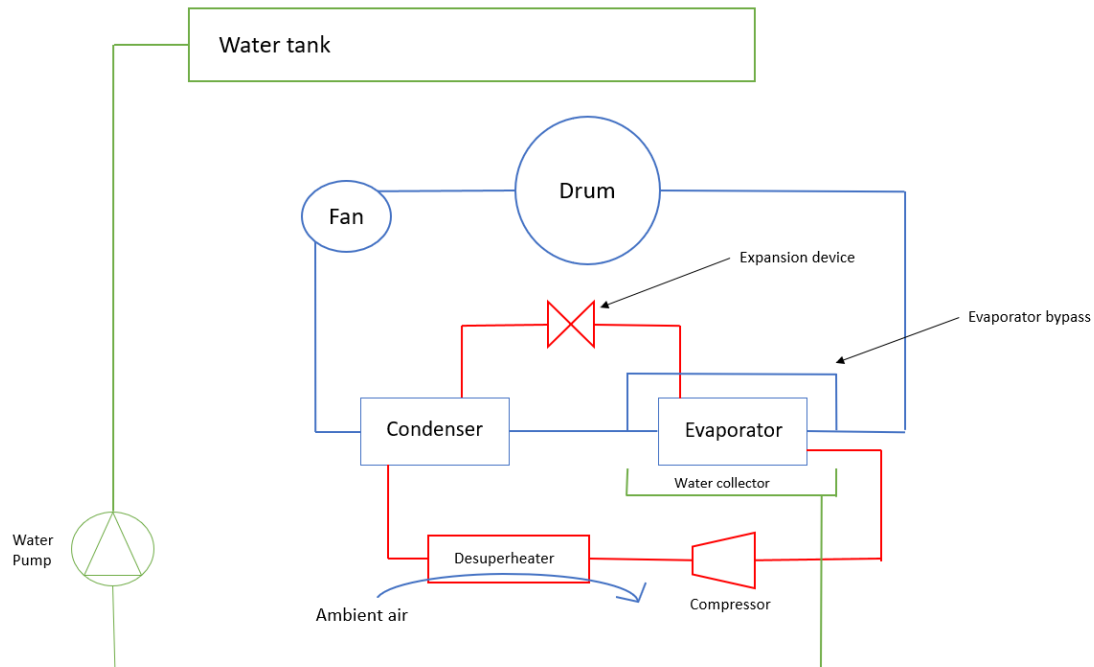


Figure 7 - System schematic for a vacuum heat pump assisted drum dryer system

1) Compressor

The compressor compresses refrigerant in gas-phase coming from the evaporator. Necessary pressure increase in the compressor depends on which refrigerant that is used in the system, ambient temperature and desired drying temperature. In small units, the compressor of choice is normally a hermetic piston compressor. It is a compact, low cost unit with the motor and piston sealed within a welded casing. This eliminates the problem of leakage through the sealings of the shaft between the engine and the piston and offers adequate compressor efficiency. Due to the hermetic seal, no parts of the compressor or its engine may be inspected or serviced. The motor and compressor itself is cooled by the suction gas, providing additional overheating of the suction gas before entering the piston. Other compressors such as hermetic scroll compressor or semi-hermetic piston compressors may be used. The efficiency of scroll compressors is lower than piston compressors, making them less desirable for this duty. Semi hermetic compressors are normally less compact than hermetic compressor, while the serviceability is limited to the rotor of the motor. As components of a household dryer is rarely

serviced during its lifetime, the semi hermetic compressor is not the obvious choice for these appliances. Semi hermetic compressors are frequently used in medium size system.

2) Condenser

The condenser is a heat exchanger adding heat to the air going to the drum, through condensing of the refrigerant. Due to its relatively compact size, low pressure loss and simple design, tube and fin heat exchangers are widely used in heat pump dryers. The refrigerant flows within the tubes of the heat exchanger, while air flows over its fins. As with all heat exchangers, the condenser causes a pressure drop in both the refrigerant circuit and air circuit. The pressure drop in the refrigerant circuit is dependent on the diameter, length, geometry and roughness of the tubing, while the pressure drop in the air circuit mainly depends on the size and shape of the fins. Though an excessively large condenser is desirable to obtain minimum temperature difference between the refrigerant and air, the excessive size would also cause excessive pressure drop that will have to be overcome by the compressor and air fan.

3) Pressure release system/valve

In larger heat pumps a thermostatic controlled valve releases pressure before the refrigerant enters the condenser. In small scale heat pumps with somewhat lower energy efficiency demands simpler systems are often used to release pressure in order to maintain low investment costs. The most common device is a capillary tube, because of its simple design, low cost and durability. A capillary tube is simply a tube with a very small internal cross-sectional area. The pressure loss is set by the internal diameter and the tube length. As the capillary tube is a static device with no moving parts, it may not be controlled during operation to accommodate for changing conditions. Proper selection of capillary tube is crucial for system performance. Due to the complex behavior of two phase flows, theoretical calculation of capillary tube length and diameter only serves as a preliminary selection. Testing is necessary to optimize the final selection.

4) Evaporator

The evaporator is a heat exchanger collecting heat from drum exhaust air. In most cases, a tube and fin heat exchanger are used, as with the condenser. The same trade-off between temperature difference and pressure loss as for the condenser also applies for the evaporator. Note that the evaporator in the heat pump cycle is the condenser in the drying cycle, as the heat pump collects heat from condensation and cooling of moist exhaust air from the drum. In this report, condenser and evaporator always refers to the heat pump cycle.

5) Desuperheater

In closed-loop systems, a desuperheater is necessary to remove latent heat from the system. The desuperheater is essentially a heat exchanger releasing heat to ambient air. In larger systems, it can also be cooled by water. In home appliances, heat losses by conduction and air leaks through the casing is often sufficient to remove latent heat from the system. A small temperature-controlled fan blowing air across the compressor exhaust pipe and the compressor itself may make an actual heat exchanger redundant.

Larger and more sophisticated heat pump systems may feature several other components in order to boost energy efficiency by a few percent. These components include suction-gas heat exchanger, subcooler and overheater[12]. For systems such as drum dryers the addition of these components does not seem to be cost worthy.

Hybrid systems, featuring an electric heater in addition to the heat pump to shorten warm-up time might be used. This will lower the energy efficiency and increase peak power demand, but shorten drying time[8]. A system sketch of hybrid system is shown in Figure 8.

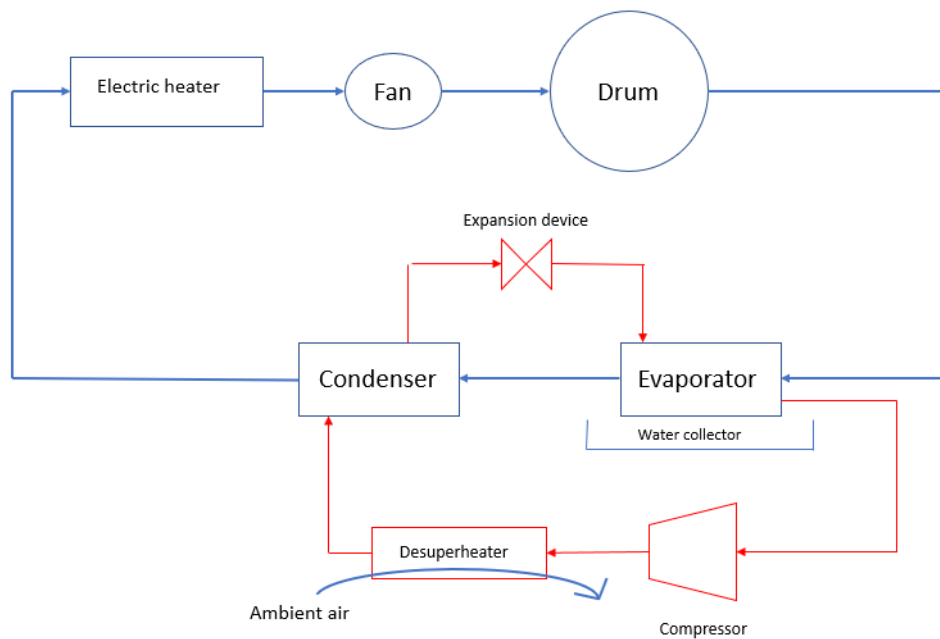


Figure 8 - Hybrid heat pump dryer including electric heater

The main drawback related to heat pump assisted drum dryers is use of refrigerants with high ODP and GWP potential. This creates high impact on environment, due to the fact that such type of systems are widely used all over the world.

The application of environmentally friendly refrigerants, increased energy efficiency, lowered drying temperatures and decreased heat rejection to the laundry room needs to make up for this drawbacks for a heat pump drum dryer to be desirable.

2.3 Refrigerants

Several natural refrigerants are environmental friendlier alternatives to HFC gases. Although HFO's and HCFC's may feature lower GWP values than HFC's, they may not automatically be regarded as environmentally friendly[13]. Both the environmental impact, flammability, combustion products, toxicity, decomposition products and production process of these gases are being questioned.

R717(Ammonia/ NH_3), R600(Isobutane), R744(Carbon-dioxide/ CO_2) and R290 (Propane) are all environmental friendly refrigerants, that may substitute HFC's. They all have zero ODP and very low GWP compared to HFCs. Ammonia pose excellent thermodynamic properties but are toxic and have a strong odor. Only a few grams of ammonia per cubic meter of air pose a danger of death by poisoning and the odor caused by lower concentrations may cause anxiety and people to evacuate. Therefore ammonia is not regarded as suitable for household appliances that are not efficiently ventilated to the outside or have the possibility of a scrubber system. As ammonia corrodes copper, it may not be used as a drop-in in systems with copper parts. Also, hermetic compressors for ammonia would have to be made without copper windings in the motor. Carbon-dioxide is an excellent alternative but requires very high pressure compared to R134a. A drum dryer using CO_2 as working fluid has been developed at NTNU, providing auspicious results[14]. The stable operating conditions of a drum dryer allows a CO_2 heat pump to run efficiently without sophisticated design or excessive amount of components. Unfortunately, the high pressure components needed are costly compared to the moderate pressure components used with HFCs, making CO_2 drum dryers disproportionately expensive. Isobutane has many of the same qualities and drawbacks as propane, especially regarding flammability. The critical temperature is higher than for propane and R134a. By its thermodynamic properties, it is interesting as a substitute for R410a, and are used in domestic chillers.

Propane is non-toxic, odorless and operates at moderate pressures similar to R134a and offers similar thermodynamic properties as R134a. Its flammability concerns in hermetic systems may easily be constrained by charge minimization and the use of properly designed compressors. Subsequently, is the most promising replacement for R134a.

2.4 Comparison of properties of R134a and R290

Both R134a and R290 is common refrigerants used in different applications. While R134a is a synthetic fabricated gas invented for use in refrigeration systems, R290 is a natural hydrocarbon found in the earth's crust.

R134a (1,1,1,2-Tetrafluoroethane) is one of the most commonly used refrigerants in small scale heat pumps, automotive AC-units, chillers and dryers[15]. Providing oil change or hydrocarbon blend, it can be used as drop-in replacement for R12[16, 17]. According to ASHRAE classifications it is not classified as dangerous, hazardous, toxic or flammable, and has very good thermodynamic properties[18]. R134a and others HFC-gasses were considered an environmental friendly alternative replacing ozone-depleting CFC-gasses that were banned by the Montreal Protocol[19]. Due to the awareness of climate changes, R134a is no longer considered environmental friendly due to its high GWP value[20].

R134a is also referred to as HFC-134a, when use as refrigerant is not specified. Several other synonyms are commonly and sometimes imprecisely used in trade and everyday speech.

R290 (Propane) is a common hydrocarbon, classified as a natural working fluid when used in refrigeration systems and heat pumps. At room temperature and ambient pressure propane is a colorless and odorless highly flammable gas. It is widely used as fuel for heating and combustion engines, and is an important raw material for petrochemical industry[21]. It offers low GWP and suitable thermodynamic properties making it interesting as substitute for R134a.

As use of propane in refrigeration systems requires higher level of purity than what is often the case with commercially available propane, refrigeration grade propane is consequently referred to as R290 in this report[22]. While propane sold as fuel includes an additive providing a distinctive smell, R290 does not include this additive, making it completely odorless. Although specifications for R290 is not found in international standards, some general data for hydrocarbon refrigerants are found in the German DIN8960 standard[23].

R290 oil compatibility is almost identical to R134. It is chemically inactive in refrigeration circuits. Some rubbers and plastics, especially chlorinated plastics, may be incompatible with hydrocarbon refrigerants. Danfoss has composed a short list of materials reported to be problematic, represented in Table 2.

Table 2 - Materials compatibility with R290 [23]

Material	Compatible
Butylic rubber	No
Natural rubber	No
Polyethylene	Depending on conditions
PP	No
PVC	No
PVDF	No
EPDM	No
CSM	No

For metallic materials NS-EN ISO 11114-1:2012[24] states for propane:

“No reaction with any common materials; however, in wet conditions the risk of corrosion from impurities shall be considered.”

For non-metallic materials *NS-EN ISO 11114-2:2013* provides a more extensive list of recommendations. The complete list is rendered in Appendix A. It lists several of the materials listed as non-compatible by Danfoss as acceptable for use with propane. Note that *NS-EN ISO 11114 series* are gas cylinder and valve standards.

Table 3 provides an overview of selected properties of R134a and R290. Data has been collected from several sources listed in the heading or together with the specific property. Values of GWP and auto-ignition temperature vary from different sources. As the exact value of these

properties are not important for this study, no further effort has been made to verify the most acknowledged value.

Table 3 - Chemical Properties of refrigerants R134a and R290[25, 26]

Properties	Unit	R134a	R290
Chemical name		1,1,1,2-tetrafluoroethane	Propane
Chemical formula		CH ₂ FCF ₃ C ₆ H ₂ F ₄	CH ₃ CH ₂ CH ₃
Synonyms and trade names		HFC-134a Norflurane Freon 134a Dymel 134a Forane 134a Genetron 134a HFA-134a Suva 134a	Refrigerant grade Propane
ASHRAE 34 Safety group		A1	A3 (highly flammable)
Auto-ignition temperature	[°C]	770 [27]	450 [28]
State at NTP		Gas	Gas
Melting point	[°C]	-103.3	-187.7
Boiling point	[°C]	-26.1	-42.1
Critical temperature	[°C]	101.1	96,7
Critical pressure	[MPa]	4.06	4,25
Molecular weight	[g/mol]	102.03	44.1
Atmospheric lifetime	[years]	14.0	0.041
GWP [20]	[-]	1430	3
ODP	[-]	0	0
Lower flammability limit (LFL) [29]	% vol g m ⁻³	- -	2.1 39
Upper flammability limit (UFL) [29]	% vol g m ⁻³	- -	9.5 177

2.5 Publications on propane in HPDD

Bellomare et al. (2015) [30] conducted analysis of hydrocarbons (R290 and R441A) as drop-in replacement of R407C in household heat pump tumble dryers.

Replacing only the compressor, their results show that total energy consumption increased by 6 % when using R290, while drying time increased by 8%. They conclude that

“it is mandatory having technology support in terms of properly designed components, in order to not deteriorate system performances when a refrigerant drop-in replacement takes place. It is possible to conclude that a rough refrigerant drop-in replacement might lead to higher energy consumption.”

Personal enquiry has been made by email to the authors regarding what compressor was used in the study. S. Minetto responded that they used a HFC compressor, thus not a compressor made for R290 [31].

D. Sánchez et. al. (2017) [32] performed an energy performance evaluation of R1234yf, R1234ze(E), R600a, R290 and R152a in comparison with R134a. Similar to the vast majority of studies on HC's in household appliances, the evaluation was based on a refrigeration system. They state that

“R290 presented an increment of COP, cooling capacity and compressor power consumption.”

Danish cooling and heating components producer Danfoss has published an Application guideline for “Practical Application of Refrigerants R 600a and R 290 in Small Hermetic Systems” [23]. Though the guide's main focus are refrigerators and cooling purposes, it is relevant for HPDD's as well. The guide is weak on citations, and does not offer a clear line between calculations, presumptions, experience and scientific results. For all easily comparable

data, the guide checks out as correct, and offers an extent of relevant data regarding application of R290.

Tecumseh Products Company LLC has published “Guidelines for the utilization of R600a and R290”[33]. It offers practical guidelines for design and operation of refrigeration units utilizing R290, with special care concerning use of Tecumseh’s products. Relevant to this study they state about capillary tube selection:

“capillary tubes selected for R404A applications should be adequate as a preliminary selection for R290. As with any capillary tube selection, system testing is necessary to determine the proper final selection.”

Tecumseh has also published a “Technical Bulletin” on hydrocarbons [34] and SECOP an application guideline for R600a and R290 in small hermetic systems [35]. This documents contain roughly the same information as the ones stated above.

2.6 Safety regulations

R134a is comprised by the EU F-gas Regulation, regulating production, usage and disposal of climate affecting HFC-gasses. R290 is not an HFC gas and is therefore not comprised by the regulation. This makes it legally less complicated to handle R290, in terms of certification of service personnel and collection of used gas[20].

IEC 60335-2-89:2010, paragraph 22.105, which is also adopted as a Norwegian NEK standard states that[36]:

“The mass of refrigerant in appliances which use flammable refrigerant in their cooling system shall not exceed 150 g in each separate refrigerant circuit.”

R290 is classified as a flammable refrigerant. There has been reported that the limit is likely to be moved to 500 g by 2018[37], but this has not been verified by other sources. Readers may note that according to LFL and UFL in Table 3, a charge of 150 g propane released into a small laundry room assumed to contain about 6 m³ of air will not provide a flammable mixture, while 500 g propane released into the same unvented room will be highly flammable.

2.7 Consequences on system design

By theoretical basis, when redesigning a R134s system for R290 the materials and dimensions of heat exchangers, tubing, filters and similar components does not need to be changed. The compressor needs to be substituted to a compressor designed for R290, featuring a slight decrease in displacement and spark-free design. The mass of refrigerant charge may be reduced by about 40%. To obtain efficient and reliable operation, capillary tube replacement is recommended.

The amount of changes to a factory production line necessary to successfully implement R290 as refrigerant in heat pump drum dryers is limited to compressor installation and system charging, as well as capillary tube design.

2.8 Important equipment for propane

Great efforts have been made to identify a commercially available compressor suited for use with R290 within the desired temperature range. Specifications of compressors from the following producers has been examined: Danfoss Compressors/SECOP, Konor Electromechanics Co., Emerson Climate Technologies, Toshiba, Hitachi, Tecumseh, Sanyo, Denso, Dorin, Bock and Mycom

Only Tecumseh are found to produce high back pressure (HBP) R290 compressors within the desired power range. HBP compressor are preferred to meet efficiency demands, and to be flexible regarding high temperature testing.

Figure 9 shows evaporation temperatures for Secop LBP, MBP and HBP compressors. As seen in the figure HBP is favorable.

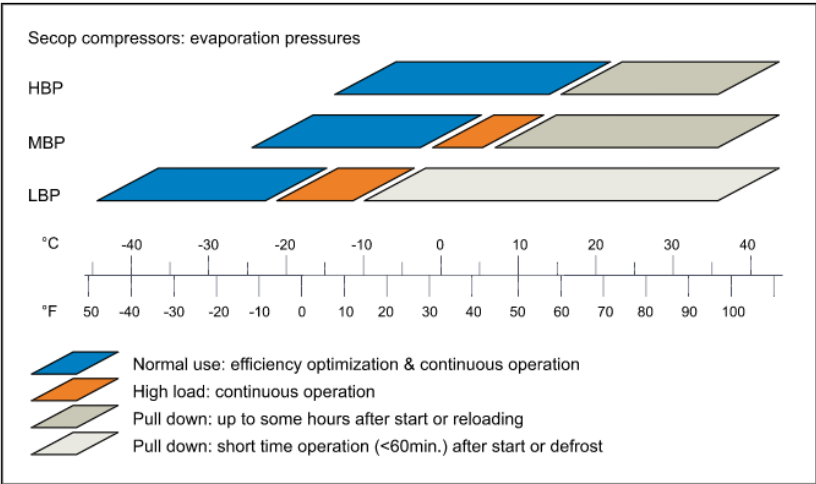


Figure 9 - Secop compressors: evaporation pressures. Figure created by Secop[38]

2.9 Drying and dehumidification

As mentioned, the driving force for drying of fabric in drum dryers are the difference in partial vapor pressure between dry air blown into the dryer and saturated air close to the fabrics. As relative humidity is defined as the ratio between the partial vapor pressure and the saturation or equilibrium vapor pressure, the relative humidity of the air needs to be much less than 100% in order to obtain drying.

The amount of water that an amount of air can hold without condensation is dependent on temperature and pressure. For a given pressure, this relationship can be expressed in a psychrometric chart, or an I-x diagram. As air pressure in the air cycle is close to ambient (atmospheric) pressure, diagram for atmospheric pressure can be used. The I-x diagram in Figure 10 shows how raising temperature increases the amount of water air can hold, thus decreasing relative humidity. Consequently, cooling moist air will cause condensation of water, and is the most common way to reduce moisture content in air. The temperature when humidity in the air will begin to condense is known as saturation temperature, or dewpoint.

An ideal closed loop drying cycle is drawn in Figure 10. From point 1 to point 2 the air absorbs water thus increasing the mixing ratio between water and dry air. Assuming adiabatic evaporation, the water extracts heat from the air in order to evaporate causing air temperature to fall while maintain constant enthalpy. From point 2 to point 3 the air is cooled while humidity condenses to liquid on the surface of the condensing unit expressed in point 4, thus decreasing the mixing ratio of the air overall airflow. The final state of the air after passing the condensing unit remains at point 3. From point 3 to point 1 the air is heated causing temperature and enthalpy to increase while maintaining constant mixing ratio, thus decreasing the relative humidity.

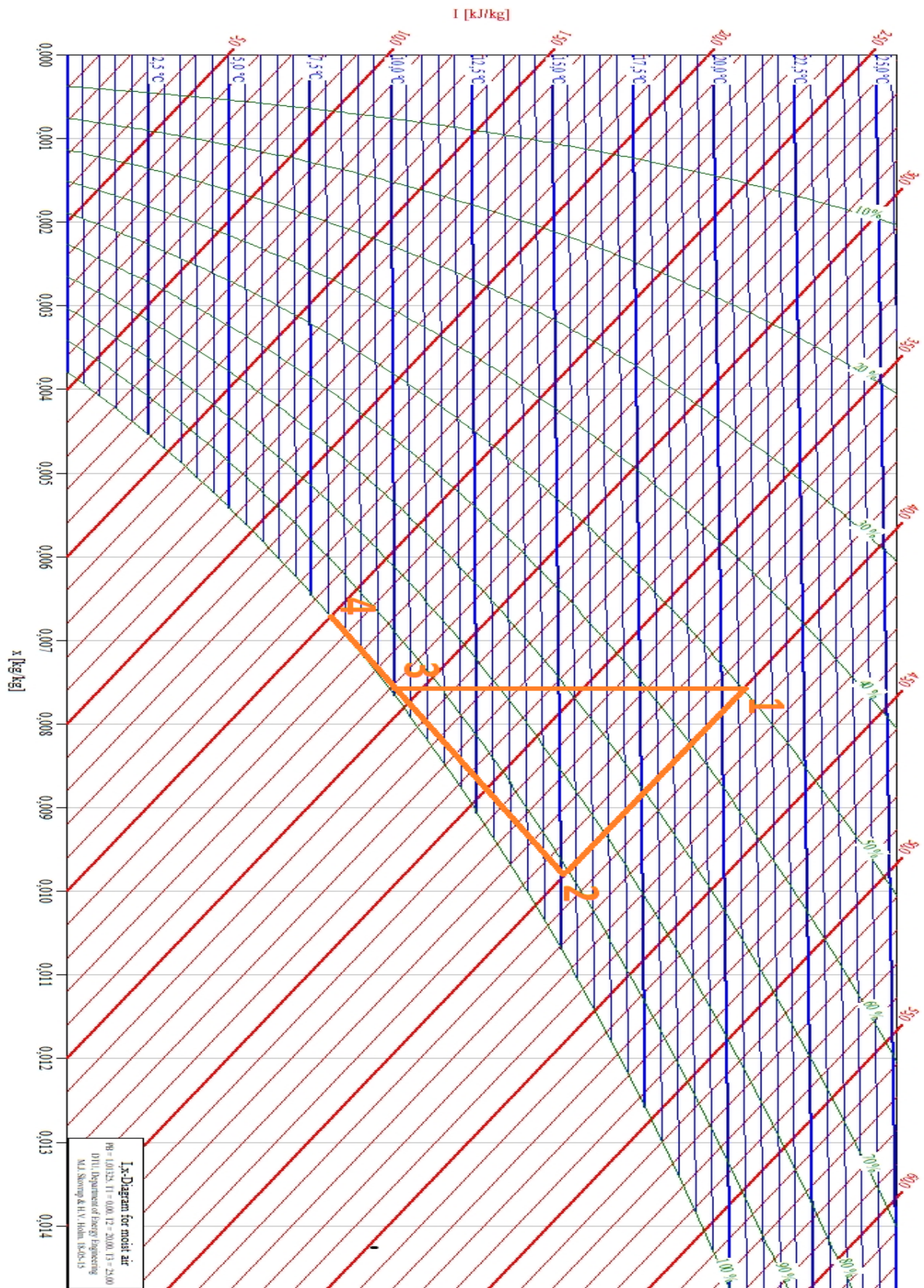


Figure 10 - I-x diagram / Psychrometric chart

The latent heat of evaporation, as well as the specific heat capacity, for water is depending on temperature and pressure. At ambient pressure (1.01 325 bara) 100°C the latent heat of evaporation is 2256 kJ/kg, while at 50°C it is increased to 2382 kJ/kg [39]. Table 4 shows the latent heat of evaporation and specific heats for water at ambient pressure and selected temperatures.

Table 4 - Specifics heats of water at 1.01 bara [39]

Temperature [°C]	C_p liquid [kJ/kg K]	C_p gas [kJ/kg K]	Heat of evaporation [kJ/kg]
0	2.11	1.72	2835
25	4.21	2.08	2443
50	4.22	2.11	2382
100	4.20	2.03	2256

The rate of drying is dependent on the amount of moisture available at the surface of the dried product. As long as moisture can be transported to the surface of the dried product at the same rate as moisture is removed from the surface, constant drying rate may be obtained, and drying rate easily calculated. This period is referred to as constant rate drying period (CRDP). As the product is dried and moisture content decreases, the rate that moisture is transported to the surface of the product limits the drying rate. The drying rate normally declines until the product is dry. This period is referred to as falling rate drying period (FRDP). The nature of moisture transport rate within the product depends on the product. For common products, tables of empiric coefficients are developed, and drying rate may be calculated by empiric formulas.

Energy efficiency of dryers are measured by Specific moisture extraction rate (SMER). Equation 1 shows the definition of SMER. As seen by the equation, high SMER values are desirable, as it means that a large amount of water is evaporated by a small amount of added energy. In a dryer, the highest SMER values are obtained throughout CRDP, while drying beyond constant rate is more energy consuming. Although, the energy needed for evaporation of water remains the same, the energy used for fans and condensation of water increases as the water removed by one unit of air decreases. This is caused by the need for an increased

difference in vapor pressure between the air and the dried product to achieve satisfying drying rates[40].

$$1) \quad SMER = \frac{\text{Amount of water evaporated}}{\text{Energy input to the dryer}}, [\text{kg/kWh}]$$

2.9.1 Operating schemes and control parameters

Excessive temperatures and uneven drying may cause quality degradation of dried products. Especially products such as food and timber are vulnerable to degradation during drying[41].

For drum dryers, maximum temperature is set by the type and quality of fabric that is dried. Degradation and excessive wear on the fabric and other parts of clothes that is dried, such as elastic bands and prints, may be caused by high drying temperatures. Lowered drying temperatures may increase the lifetime of frequently dried fabric and clothes, thereby reducing environmental impact from this industry, as well as consumer costs. To a large extent, uneven drying is avoided using a rotating drum ensuring even airflow through the clothes.

The refrigerant pipes in the heat pump circuit are measured to have an outer diameter of 8mm. Measurements of the diameter of the remaining pipes are shown in Table 5.

Table 5 - Pipe diameter

Pipe	Outer diameter
Condenser inn/out	8 mm
Evaporator in/out	8 mm
Condenser tubing	7 mm
Evaporator tubing	7 mm
Capillary tube	2.2 mm
Capillary tube expansion chamber	17 mm

The internal diameter of the original capillary tube is measured to be 1.0mm, while its length is 78.cm.

The original compressor are found to have a rated displacement of 7.5 cm³ and input power of 300W. Appendix C contains the Product Data sheet, providing additional information. On request, the producer informs that the compressor is lubricated by JX-NOE L22E oil [43]. Furthermore, the following specifications are found on the compressor plate:

Producer: Rechi Precision

Model: 39E073B

Configuration no: R&UJYA

Serial no: Q/FE12Q1KDA5487C

220-240V 50 Hz Phase: 1 L.R.A.: 5.5 Refr: R-134a

The rated input power of the main components of the original dryer is shown in Table 6. Input power for the compressor and compressor ventilator fan has been provided by the producers[44, 45], and the water pump from the Bosch UK website[46]. On the combined drum and drum fan engine no producer markings are found. Unfortunately, Bosch has not been willing to disclose any technical specifications regarding this engine[47].

The availability of specifications and rated performance of the drum dryer and its components are limited, as Bosch has not been willing to enclose any further technical data or drawings for use in this study[48].

The maximum combined electric power pulled by the dryer is stated to be 1000W at 220 -240V by markings on the dryer. Refrigerant charge is stated to be 0.22kg of R134a.

Table 6 - Rated input power of the drum dryer's original main components

Component	Producer	Bosch part number	Rated input power
Compressor	Rechi Precision	00145545	300W
Fan compressor ventilator	Sunon	00651456	11W
Drum and drum fan engine	Unknown	00145443	Undisclosed
Water pump	Unknown	00145388	26W
Total rated input power			337 + drum/fan eng.

The compressor and drum engine are phase compensated by capacitors in parallel. The capacitors are 9uF for the drum engine and 15uF for the compressor.

As design expectations are difficult to come by, and Bosch is unwilling to disclose specifications for the original dryer, presumptions and measurements in Table 7 has been made for initial system design. The presumptions are based on literature review[4, 8, 49] and the authors considerations based on thermodynamics and mechanical principles.

Table 7 - Design specifications

Parameter	Unit	Value
Initial moisture content in fabric	%	33
Terminal moisture content in fabric	%	-
Moisture extraction rate	[kg h ⁻¹]	1
Airstream trough drum	[kg h ⁻¹]	170
Relative humidity of moist air at drum outlet through CRDP	%	85
Expected air leakage from drum	%	25
Maximum power consumption for entire system	[VA]	550
Maximum combined power consumption for fans, pump, and drum engine	[VA]	250
Power available for compressor	[VA]	300
Condensation temperature (steady state)	[°C]	50
Evaporation temperature (steady state)	[°C]	20
Evaporator superheat (steady state)	[K]	-
Condenser subcooling (steady state)	[K]	-
Isentropic efficiency of compressor (steady state)	[-]	-
Volumetric efficiency of compressor (steady state)	[-]	-

In all types of drum dryers, air leakage from the system seems inevitable[49]. Air leakages may be up to 40% of the total air volumetric flow.

3.2 Equipment

The following equipment has been used:

- Drum dryer as described in section 3.1
- Instrumentation and logging equipment as described in section 3.5
 - Computer: Dell OptiPlex GX280
- Fabric as described in section 3.3
- Washing machine/centrifuge: AEG LN58460
- Scale: Mettler Toledo XS32001LX

3.2.1 Compressor

At adequate temperatures R290 inhibits higher $\Delta h_{\text{condensation}}$ than R134a, providing the need for lower refrigerant mass flow. On the other hand, the density of R290 is lower than of R134a, and almost makes up for the increased $\Delta h_{\text{condensation}}$ in terms of mass flow. Equation 2 and Equation 3 may be used to calculate the alteration in mass flow and volume flow. While $\Delta h_{\text{condensation}}$ is the enthalpy change during condensation of the appropriate refrigerant, v_g is the specific volume of the refrigerant at the compressor inlet. Both values are found in tables.

$$2) \quad \dot{m}_{\text{Ratio}} = \frac{\Delta h_{\text{condensation},R134a}}{\Delta h_{\text{condensation},R290}}$$

$$3) \quad \dot{v}_{\text{Ratio}} = \frac{\frac{\Delta h_{\text{condensation},R134a}}{v_{g,R134a}}}{\frac{\Delta h_{\text{condensation},R290}}{v_{g,R134a}}}$$

Assuming condensation temperature of 50°C and suction gas temperature of 15°C, the mass flow ratio is calculated to 0.57 and the volume flow ratio to 0.84.

Multiplying the displacement of the original R134a compressor with the volume flow ratio provides a displacement for the R290 compressor at 6.3cm³

After evaluation, a Tecumseh AE4430U-FZ1A compressor has been chosen for the rebuild. The main specifications are shown in Table 8. The product data sheet is found in Appendix D.

Table 8 - Tecumseh AE4430U-FZ1A specifications

Producer	Model number	Type	Displacement[cc]	Input power [W]
Tecumseh	AE4430U-FZ1A (AE4430U-FZ)	Hermetic Reciprocating	6.12	315

3.2.2 Heat exchangers

The original heat exchangers are assumed to be adequate for R290. They are both counter flow fin and tube types. Although the sizing is not optimal for R290, the original heat exchangers will not be altered. Sintef has developed a computer program for design of heat exchangers, named HXsim. At the time of writing, a license and working edition of HXsim has not been obtained despite efforts to do so.

3.2.3 Refrigerant charge

The traditional way of calculation refrigerant charge is by dividing the internal volume of the high-pressure side components and tubing by the specific volume of liquid refrigerant. The fraction is stated by Equation 4. Determining the internal volume of the components may be complicated and prone to measurement errors if not stated by the producer.

$$4) \quad m_{\text{Refrigerant}} = \frac{\text{High - pressure side internal volume}}{\text{Liquid refrigerant specific volume}}$$

Assuming that the length of tubing at the high-pressure side of the system remains the same, the ideal R290 charge may be calculated from the original R134a charge. Equation 5 may be used. m_{R134a} is the factory charge of R134a, while v_l is the specific volume of saturated liquid refrigerant at condensation temperature.

$$5) \quad m_{R290} = m_{R134a} \cdot \frac{v_{l,R134a}}{v_{l,R290}}$$

Assuming 50°C condensation temperature, R290 charge is 91g. The factory R134a charge is 220g.

Multiplying refrigerant charge with the refrigerants GWP value provides the total global warming potential of the charge expressed in CO₂ equivalents. Based on the values above, the R134a charge equivalents 295kg CO₂, while the R290 charge equivalents 0.273kg CO₂. However the charge should be optimized with respect to working conditions and size of heat exchangers.

3.3 Experimental setup and procedure

To ensure comparable results, the drum dryer has been modified so that the compressor, compressor cooling fan, drum engine and drum fan is controlled by mechanical switches. This ensures that the programming of the original control does not influence the results. The switches are on/off, meaning that the speed of the electric motors cannot be altered.

The wiring is made so that one switch controls the compressor and compressor cooling fan, and one switch controls the rotation engine and fan. The compressor cooling fan can be unplugged manually. As the drum and fan is run by a combined motor and combined shaft, drum rotational speed and fan speed is fixed to each other. The pump draining the water collector is controlled by a manual switch that needs to be depressed continuously for the pump to run.

The tests are run with a test load of 2.632 kg fabric, consisting of various cotton. The fabric is then soaked in water, and centrifuged at up to 1400 rpm in a AEG LN58460 washing machine to ensure adequate moisture distribution. The moisture content mimics the residual moisture after a standard washing program in an ordinary washing machine. The fabric is then weighed and loaded into the dryer. The compressor cooling fan are unplugged during experiments, and temperatures monitored by the operator to ensure unarmful temperatures. Four different experimental setups has been applied;

Setup 1: Fabric centrifuged at 1400 rpm. The dryer is run for 80 minutes. The fabric is the taken out for the dryer and weighed.

Setup 2: Fabric centrifuged at 1400 rpm. The dryer is run for 80 minutes. Every 10 minutes the fabric is taken out of the dryer and weighed. The compressor is shut down during weighing.

Setup 3: Fabric centrifuged at 1400 rpm. The dryer is run for 120 minutes. The fabric is then taken out of the dryer and weighed.

Setup 4: Fabric centrifuged at 600rpm. The dryer is run for 80 minutes. The fabric is the taken out for the dryer and weighed.

The amount of water removed from the fabric by the dryer can be calculated as the difference in weight before and after drying. To allow for calculation of leakage from the dryer, the condensed water is collected and weighed. Since there is no sump for the pump in the water collection tray, the tray is filled with water and pumped down to the level achievable by the pump before experiments. During experiments, the pump is run repetitively while the water is collected to ensure that the evaporator is not submerged, thus affecting results. At the end of experiments, the pump is run until the water level has again reached the minimum level achievable by the pump, ensuring that the amount of water collected for weighing is equal to the amount condensed during drying.

Figure 12 shows the experimental rig with the drum dryer, control cabinet and a computer used for logging.



Figure 12 - Experimental rig

3.3.1 Standardized procedure

A practical procedure has been developed for the experiments. To ensure comparable results, this procedure is followed in the same order for every experiment. Table 9 shows the procedure. The dryer is allowed to rest for at least 7 hours between experiments, to ensure that internal temperatures approaches equilibrium with the ambient between experiments.

Table 9 - Standardized procedure

Step	Description	Notes
1	Startup of the computer and control cabinet	
2	The fabric is soaked and centrifuged	
3	Filling and pumping of the water collection tray	
4	Emptying and weighing of the water collector	
5	Startup of the LabView VI and logging	Always check that logging is running
6	Weighing of the centrifuged fabric	Weight is logged manually
7	Feeding of fabric into the drum	Set timer for draining and total drying time
8	Simultaneous start of the drum engine, drum fan and compressor	By use of manual switches
11	During drying: Pumping of the water collector every 20 th minute	Manual operation
10	Drum engine, drum fan and compressor are stopped after time depending on setup	By use of manual switches
11	Weighing of the dried fabric	Weight is logged manually
12	Pumping of the water collection tray	Manual operation
13	Weighing of the collected water	Weight is logged manually
14	Cleaning of the drum exhaust air filter	
15	Shutdown of logging, LabView, the computer and control cabinet	

3.4 Rebuild

To allow the compressor to be changed the R134a system was emptied, instrumentation connected to the heat pump circuit removed and the pipes cut as close to the original compressor as possible. Then the compressor was removed, and cabinet and compressor mountings adapted to fit the new R290 compressor. The R290 compressor were mounted within the original cabinet, maintaining almost the same amount of air leaks and insulation as before, minimizing the change in heat loss compared to the R134a system. Due to the increased outer dimensions of the R290 compressor, the compressor cooling fan had to be removed from its mountings. As the fan is mounted in an opening in the casing, the fan is temporarily placed over the opening for experiments to avoid influencing heat loss. The fan has not been run for any experiments other than initial system behavior tests.

The pipes connected to the compressor were bent and adapted to fit the new compressor, before being soldered to the suction and discharge pipes. A valve was soldered to the process pipe of the compressor, to serve as a service valve for experiments. To obtain a hermetically sealed system permitted for non-laboratory use, this pipe would have to be sealed by soldering.

The thermocouples removed prior to the rebuild were reinstalled in the same position using the same fastening and insulation method as before. The pressure sensors were reconnected to the same connectors as before. Prior to recharge, the system was pressure-tested with nitrogen for 16 hours and all joints and connections inspected using soapy water.

Initially, the system was charged with 100g of R290, including refrigerant left in the pipes between the canister and the service valve. The first experiment revealed excessive overheating at the compressor suction pipe, suggesting that the charge was less than ideal. An extra charge of 15g R290 were added to the system, making the total charge 115g. At this charge the overheating was considered to be ideal at 2-4 K overheat. Further charge optimizing is performed in section 4.2.5.

3.5 Instrumentation

The original drum dryer has been somewhat modified, and sensors mounted for previous experiments made by other students. Sensor values are logged using a LabVIEW program originally designed for a CO₂ HPDD by technicians at the NTNU laboratory. The program has been edited to provide the desired data for this thesis. Sensor values are logged and saved as Excel-files for analysis, at a time interval set to 2 seconds. Due to processing time, the real time interval is approximately 3 seconds. The LabVIEW block diagram is shown in Figure 13.

Data acquisition is done using National instruments cDAQ-9178. NI cDAQ-9178 provides a USB interface compliant with almost all computers available.

In addition to the sensors connected to the drum dryer, input power is measured by a transducer connected to the feed wires. Input power for the combined drum/ drum fan engine and the compressor is measured separately. Measurements are performed using a DEIF TAP-210DG/3 transducer.

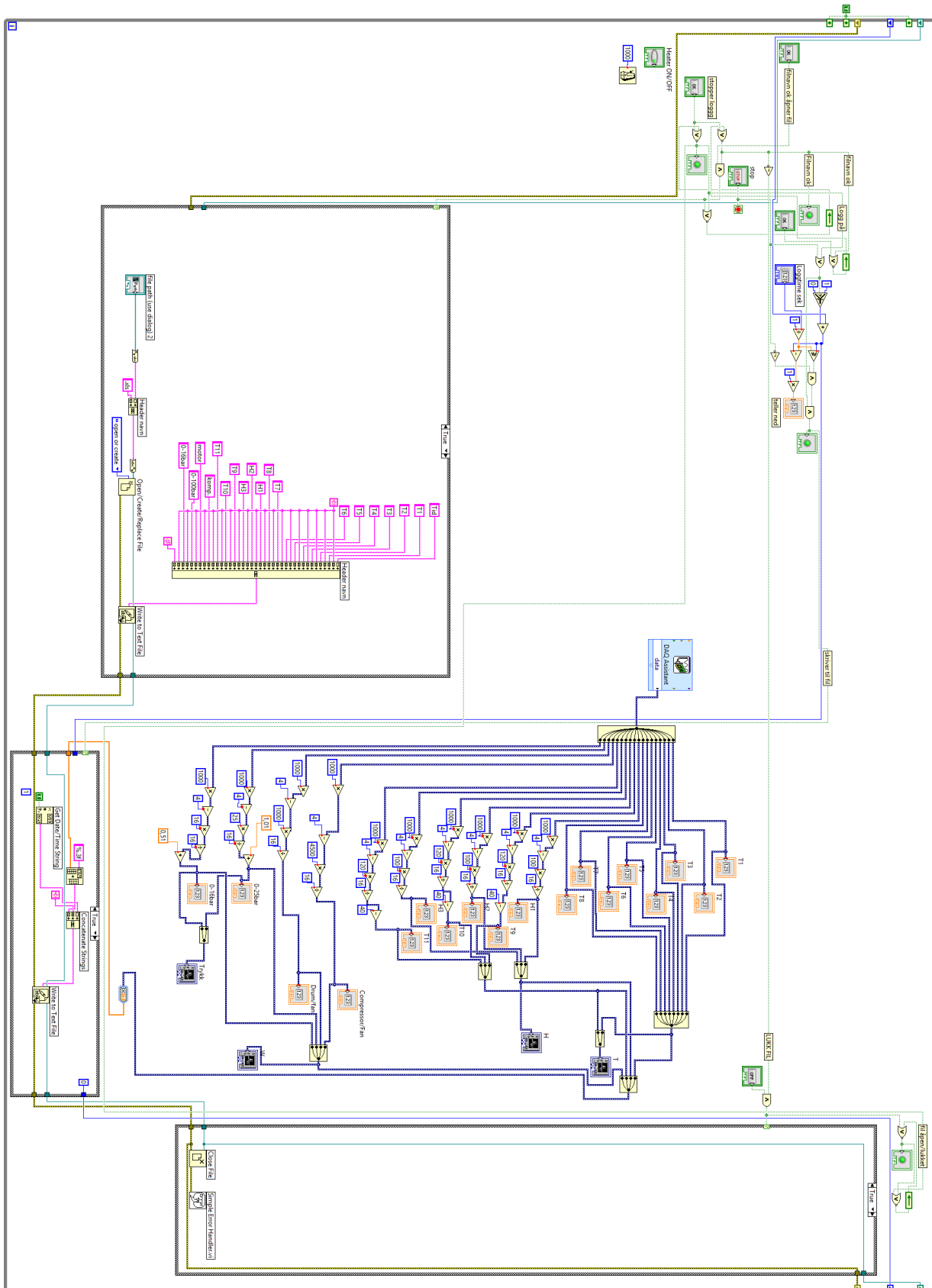


Figure 13 - Printout of the LabVIEW Block Diagram

As seen in Figure 14 the system is equipped with several thermistors and hygrometers. T1-T7 are thermistors attached to the pipes of the heat pump circuit. The thermistors are partially insulated against the ambient. T8 thermistor is not in use. It is “stored” in the cable tray, where it may serve as a reference of the ambient temperature close to the drum dryer. T9/H9, T10/H10 and T11/H11 are combined thermocouples and hygrometers. They are placed in the airstream of the dryer circuit as shown in the figure.

The sensors used for previous studies includes thermistors T1 – T6, and the combined thermocouples/hygrometers T9-T11/H9-H11. The placement of this sensors has been evaluated after processing initial experiments, and the physical placement of several sensors has been altered as the placement were not optimal for correct measurements. This includes sensor H9/T9, H10/T10 and T5. Thermistor T7 has been placed in the previous position of T5. The schematic placement of all sensors, except T7, remain the same. Pressure sensors P1 and P2 has been added to the system.

Ideally, an air flow meter would be placed in the airstream. Unfortunately, no laminar flow is found in the airstream of the drum dryer. I.e. airflow would have to be measured in turbulent flow, providing at best unreliable measurements.

The temperature and humidity in the airstream (T9/H9, T10/H10 and T11/H11) are measured using VAISALA Humidity and temperature transmitters with Remote Probes.

Pressure is measured using a Druck PTX 110/W pressure transmitter at low pressure (P1) and an Endress+Hauser Cerabar PMC731 digital pressure transmitter at high pressure (P2). Calibrated pressure range is respectively 0-16 bara and 0-40 bara.

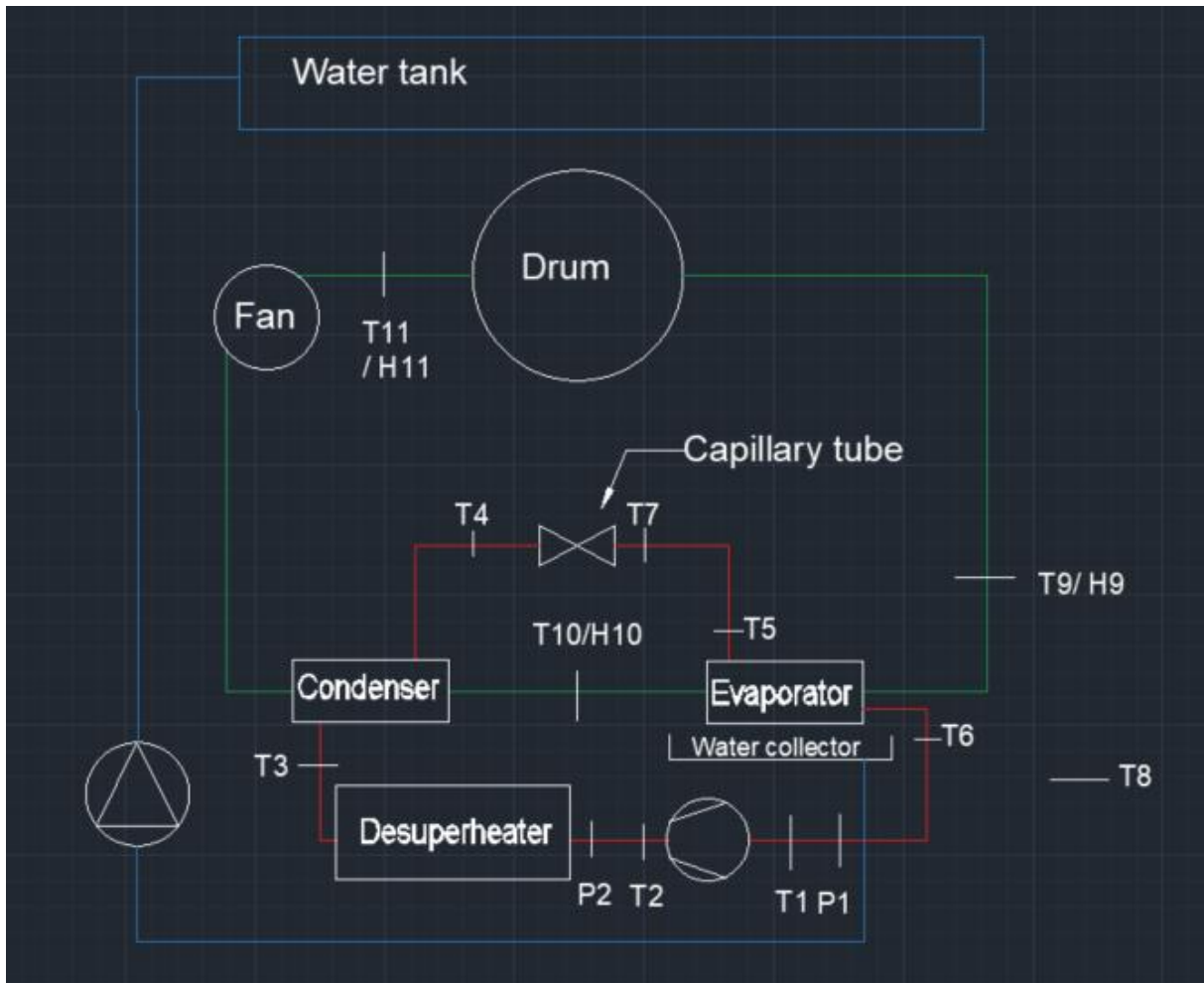


Figure 14 – Instrumentation

Figure 15 shows the physical position of sensors T1-T6, and T10/H10 before repositioning, while Figure 16 show the repositioned sensors including T7. The remaining sensors are placed in components that were dismantled to access the evaporator and condenser. The placement of T11/H11 were not altered and are seen in Figure 17. The dismantled cover with the sensor is mounted to mounts to the rear of the dryer, covering the exposed fan and drum inlet.

Figure 18 shows the final position of T9/H9 after repositioning. The arrow in the figure indicates the previous position. The actual previous position are hidden by the plastic, and may not be seen in the figure.

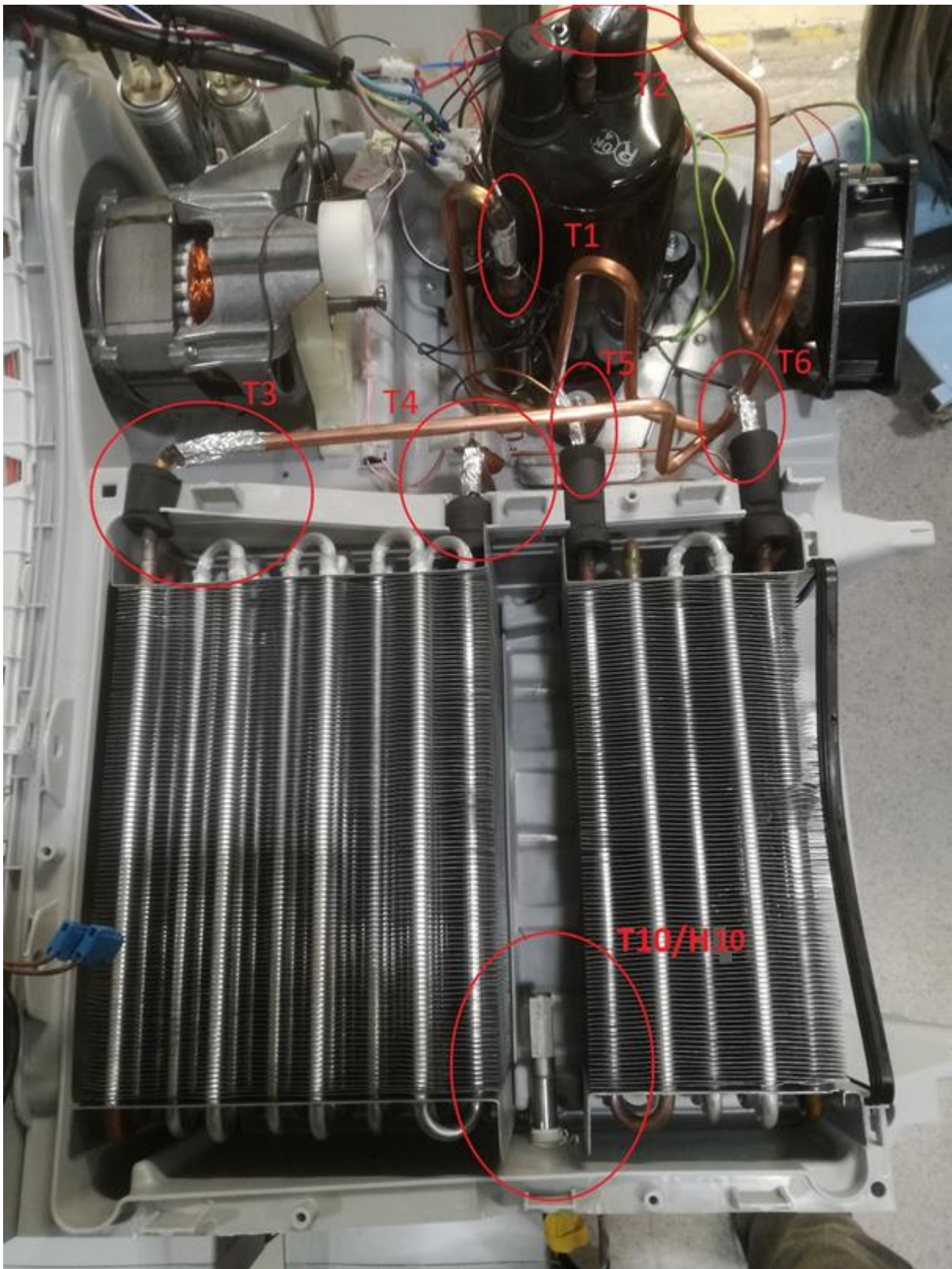


Figure 15 - Initial sensor placement

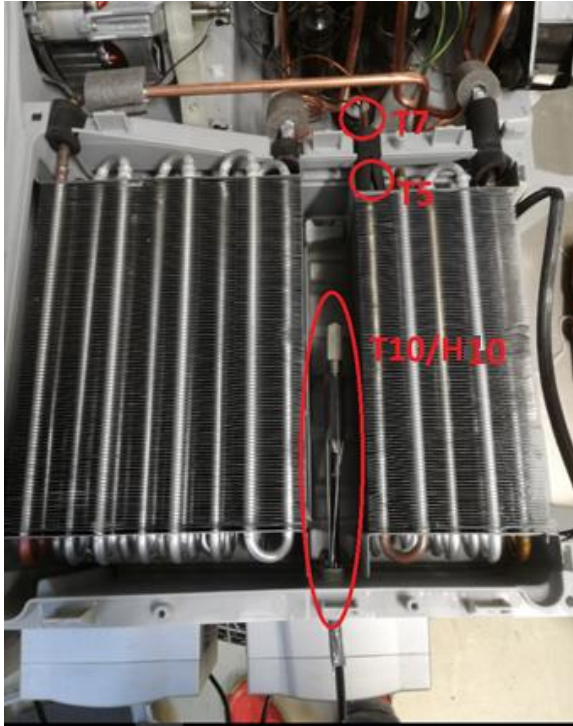


Figure 16 - Repositioning of T10/H10, T5 and T7



Figure 17 - T11/H11 position



Figure 18 - T9/H9 position

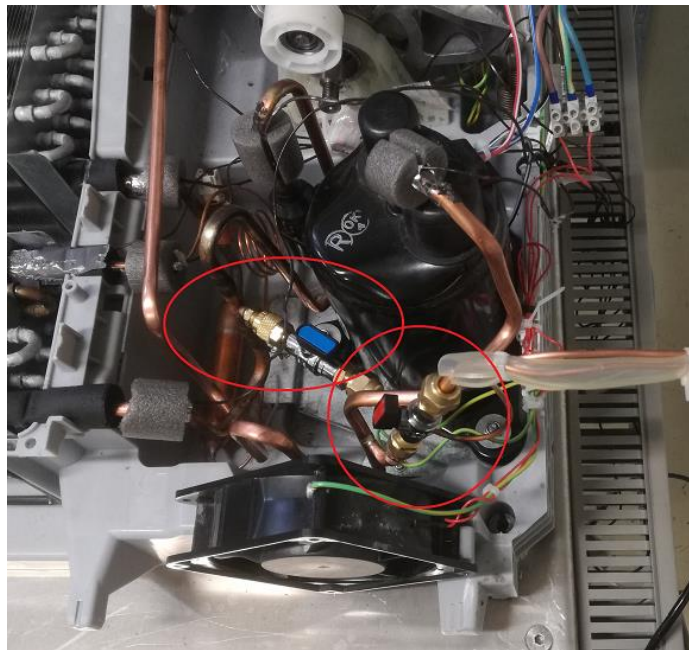


Figure 19 - Pressure transmitters connections before rebuild

The physical placement of the connections for the pressure transmitters P1 and P2 before the rebuild is shown in Figure 19. Figure 20 shows the placement of the mentioned sensors after the rebuild.

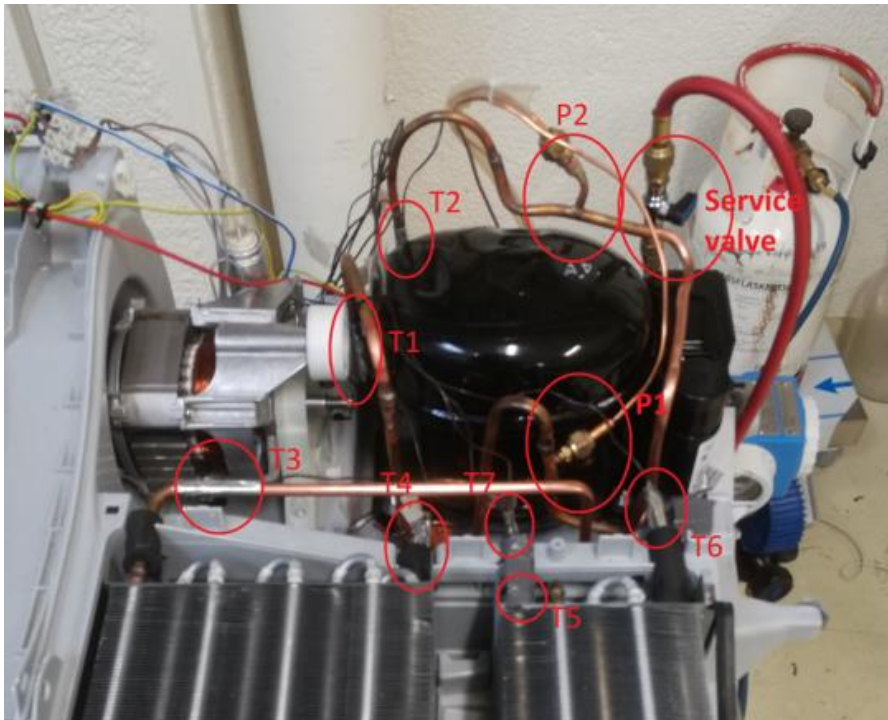


Figure 20 - Sensor positions and transmitter connections after rebuild

3.5.1 Calibration

Calibration of the humidity sensors are carried out according to the Vaisala HUMICAP® Humidity and Temperature Transmitter Series HMT330 user manual[50], using the Vaisala HMK15 Humidity Calibrator. The Push Buttons procedure were chosen, utilizing standardized LiCl and NaCl solutions. The procedure is thoroughly explained in the mentioned user's manual.

Pressure transmitters are calibrated using FLUKE 719 100G Pressure Calibrator.

3.6 Data processing

Data acquired during experiments are processed in order to calculate relevant parameters that can not be measured directly.

3.6.1 Calculation of absolute humidity and mixing ratio

Humidity in air is often measured by a hygrometer measuring the relative humidity, i.e. the portion of humidity in the air relative to the humidity of saturated air at the same temperature. Proper post processing and discussion of collected data requires computerized calculation of absolute humidity and mixing ratio from relative humidity measurements. The humidity conversion formulas in the following paragraphs are published by VAISALA, the producer of the hygrometers used in this thesis[51].

Relative humidity is defined by Equation 6, where RH is the relative humidity in percent, P_w is the water vapor pressure and P_{ws} is the water vapor saturation pressure.

$$6) \quad RH = \frac{P_w}{P_{ws}} \cdot 100\% \quad [\%]$$

Equation 6 may be rewritten to Equation 7, for calculation of P_w from P_{ws} and RH.

$$7) \quad P_w = P_{ws} \cdot \frac{RH}{100\%}$$

Within the limited temperature range that is relevant to this thesis, the water vapor saturation pressure (P_{ws}) may be calculated from Equation 8. A, G and T_n are constants found in Table 10, while t is the temperature in degrees Celsius.

$$8) \quad P_{ws} = A \cdot 10^{\left(\frac{G \cdot T}{T + T_n}\right)} \cdot 10^2 \quad [Pa]$$

Table 10 - Constants for Equation 8

	A	G	Tn	max error	Temperature range
Water	6.116441	7.591386	240.7263	0.083 %	-20...+50°C
	6.004918	7.337936	229.3975	0.017 %	+50...+100°C
ice	6.114742	9.778707	273.1466	0.052 %	-70...0°C

The mixing ratio, X, is calculated using Equation 9. P_{tot} is the total ambient pressure.

$B = 621.9907$ is a constant valid for air. For other gases B needs to be calculated based on molecular weight of water and the gas.

$$9) \quad X = B \cdot \frac{P_w}{P_{tot} - P_w} \quad [g \text{ water}/kg \text{ dry air}]$$

For the case of a drum dryer, the total pressure in the air cycle can be assumed to be equal to atmospheric pressure.

Absolute humidity, AH, is calculated using Equation 10, where C is a constant, and t is the temperature in kelvin. $C = 2.16679 \text{ gK/J}$

$$10) \quad AH = C \cdot \frac{P_w}{t} \quad [g/m^3]$$

For single step calculation of mixing ratio, Equation 7 and Equation 8 are inserted into Equation 9, resulting in Equation 11

$$11) \quad X = B \cdot \frac{A \cdot 10^{\left(\frac{G \cdot T}{T+T_n}\right)} \cdot 10^2 \cdot \frac{RH}{100\%}}{P_{tot} - A \cdot 10^{\left(\frac{G \cdot T}{T+T_n}\right)} \cdot 10^2 \cdot \frac{RH}{100\%}} \quad [g \text{ water}/kg \text{ dry air}]$$

For a similar calculation of absolute humidity, Equation 7 and Equation 8 are inserted into Equation 10, resulting in Equation 12.

$$12) \quad AH = C \cdot \frac{A \cdot 10^{\left(\frac{G \cdot T}{T+T_n}\right)} \cdot 10^2 \cdot \frac{RH}{100\%}}{t} \quad [g/m^3]$$

3.6.2 Other calculations

The heat that needs to be added to the drum to achieve evaporation of moisture corresponds to condenser heat flow (Q_c). Heat that needs to be added can be calculated from Equation 13 where h_{fg} is latent heat of evaporation, c_p specific heat, ΔT temperature rise in the drum and ER evaporation rate.

$$13) \quad Q_c = (h_{fg} + c_p \cdot \Delta T) \cdot \frac{ER}{3.6}$$

Log mean temperature difference (LMTD) may be calculated using Equation 14, where ΔT_A is the temperature difference between the stream of refrigerant and air at end A, and ΔT_B is the temperature difference between the two streams at end B. Due to the nature of boiling and condensation of multi-phase flow in tubes, condensation and evaporation temperature is used as input for refrigerant temperature regardless of overheating and subcooling[52].

$$14) \quad LMTD = \frac{\Delta T_A - \Delta T_B}{\ln\left(\frac{\Delta T_A}{\Delta T_B}\right)}$$

Figure 21 shows a flow chart of how the LMTD is calculated based on the data log from experiments. As seen, condensation and evaporation temperatures are derived from saturation tables for the applied refrigerant. Table input is condensation and evaporation pressure. Figure 21 shows a flow chart of how the LMTD is calculated based on the data log from experiments. As seen, condensation and evaporation temperatures are derived from saturation tables for the applied refrigerant. Table input is condensation and evaporation pressure.

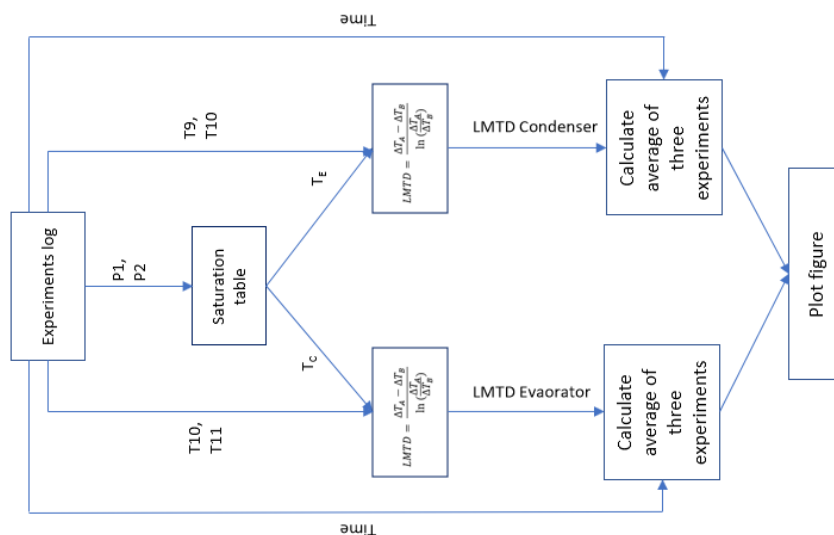


Figure 21 – Flow chart: LMTD calculation

The instantaneous Coefficient of performance (COP_H) for the heat pump may be calculated from measurements using Equation 15. COP_H annotates that COP relative to heating duty is used. Q_c is evaporator heat transfer rate, $P_{el, compressor}$ the electric power input to the compressor motor, $h_{2, real}$ the tabulated enthalpy at the compressor outlet, $h_{4, real}$ the tabulated enthalpy at the condenser outlet and $\dot{m}_{refrigerant}$ the mass-flow of refrigerant.

$$15) \quad COP_H = \frac{Q_e}{P_{el, compressor}} = \frac{h_{2, real} - h_{4, real}}{\frac{P_{el, compressor}}{\dot{m}_{refrigerant}}}$$

Total compressor efficiency is calculated using Equation 16. W_{is} is the amount of work necessary assuming isentropic compression, E_{el} is the real electric energy input to the compressor motor, $h_{2, isentropic}$ is the enthalpy after compression assuming isentropic compression, $h_{1, real}$ is the real enthalpy at the compressor inlet, $h_{2, adiabatic}$ is the enthalpy after compression assuming real adiabatic compression,

$$16) \quad \eta_{compressor} = \frac{W_{is}}{E_{el}} = \frac{h_{2, isentropic} - h_{1, real}}{h_{2, adiabatic} - h_{1, real}} = \frac{h_{2, isentropic} - h_{1, real}}{\frac{P_{el, compressor}}{\dot{m}_{refrigerant}}}$$

Calculating $h_{2, isentropic}$ is done using P-t and P-s tables for the applied refrigerant. The steps are shown in Figure 22.

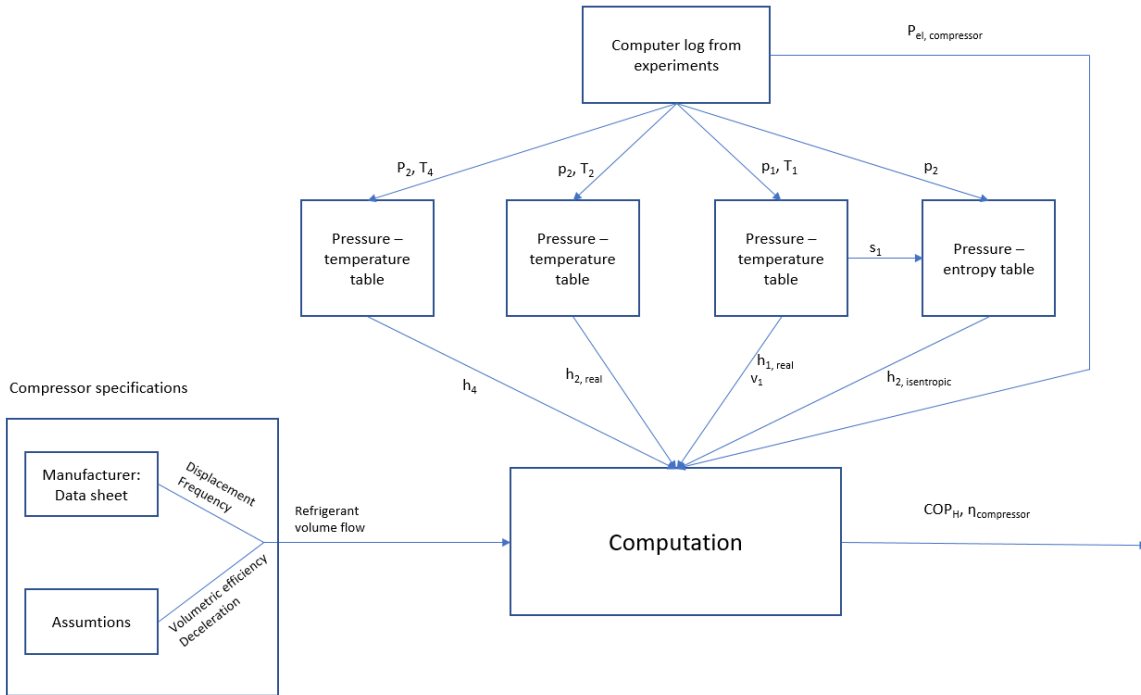


Figure 22 – Flow chart: COP_H and compressor efficiency calculation

Airflow is calculated using output from the hygrometers. Using Equation 12 absolute humidity is calculated, providing input for Equation 17. Equation 17 assumes that there is no leakage of air in or out of the system. AH_x is absolute humidity, where the number substituting the x refers to the applied hygrometer. $\Delta m_{water,weighed,fabric}$ is the change in the amount of water in the dried fabric measured by weighing.

$$17) \quad Airflow = \frac{\int_{t=0}^{exp\ end} (AH_9 - AH_{11}) dt}{\Delta m_{water,weighed,fabric}} = \frac{\int_{t=0}^{exp\ end} (AH_9 - AH_{11}) dt}{\Delta m_{water,weighed,fabric}} = \frac{\int_{t=0}^{exp\ end} (\Delta AH) dt}{\Delta m_{water,weighed,fabric}}$$

Knowing the airflow of the system, instantaneous specific moisture extraction rate may be calculated using Equation 18. $P_{el,motor}$ is electric power input to the drum and drum fan motor.

$$18) \quad SMER = \frac{\Delta AH \cdot Airflow}{P_{el,compressor} + P_{el,motor}}$$

Average SMER may be calculated based on intermediate and end-of-experiment weighing of the dried fabric. Equation 19 shows the calculation.

$$19) \quad SMER = \frac{\Delta m_{water,weighed,fabric}}{E_{el,compressor} + E_{el,motor}} = \frac{\int (\Delta AH \cdot Airflow) dt}{\int (P_{el,compressor} + P_{el,motor}) dt}$$

Moisture ratio based on intermediate and end of cycle weighing of the dried fabric may be calculated using Equation 20.

$$20) \quad MR = \frac{\omega_t - \omega_{end}}{\omega_0 - \omega_{end}}$$

ω is calculated using Equation 21, where m_{water} is the mass of water and $m_{dry fabric}$ is the mass of dry fabric.

$$21) \quad \omega = \frac{m_{water}}{m_{dry fabric}}$$

4 Experiments

A series of experiments has been performed during the fall of 2017 and the spring of 2018. The results are presented in this chapter, along with evaluation of the presented results. To avoid confusing, the terms DC-COP and DC-SMER is introduced. The terms refers to the average COP and SMER throughout one drying cycle according to setup 1 defined in Section 3.3. Superior values of DC-COP and DC-SMER will define the best performing refrigerant at this duty. Average COP and average SMER is used regarding the average values of repetitive experiments.

4.1 Overview

Table 11 shows an overview of valid experiments providing the data for the evaluation of the system.

A large quantity of experiments has been performed to investigate system behavior and to check for errors, leaks and instabilities. The results of these experiments are not satisfactory accurate and reliable to be included as data for this thesis, and are not mentioned in the table. A complete list of experiments is found in Appendix B.

COP calculation relies on data from the pressure transmitters, hence COP is not calculated for experiments performed prior the pressure transmitter installation. SMER listed in the table is calculated from the weight of the fabric before and after drying, and the measured power consumption. Experiments according to setup 2 is performed with intermediate weighing of the fabric. SMER in these experiments are influence by the repetitive shutdown and startups and are not therefor not listed in Table 11. In reference to the table, the “Original” capillary tube is 78.5cm with an internal diameter of 1.00mm. Note that the table lists the experiments chronologically based on when they are performed. Repetitive experiments on the same charge level is therefore not necessarily listed in subsequent order.

Table 11 - Valid experiments

Nr.	System	Charge	Capillary tube	Setup	SMER	COP	Comments	No pressure sensors
1	R134a	220g	Original	Setup 1	1.68	-		
2	R134a	220g	Original	Setup 2	1.92	-		
3	R134a	220g	Original	Setup 2	-	-	Intermediate weighing	
4	R134a	220g	Original	Setup 2	-	-	Intermediate weighing	
5	R134a	220g	Original	Setup 3	-	-	Intermediate weighing	
6	R134a	220g	Original	Setup 4	2.09	-		
7	R134a	220g	Original	Setup 1	1.70	3.85		
8	R134a	220g	Original	Setup 1	1.69	3.88		
9	R134a	220g	Original	Setup 1	1.69	3.66		
REBUILT SYSTEM BELOW THIS LINE								
10	R290	100g	Original	Setup 1	1.65	3.80		
11	R290	115g	Original	Setup 1	1.73	4.19		
12	R290	115g	Original	Setup 1	1.67	3.72		
13	R290	115g	Original	Setup 1	1.73	4.00		
14	R290	115g	Original	Setup 2	-	-	Intermediate weighing	
15	R290	115g	Original	Setup 2	-	-	Intermediate weighing	
16	R290	115g	Original	Setup 2	-	-	Intermediate weighing	
17	R290	115g	Original	Setup 4	2.13	4.28		
18	R290	115g	Original	Setup 3	1.22	3.95		
19	R290	125g	Original	Setup 1	1.74	4.18		
20	R290	135g	Original	Setup 1	1.71	3.93		
21	R290	135g	Original	Setup 1	1.67	3.82		
22	R290	135g	Original	Setup 1	1.69	4.01		
23	R290	125g	Original	Setup 1	1.62	3.96		
24	R290	125g	Original	Setup 1	1.64	3.82		
25	R290	125g	Original	Setup 1	1.68	3.87		
26	R290	125g	Original	Setup 1	1.69	3.89		
27	R290	125g	Original	Setup 1	1.72	3.85		
28	R290	100g	Original	Setup 1	1.72	3.97		
29	R290	100g	Original	Setup 1	1.67	3.86		
REPLACED CAPILLARY TUBE BELOW THIS LINE								
30	R290	115g	D = 1.00mm L = 42.0cm	Setup 1	1.60	3.74	Inadequate capillary tube length	
31	R290	115g	D = 1.00mm L = 120.0cm	Setup 1	1.68	3.87		
32	R290	135g	D = 1.00mm L = 120.0cm	Setup 1	1.68	4.03		
33	R290	150g	D = 1.00mm L = 120.0cm	Setup 1	1.72	4.09		
34	R290	150g	D = 1.00mm L = 120.0cm	Setup 1	1.68	3.99		
35	R290	150g	D = 1.00mm L = 120.0cm	Setup 1	1.80	4.00		
36	R290	150g	D = 1.00mm L = 120.0cm	Setup 1	1.71	3.91		
37	R290	150g	D = 1.00mm L = 120.0cm	Setup 1	1.69	3.92		

4.2 Results and discussion

An extensive compilation of plots from valid experiments are found in Appendix D-D. Complete experiments logs are not suited for representation in .pdf or analog format. They are therefore found as digital excel files in Appendix D-A.

The main results are presented in this section. If nothing else is stated for the specific figure, the figure is based on experiments performed on R134a system with unaltered factory charge of refrigerant stated to be 220g, and R290 system with the original capillary tube charged with 115g refrigerant.

Since drying beyond 3-5% residual moisture in the fabric is found to significantly affect results, the 80 minutes drying cycle is applied for the majority of the experiments. At very low residual moisture relatively small deviations in initial moisture content and ambient conditions introduce large deviations in system behavior. Within the 80 minutes system behavior is found to be comparable.

4.2.1 Drying process

A curve of the drying process is plotted at every 10th minute of drying in Figure 23 and Figure 24. The plot is the average of three identical experiments for each refrigerant. The plotted values are instantaneous thermocouples/hygrometer values. Figure 23 shows R134a while Figure 24 shows R290. As seen higher mixing ratio is obtained using R134a than R290, as a result of elevated drying temperatures. The plotted points on the curve are the same as expressed in Figure 10.

The relative humidity observed at the drum outlet decreases as the fabric dries. Obtaining close to saturation of the air at the drum outlet throughout the drying cycle would require the air to have increased retention time in the drum, and possibly enhanced guidance of the air through the fabric. This would increase drying time and complicate drum design. The increase in moisture ratio during heating of the air suggests that some air bypasses the heat pump unit, or is exchanged to the ambient through air leaks. As the T10/H10 sensor is centered in the airstream shortly after the evaporator, it does not measure parameters of the air bypassing the

evaporator. The T11 sensor is positioned further away from the condenser, allowing air that has bypassed the evaporator and/or the condenser to mix with dried air. From a practical design point of view, a certain degree of heat pump bypass as well as air-leaks is expected.

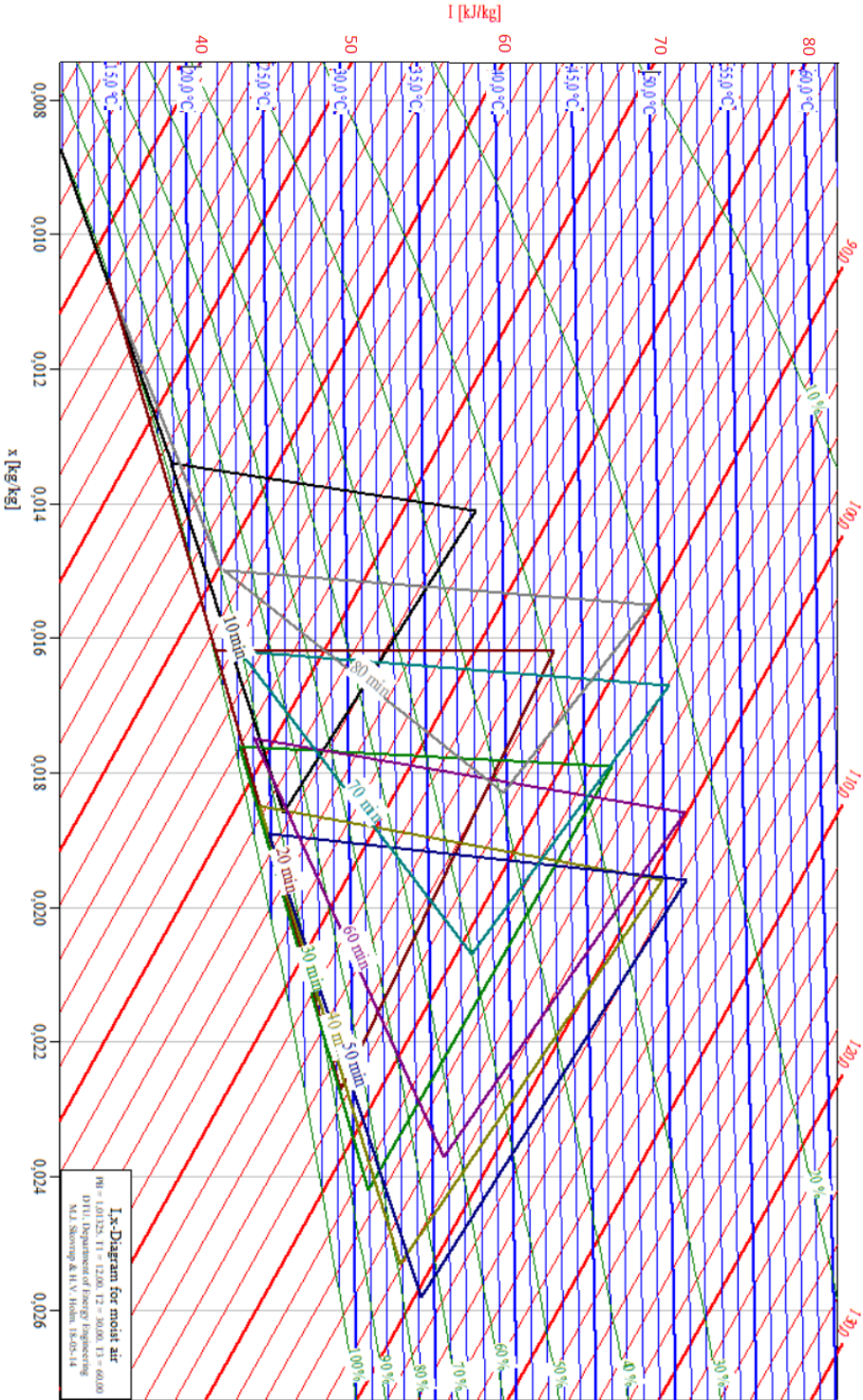


Figure 23 - IX Diagram with plots for drying with R134a at 220g charge

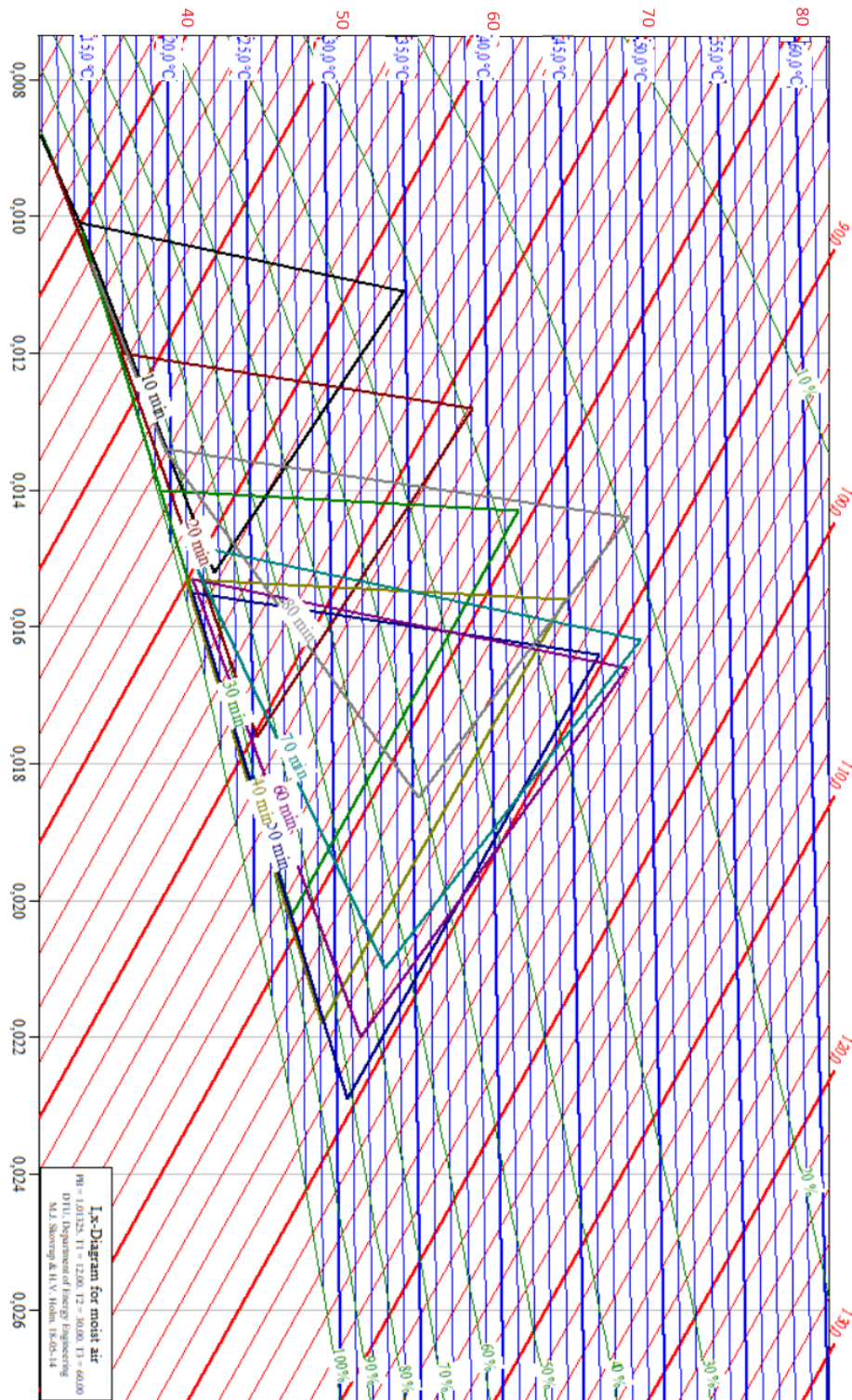


Figure 24 - IX diagram with plots for drying with R290 at 115g charge

The moisture ratio of the drying fabric is plotted in Figure 25. The moisture ratio is calculated based on initial weighing and hygrometer readings throughout the experiments. The plotted value is the average of three identical experiments on each refrigerant.

Regression analysis of the data shows that the inflection point of the R134a curve is at 39.0 minutes while the inflection point of the R290 curve is at 44.6 minutes. The inflection point indicates the time where the fastest decline in moisture ratio is observed., i.e. the highest moisture extraction rate. The difference appears to be due to the more rapid temperature increase in the R134a system observed and discussed in section 4.2.2, causing the moisture extraction rate to peak earlier than for the R290 system. The peak and development in moisture extraction rate is observed in Figure 39 on page 70.

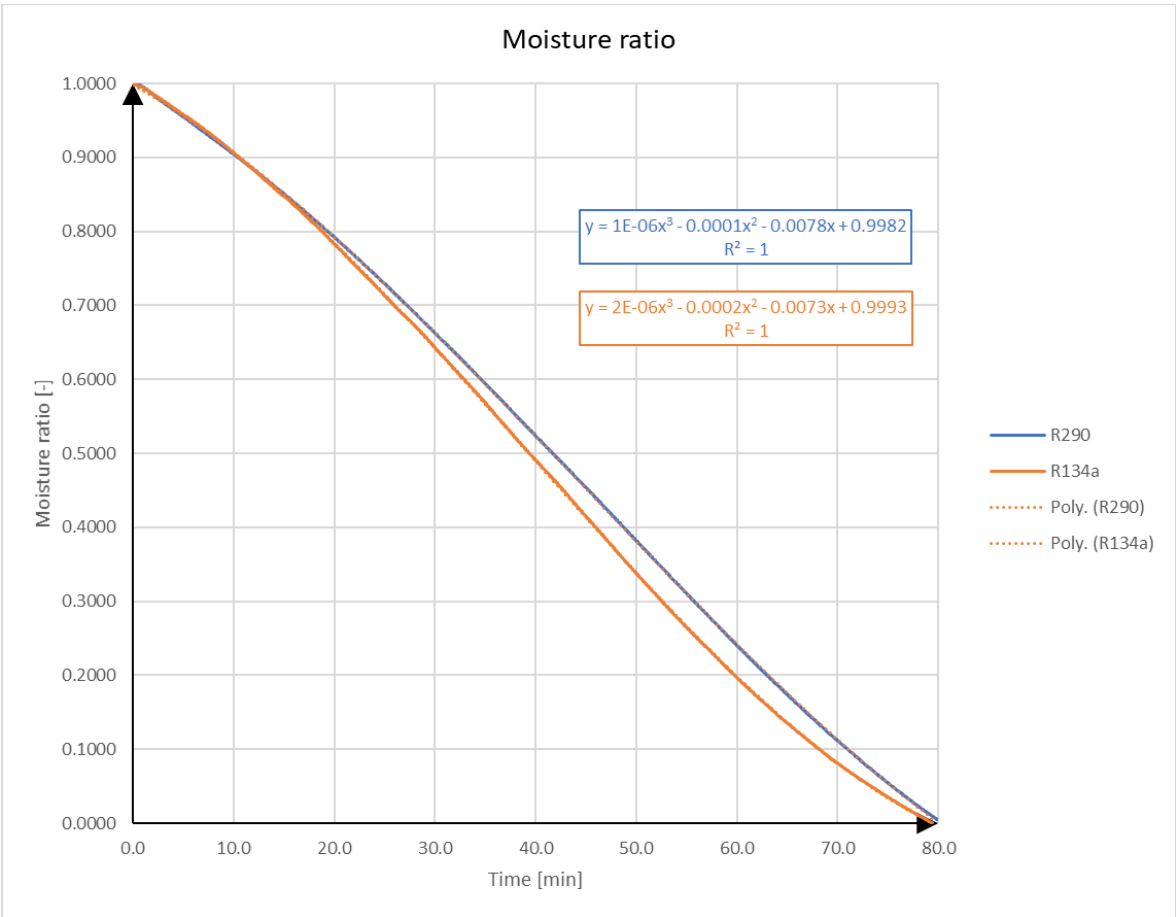


Figure 25 – Moisture ratio at 220g R134a and 115g R290 charge

4.2.2 Heat exchange and temperature development

Figure 26 shows the development of the Log mean temperature difference of the evaporator and condenser when charged with R134a and R290. The plot displays the average of three identical 80 minutes experiments on each refrigerant. Condensation and evaporation temperature are calculated from measured condensation and evaporation pressure, while the measured temperatures of the airstream are applied directly to the LMTD formula. This implies that the condensation and evaporation temperature is assumed to be constant at saturation temperature. The LMTD equation does not allow for applying subcooling and overheating to the formula. This is drawback of applying LMTD to heat exchangers where condensation and evaporation takes place in combination with subcooling and/or overheating. Pressure loss across the heat exchangers effects the saturation temperature, which declines as the pressure drops. No approximations are made for the pressure loss while calculating the LMTD. Pressure loss in the heat exchangers are calculated and discussed in relation to Figure 33 on page 62. The LMTD are calculated for each instance of data saved to the log file, approximately for every third second throughout the experiment. The plot shows that the LMTD of both the evaporator and condenser decreased slightly when charged with R290 compared to R134a, indicating slightly superior heat transfer characteristics of R290.

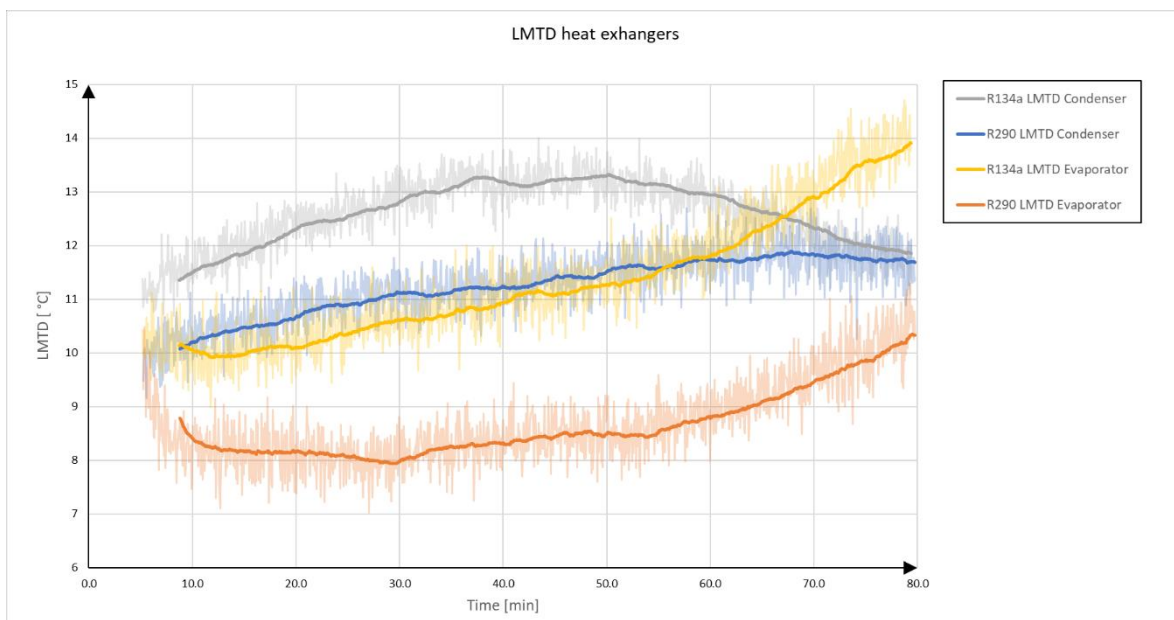


Figure 26 - LMTD heat exchangers at 220g R134a and 115g R290 charge

Towards the end of the drying cycle the Evaporator LMTD increases significantly, while the R134a Condenser LMTD decreases. R290 Condenser LMTD appears to decrease slightly. The increase in evaporator LMTD is a result of the decrease in moisture ratio of the air coming from the drum, seen in Figure 27 and Figure 28. Moist air features improved heat transfer characteristics compared to dry air, providing lower LMTD while the air is moist. Figure 27 and Figure 28 shows the average relative humidity and temperature of the air cycle measured by the combined hygrometer and temperature sensors. The higher condensation and evaporation temperatures of R134a as well as the more rapid increase in temperature provides increased temperature of the air entering the drum.

The condenser LMTD is linked to the amount of subcooling at the condenser outlet, seen in Figure 32 on page 61. LMTD assumes constant condensation temperature equal to saturation temperature at the condenser inlet. Increased subcooling implies that a larger part of the condenser contains refrigerant at temperatures below condensation temperature. This requires the smaller part of the condenser filled with refrigerant at condensation temperature to transfer more heat through a smaller surface area, demanding increased temperature difference. Due to the decrease in subcooling at the R134a condenser outlet towards the end of the drying cycle, a decrease in the LMTD is observed.

The original condenser and evaporator designed for R134a is used with both refrigerants. The decrease in LMTD while charged with R290 suggests that the refrigerant side (tubing) of the heat exchangers may be reduced when designing a drum dryer for R290. Reduction in the tube length of the tube and fin heat exchangers causes reduction in refrigerant pressure loss across the heat exchangers. Reduced pressure loss is desirable due to the reduction in compressor work needed, though an increase in the LMTD increases the necessary pressure ratio provided by the compressor, thereby increasing necessary compressor work. Investigation of the optimum point when designing the heat exchangers is not a prioritized part of this study, although a potential for energy saving is noted and a potential for reduced investments costs.

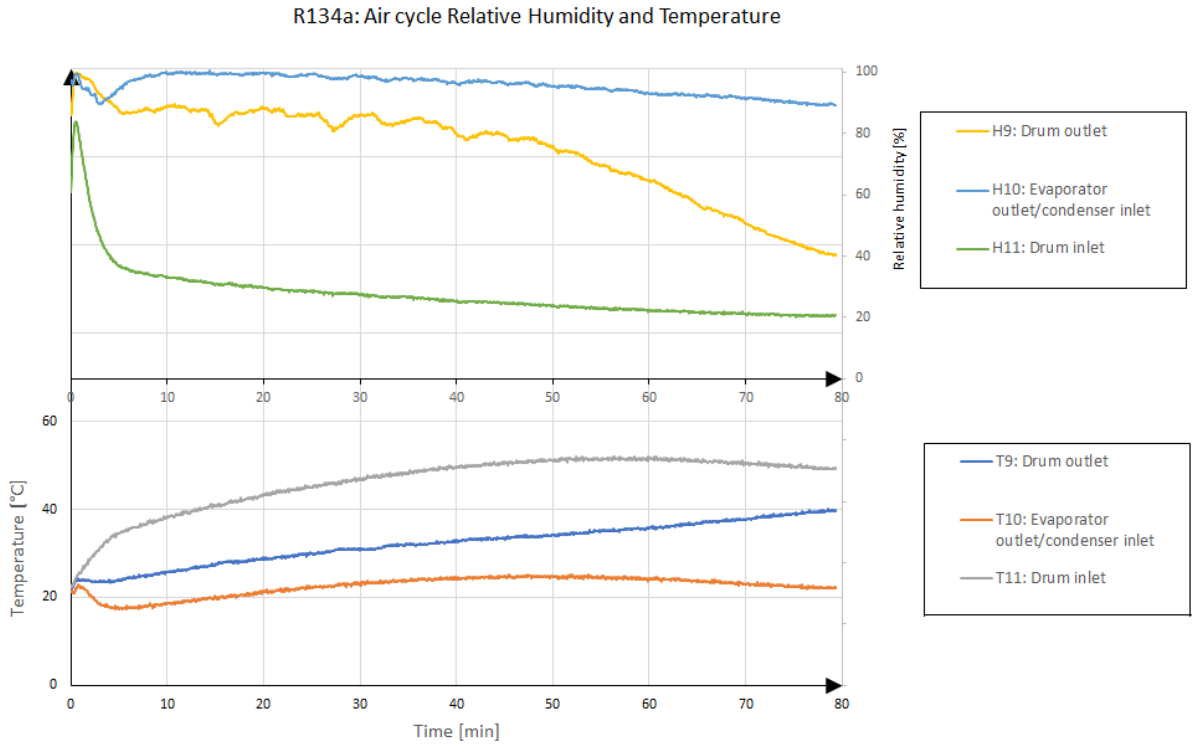


Figure 27 - R134a Air cycle Relative Humidity and Temperature at 220g charge

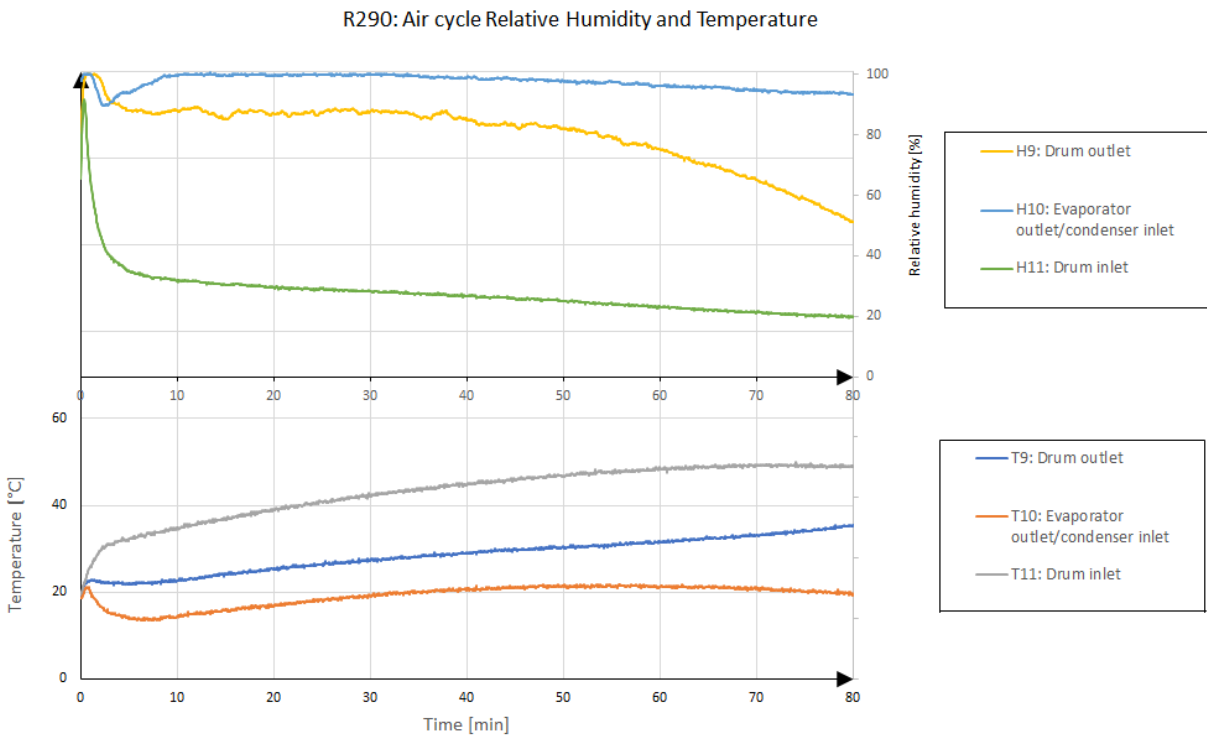


Figure 28 - R290 Air cycle Relative Humidity and Temperature at 115g charge

Figure 29 shows the condensation and evaporation temperature calculated from measured condensation and evaporation pressure. The temperatures are calculated for each instance of data saved to the log file, approximately for every third second throughout the experiment. It shows a slight decrease in condensation temperature when charged with R290 compared to R134a. The plot displays the average of the same three identical 80 minutes experiments as in Figure 26. As the figure is based on pressure measurements close to the condenser inlet and evaporator outlet, it expresses the maximum condensation temperature and minimum evaporation temperature. Temperature glide throughout condensation and evaporation is inevitable due to the cohesion of saturation pressure and temperature. As seen by Figure 32 on page 61 the subcooling at the condenser outlet declines towards the end of the drying cycle, causing less heat exchange to be performed at temperatures below saturation temperature.

The decline in evaporation temperature towards the end of the drying cycle observed in Figure 29 is the sum of the effect of increased LMTD and increased air temperature difference demand across the evaporator.

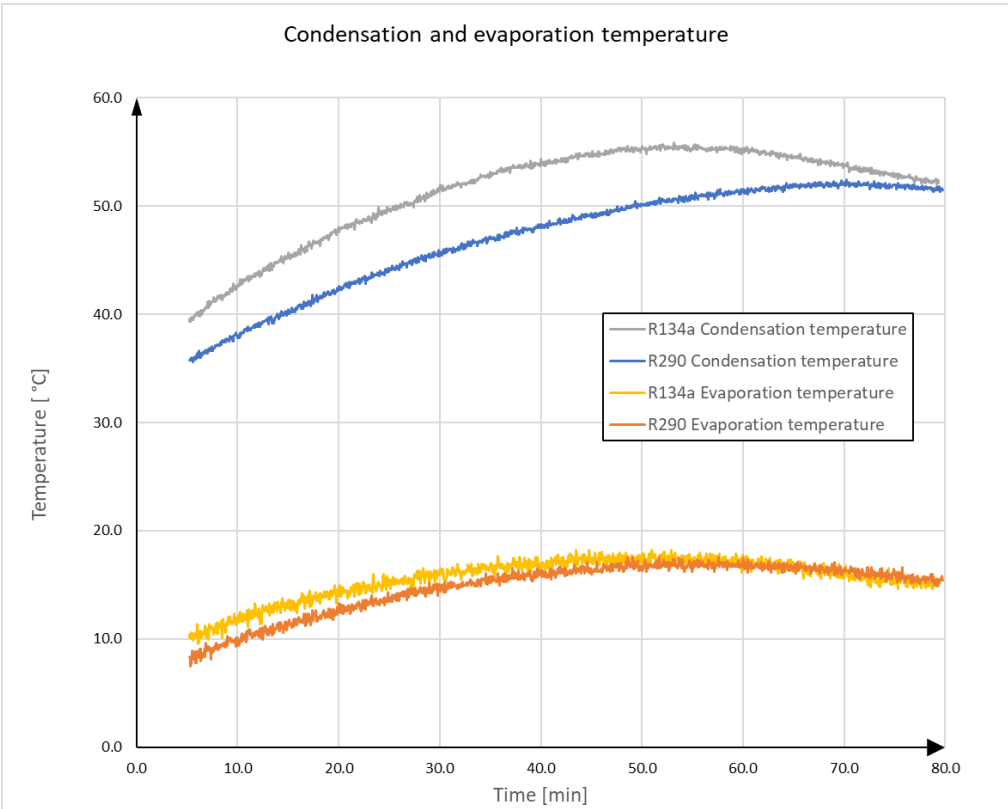


Figure 29 - Condensation and evaporation temperature at 220g R134a and 115g R290 charge

Maximum evaporation temperature is observed at the end of CRDP, indicating that the condensation temperature increases as long as the humidity of the drum exhaust is close to its maximum, providing the best heat transfer coefficients and availability of energy. As the humidity of the drum exhaust air declines when entering FRDP, increased LMTD is demanded as seen in Figure 26.

At maximum humidity, maximum energy is available at a given temperature. When moisture ratio declines less energy is available in the air, demanding increased cooling of the airstream through the evaporator to maintain the heat flow. This is supported by the observation of decreased air temperature out of the evaporator, as well as increased temperature going into the evaporator. The increase in temperature difference is seen in Figure 27 and Figure 28. This demands the evaporation temperature to decline.

Condensation temperature is linked to the evaporation temperature by the compressor pressure ratio and characteristics of the refrigerant. As it is also affected by the temperature of air coming from the evaporator, in terms of cooling load applied, the final condenser pressure is determined by the evaporation temperature and cooling load. As condensation temperature and cooling load declines simultaneously, the evaporation temperature declines slightly less than evaporation temperature for the R290 condensation. The excess decrease in R134a condensation temperature is discussed earlier in reference to the LMTD calculation and subcooling of the refrigerant.

Figure 30 shows the temperature development in the heat pump cycle throughout the drying cycle while charged with R134a. Figure 31 shows the same development while charged with 115g R290. The plotted temperatures are the average of thermistor readings recorded from three experiments on each refrigerant. The placement of the sensors is shown in the system schematic in Figure 14.

All experiments show a decline in overall system temperatures when entering FRDP. This is seen in, Figure 30 and Figure 31, as well as Figure 29, Figure 27 and Figure 28. The relative development between the temperatures of the heat pump circuit and air circuit is discussed

earlier. The lack of accumulation of heat in the system throughout the cycle is not discussed. In a adiabatic system the energy added by the compressor would remain in the system, causing temperature to increase as long as energy is added to the system. Heat accumulation is observed throughout CRDP, but a reduction in accumulated heat is observed through FRDP. Note that it is stated in section 3.3 that the compressor cooling fan is unplugged throughout the experiments.

The reduction in accumulated heat is assumed to be caused by the large heat loss to the ambient from the drum dryer. The amount of heat loss from the systems components with temperatures above ambient is much larger than the heat gain from components with temperatures below ambient. The components with temperatures somewhat below ambient is limited to the evaporator, tubing between the evaporator and the compressor and the short bit of airstream between the evaporator and condenser. The compressor, desuperheater tubes and capillary tube, as well as the drum and most of the air ducts are significantly above ambient temperature. As the main heat loss appears to take place between the drum fan and drum outlet, the overall system temperatures are allowed to be dictated by the evaporation temperature

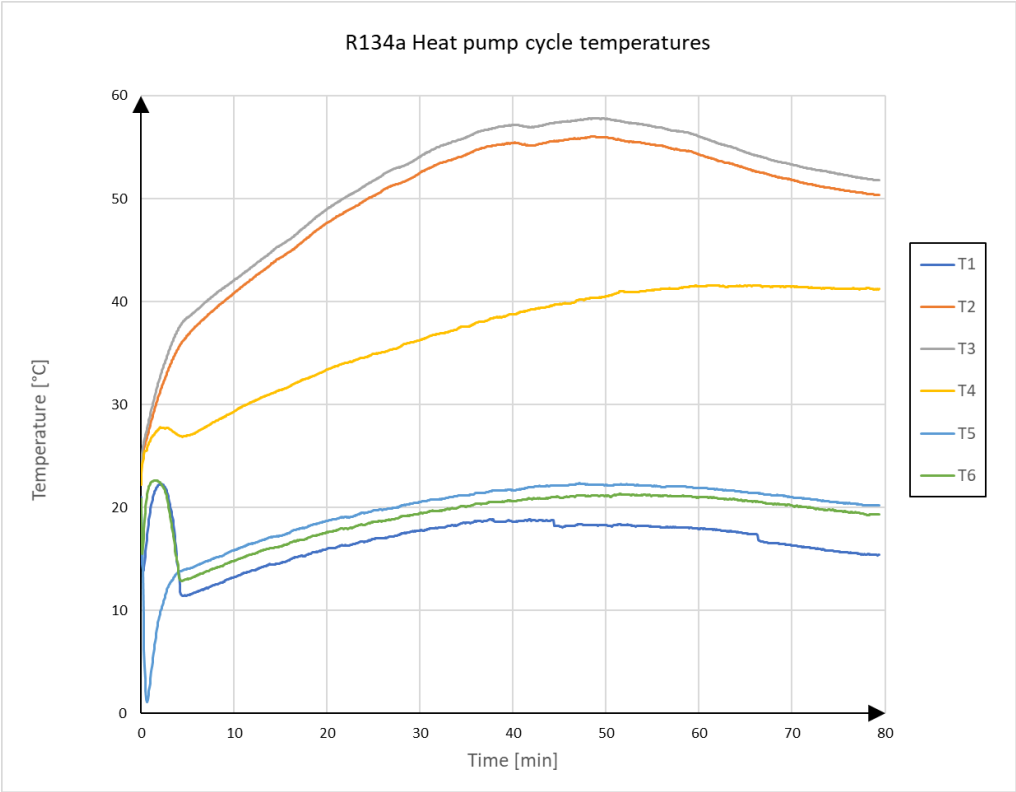


Figure 30 - R134a heat pump cycle average thermistor temperatures at 220g charge

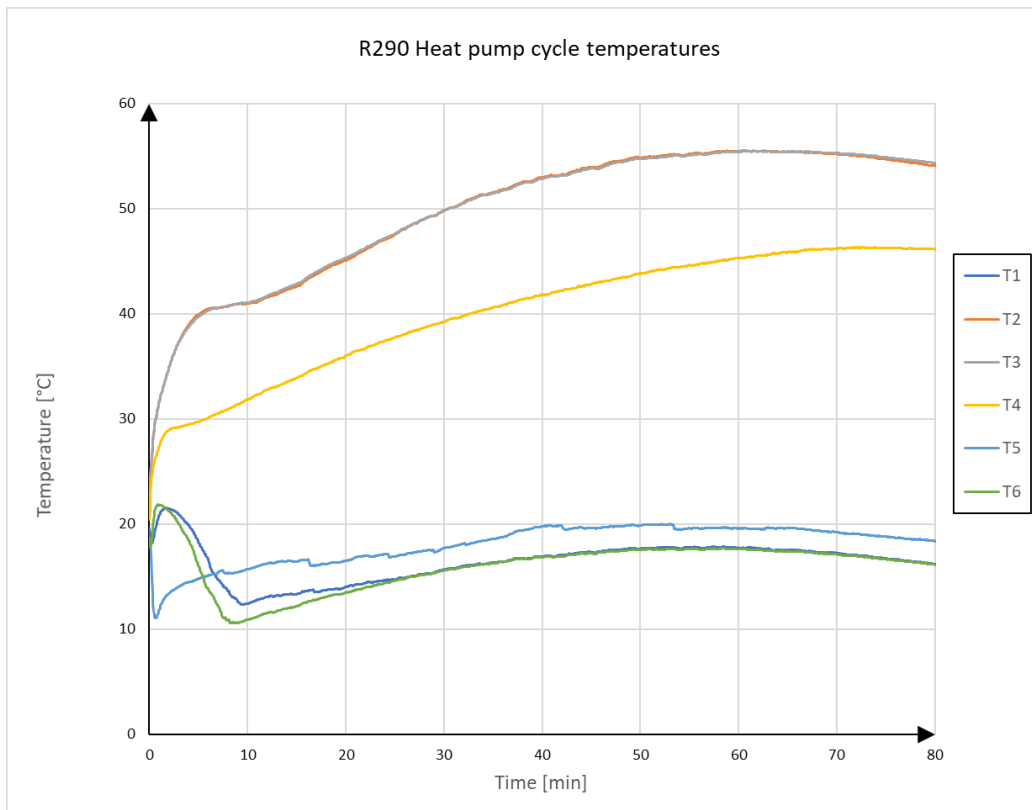


Figure 31 - R290 Heat pump cycle average thermistor temperatures at 115g charge

The difference between the condensation and evaporation temperature seen in Figure 29 and respectively the T4 and T6 temperatures seen in Figure 30 and Figure 31 indicates the subcooling and superheat at the condenser and evaporator outlet. While excessive subcooling in the counter flow heat exchangers is unproblematic, excessive superheat at the evaporator outlet is highly undesirable due to COP reduction and increased compressor outlet temperatures. Although excessive subcooling leads to more compressor work, the negative effects of excessive overheating have larger impact on system performance. The subcooling at the condenser outlet and overheating at the compressor inlet is plotted in Figure 32. The plotted values are calculated from pressure transmitters and thermocouple readings as described in section 3.6.2, neglecting pressure losses.

The high-pressure side pressure measurement is performed between the compressor outlet and condenser inlet. As the condensation temperature is calculated based on the condensation pressure being constant at P2 pressure, the calculation of subcooling at the condenser outlet is

assumed to overpredict real subcooling. Maintaining overheating at the compressors cylinder inlet valve is imperial to avoid destroying the compressor. Hermetic suction gas cooled compressors are used in the drum dryer, providing additional overheating between the compressor and cylinder inlet. This allows for operation at low overheating at the compressor inlet.

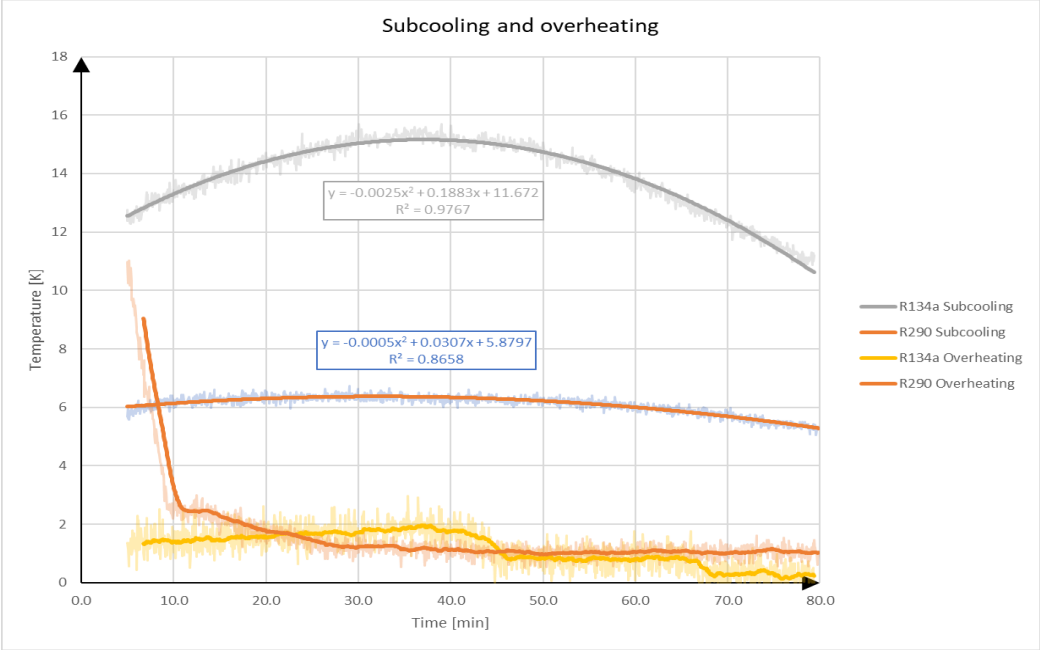


Figure 32 - Subcooling at the condenser outlet and overheating at the evaporator outlet at 220g R134a and 115g R290 charge Charge adjustment in order to obtain ideal superheating at the evaporator outlet and compressor inlet after rebuilding is discussed in section 3.4 as well as in section 4.2.6. The development of subcooling and overheating, as well as heat transfer and saturation temperatures are discussed earlier in this chapter.

Observation that evaporator inlet temperature (T5) is higher than the evaporator outlet temperature (T6) indicates significant pressure loss in the evaporator. Assuming no pressure loss, the evaporator outlet temperature should be higher than the inlet temperature due to refrigerant temperature glide and overheating at the outlet. As discussed earlier, the pressure loss is dependent on the size of the evaporator.

Neglecting pressure loss between the evaporator outlet and the P1 pressure transmitter fitting, as well as refrigerant temperature glide, pressure loss is calculated based on evaporator inlet

temperature (T5) and evaporator outlet pressure (P1). At the evaporator inlet the refrigerant exists as multiphase flow at saturation temperature, allowing for extraction of inlet pressure from saturation tables. The plotted value is the difference between the saturation pressure at T5 temperature and the pressure measured by the P1 transmitter. Significant pressure loss is calculated across the evaporator.

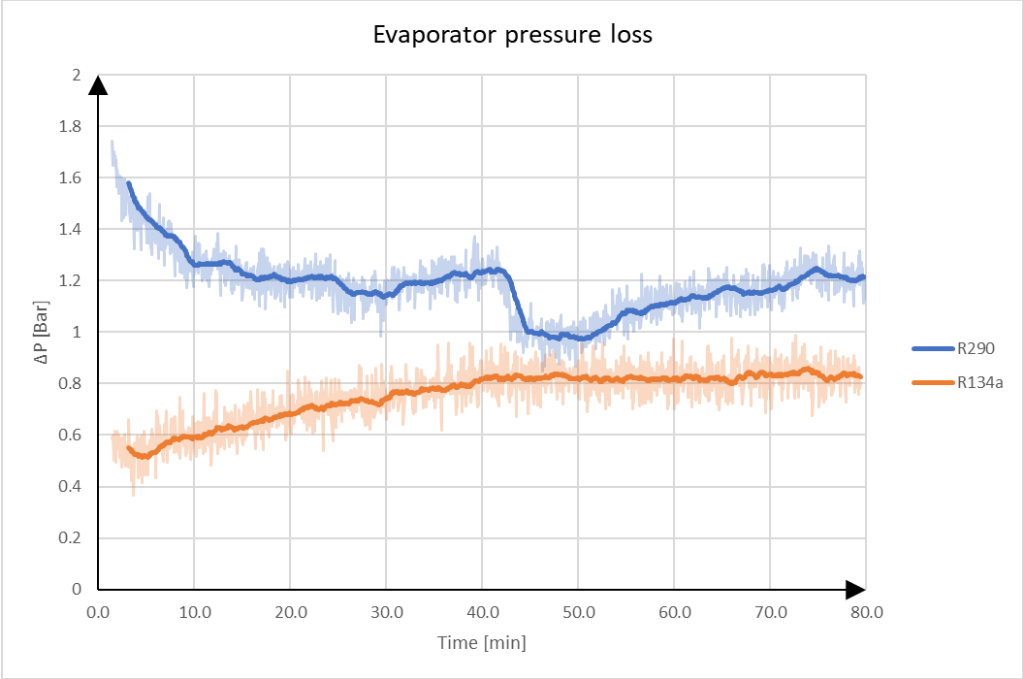


Figure 33 - Evaporator pressure loss at 220g R134a and 115g R290 charge

More volatile behavior is observed for the pressure loss in the R290 evaporator than the R134a evaporator. No obvious reason for this behavior is observed. Statistical analysis suggests that the volatile behavior displayed may be caused by large deviation in measurements between the experiments. Statistically difference between the R290 and R134a pressure loss is not found at any point of time due to the large variation.

The condenser is larger than the evaporator, indicating that the pressure loss across the condenser is larger than across the evaporator. Due to subcooling at the condenser outlet, pressure loss calculation analog to the calculation performed for the evaporator may not be done.

4.2.3 System performance

Figure 34 shows the average COP of three identical experiments on each refrigerant plotted over the total length of the experiment. The calculated average COP of R290 is slightly higher than the COP of R134a. The decline in COP is caused by the increased demand for work to be done to maintain drying rates while the fabric dries. Though compressor efficiency is maintained or increased, the increases pressure ratio demanded requires more energy to be added to the compressor.

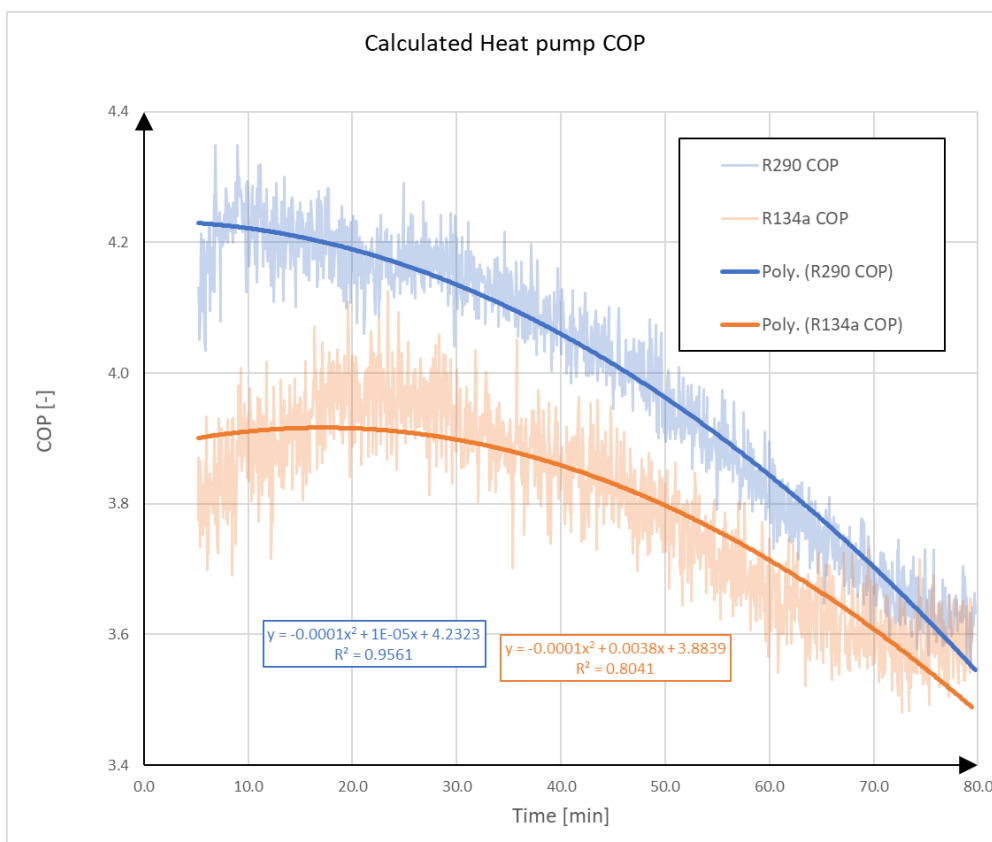


Figure 34 – Calculated Heat Pump COP at 220g R134a and 115g R290 charge

As well as the properties of the heat pump components and refrigerant, the COP is dependent on the initial state of the system, ambient temperature and humidity and moisture content in the dried fabric. The mentioned variables are kept as close to constant as allowable by the facilities of the laboratory.

Over the time of the experiment, the development of the COP is mainly dependent on suction pressure, suction temperature and the pressure ratio. After steady operation is obtained, the development of pressure and temperature is linked to the moisture content of the dried fabric. As discussed earlier increased LMTD of the evaporator and condenser reduces the COP.

Figure 35, Figure 36 and Figure 37 shows calculated compressor efficiency. Figure 35 and Figure 36 show data points calculated from measurements approximately every third second of three identical experiments on each refrigerant, as a function of suction pressure and pressure ratio. Data points from all three experiments are included. The first five minutes of each experiment is excluded, due to the unsteady system behavior at startup.

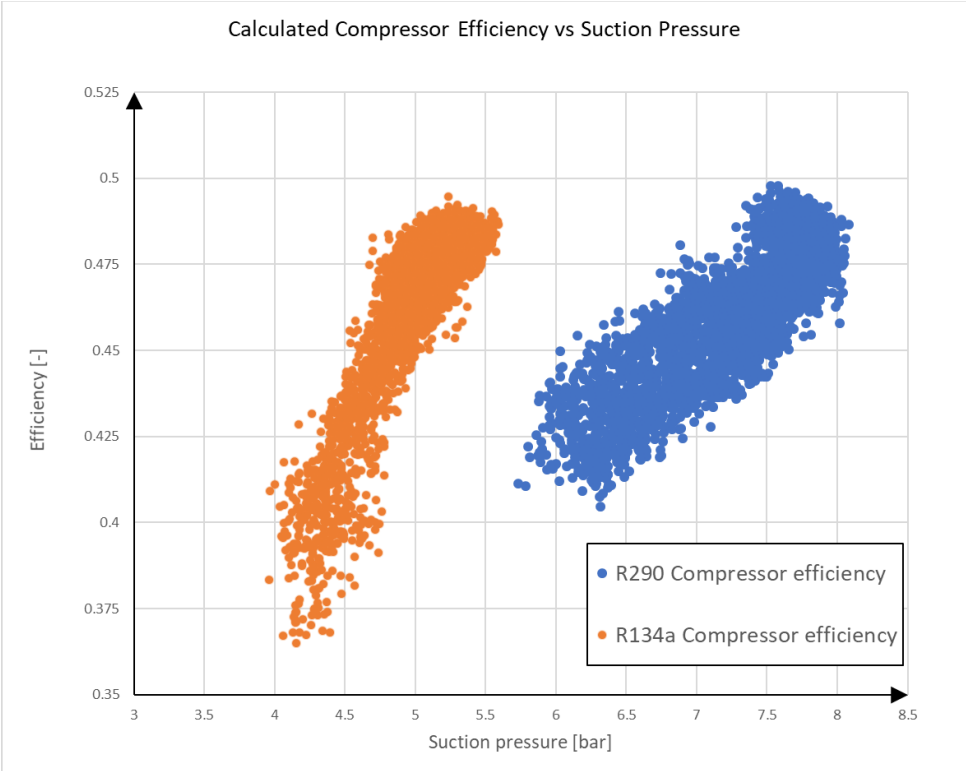


Figure 35 - Calculated Compressor Efficiency vs Suction pressure at 220g R134a and 115g R290 charge

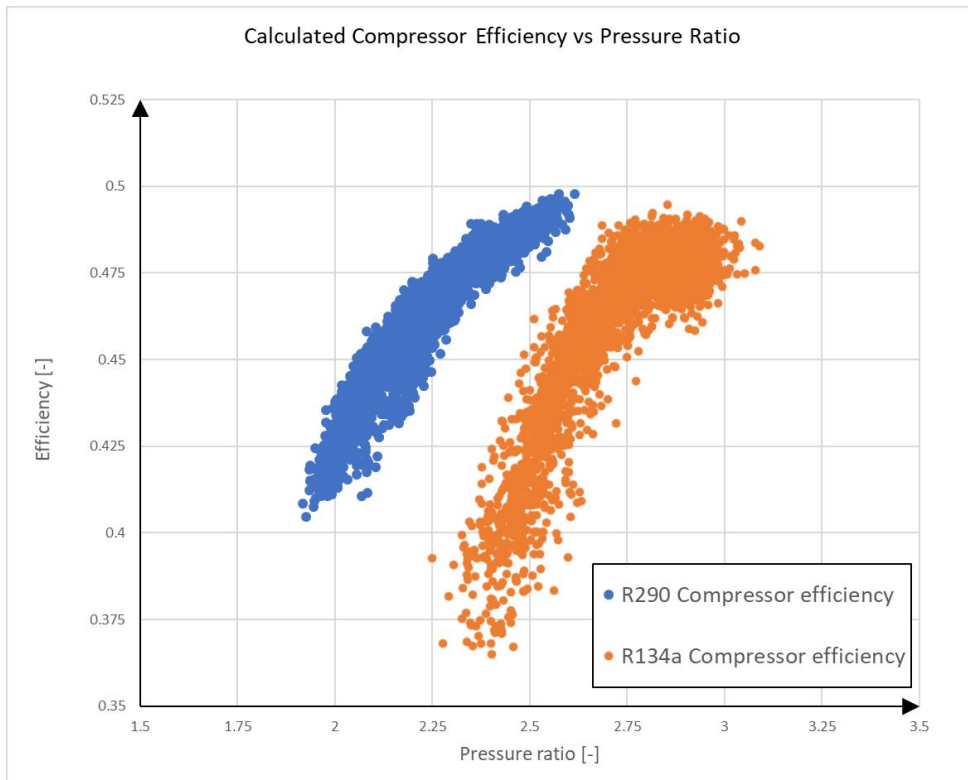


Figure 36 - Calculated Compressor Efficiency vs Pressure Ratio at 220g R134a and 115g R290 charge

Correlation factors for the data shown in Figure 35 and Figure 36 are stated in Table 12.

Table 12 - Compressor efficiency correlation factors

	Correlation: Efficiency vs suction pressure	Correlation: Efficiency vs Pressure ratio
R134a	0.89	0.88
R290	0.84	0.93

Due to the use of a capillary tube as the throttling component, the suction pressure and pressure ratio is mutually dependent. Keeping system components unaltered, increased suction pressure leads to higher pressure ratio within the investigated pressure range.

The strong correlation between suction pressure, pressure ratio and compressor efficiency prove the importance of selecting correct compressor parameters when designing a heat pump assisted

drum drying system. Failing to maintain ideal suction pressure and pressure ratio during the main parts of the drying process diminishes the efficiency of the compressor and hence the overall system. Pressure ratio vs efficiency charts are often available from the compressor manufacturer.

Figure 37 shows the average compressor efficiency of three identical experiments on each refrigerant plotted over the total length of the experiment. For both refrigerants, the maximum compressor efficiency is only maintained for a relatively short period of time. The results for R290 indicates that maximum compressor efficiency is not obtained during the experiments, indicating potential for energy savings by redesigning system components or optimizing refrigerant charge. The most relevant component is assumed to be the capillary tube.

The behavior indicates that though the operating conditions of the drum dryer is relatively stable, more complex compressor and pressure reduction control would increase efficiency especially towards the end of the drying cycle. Increased energy efficiency demands may allow for replacement of the capillary tube for a relatively cheap thermoelectric valve. As seen by Table 12 achieving optimal pressure ratio is key to efficient compressor operation.

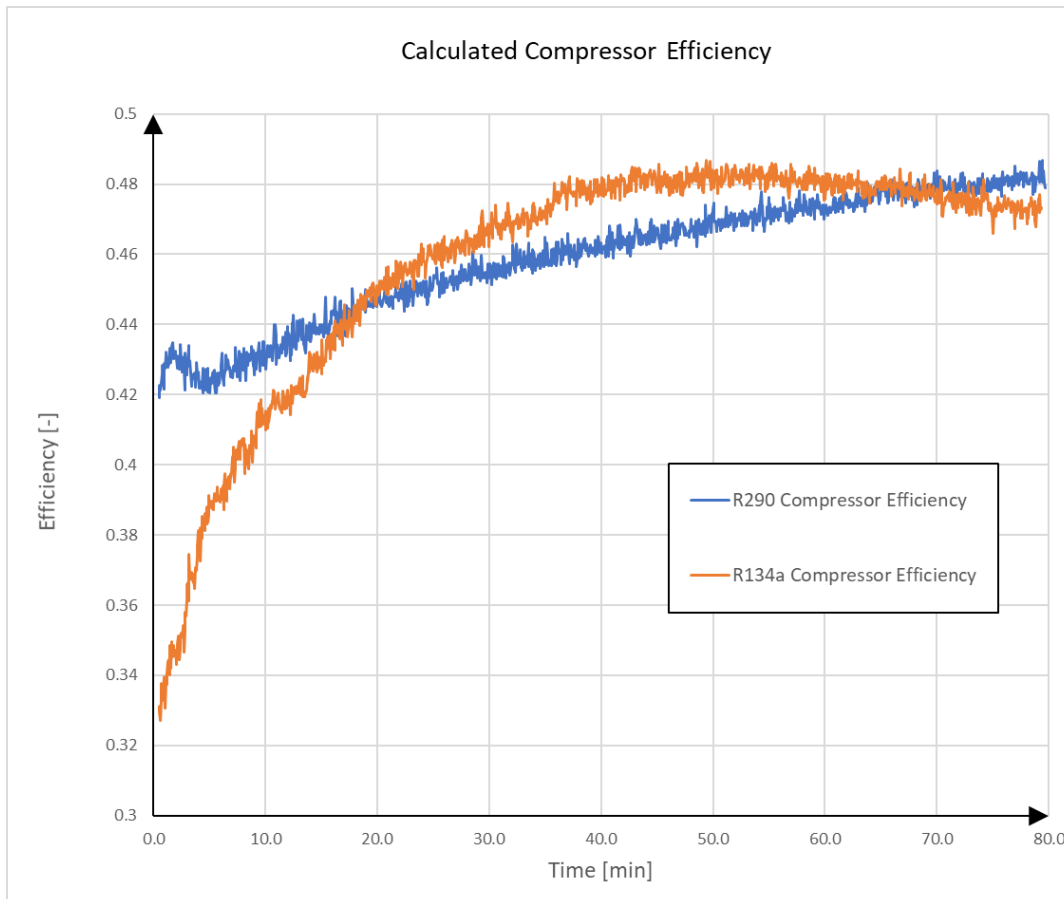


Figure 37 - Calculated Compressor Efficiency at 220g R134a and 115g R290 charge

Increasing compressor efficiency by reducing the clearance volume ratio, friction losses and electrical losses leads to improved overall system efficiency. The selection of high quality components represents a tradeoff between energy efficiency and investment costs. Maintaining maximum efficiency of a lower quality compressor may prove to be a more financially efficient way of improving efficiency than selecting a higher quality compressor.

4.2.4 Drying kinetics

The average DC-SMER obtained by the R134a system is 1.69 kg/kWh, while the highest average DC-SMER obtained by the R290 system is 1.71 at 115g charge. This is an increase of 1%.

Figure 38 shows the Specific moisture extraction rate (SMER), based on hygrometer measurements. The SMER are calculated for each instance of data saved to the log file, approximately for every third second throughout the experiment. The plotted value is the average of three identical experiments on each refrigerant. To improve readability, the actual data is faded in the background, while regression lines are drawn in the foreground.

The absolute value of SMER is vulnerable to errors in the calculated airflow and air leaks of the system. As airflow and air leaks due to the fixed fan speed and static ambient conditions are assumed to be constant, the relative development of SMER do not share this vulnerability. To adjust for errors caused by deviations in air leaks and small changes in sensor positions caused by rebuilding and adjustments, hygrometer SMER from each experiment is calibrated against SMER calculated from fabric weigh. This is done by calculating an equivalent airflow for each experiment, and using this airflow for SMER calculation.

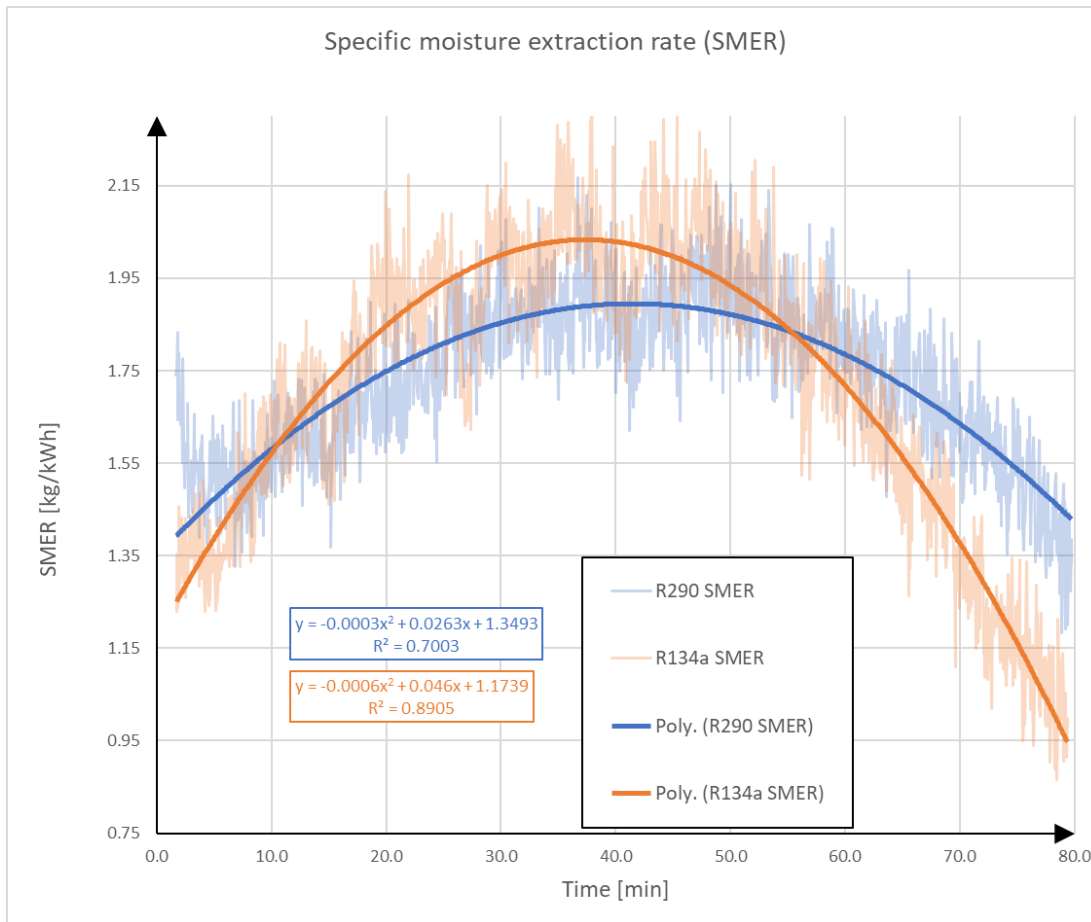


Figure 38 - Specific moisture extraction rate (SMER) calculated from hygrometers at 220g R134a and 115g R290 charge

As discussed in chapter 4.2.1 and 4.2.2 the temperature of the R134a system increases faster than for the R290 system. It is pointed out that this leads to faster increase in both SMER and MER rates, which is observed by the figures. SMER correlates to the COP of the heat pump, meaning that improved heat pump efficiency should improve SMER. Though, more factors contribute to the SMER, mainly the energy used to rotate the drum and run the drum fan. It is also assumed to be significantly affected by the amount and location of air leaks. Rotating the drum becomes less energy consuming as the fabric dries, and the weight of the content of the drum declines. Subsequently, high initial drying rates may contribute to increased SMER, though COP declines.

MER curves based on the same data as Figure 38 are plotted in Figure 39. The same weaknesses as for the SMER curves applies for MER. It is therefore calibrated in the same way as for SMER. It may be seen that the MER curve of R134a peaks earlier and more decisive, followed

by a more rapid decrease in MER than what is observed for R290. As mentioned in section 4.2.1, Figure 39 relates to Figure 25 on page 53.

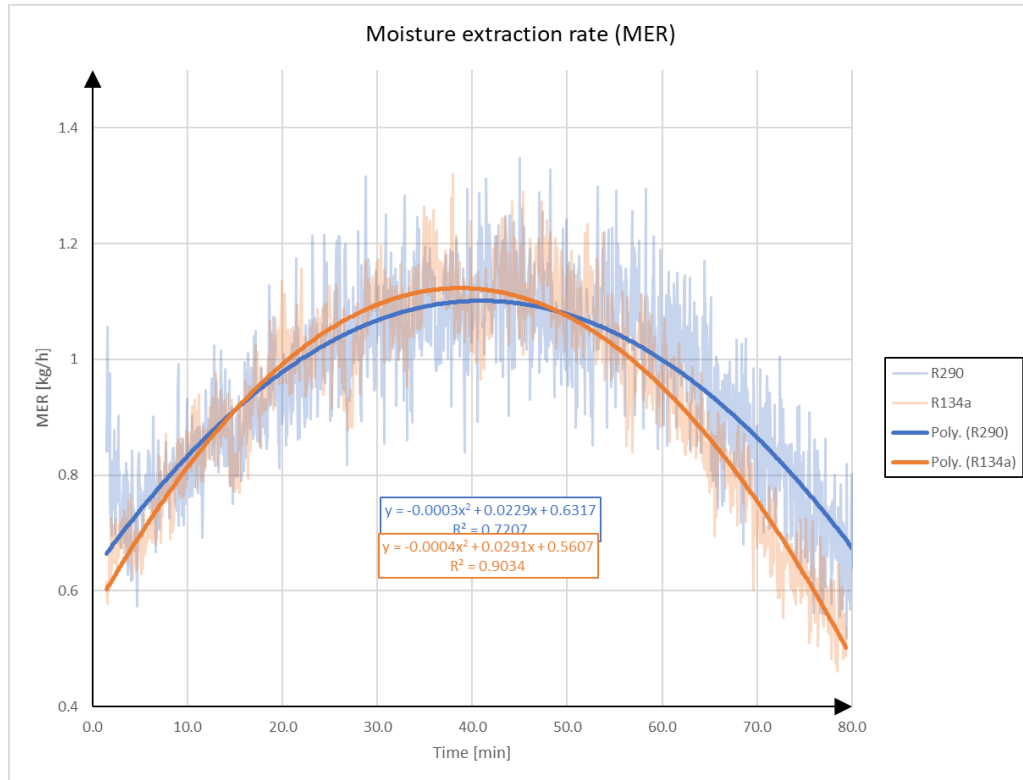


Figure 39 - Moisture extraction rate calculated from hygrometers at 220g R134a and 115g R290 charge

4.2.5 Charge optimization

A series of experiments has been performed to investigate the ideal refrigerant charge, using the original capillary tube designed for the R134a system. Figure 40 shows the DC-COP, DC-SMER calculated from hygrometers readings, DC-SMER calculated from fabric weight difference and moisture extraction rate (DC-MER) in the same figure. The plotted values are the average based on a various number of experiments at each charge level, with vertical bars showing the standard deviation. In order to establish as statistically reliable results as possible within the available time, repetitive experiments have been performed at charge levels having the largest standard deviations on COP after three experiments.

The displayed equations show the equations for the regression lines for the calculated DC-COP and DC-SMER calculated from fabric weight, along with its R^2 value.

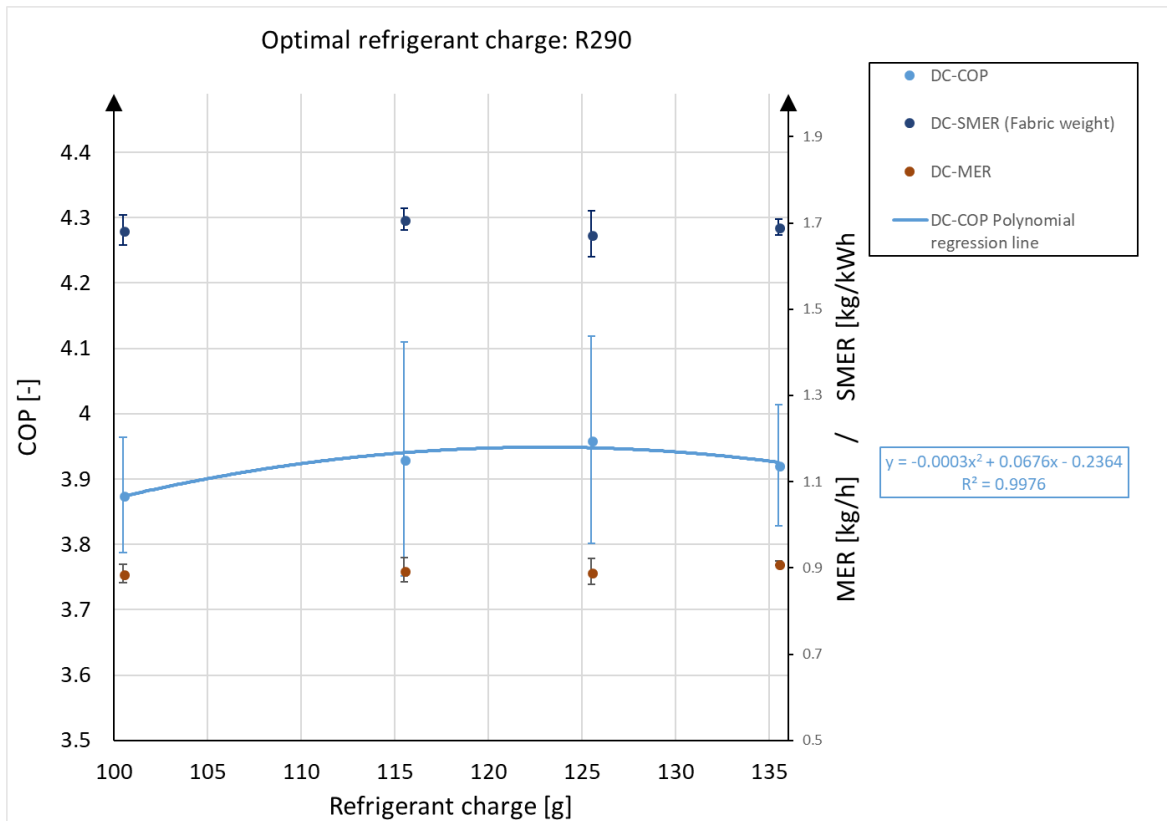


Figure 40 - Optimal R290 charge

By differentiating the DC-COP regression line equation, the refrigerant charge providing the maximum value may be calculated. Calculating for the displayed equation estimates that maximum DC-COP are obtained at a charge of 123g R290.

Figure 41 shows how the heat pump COP develops over the total time of the experiments. The plotted values are the average of three to five identical experiments at each charge level. Figure 42 shows SMER based on hygrometer readings from the same experiments. To improve readability, the actual data are faded in the background while regression lines are drawn in the foreground of the plot. The data and experiments used to plot Figure 41 and Figure 42 is the same as for Figure 40.

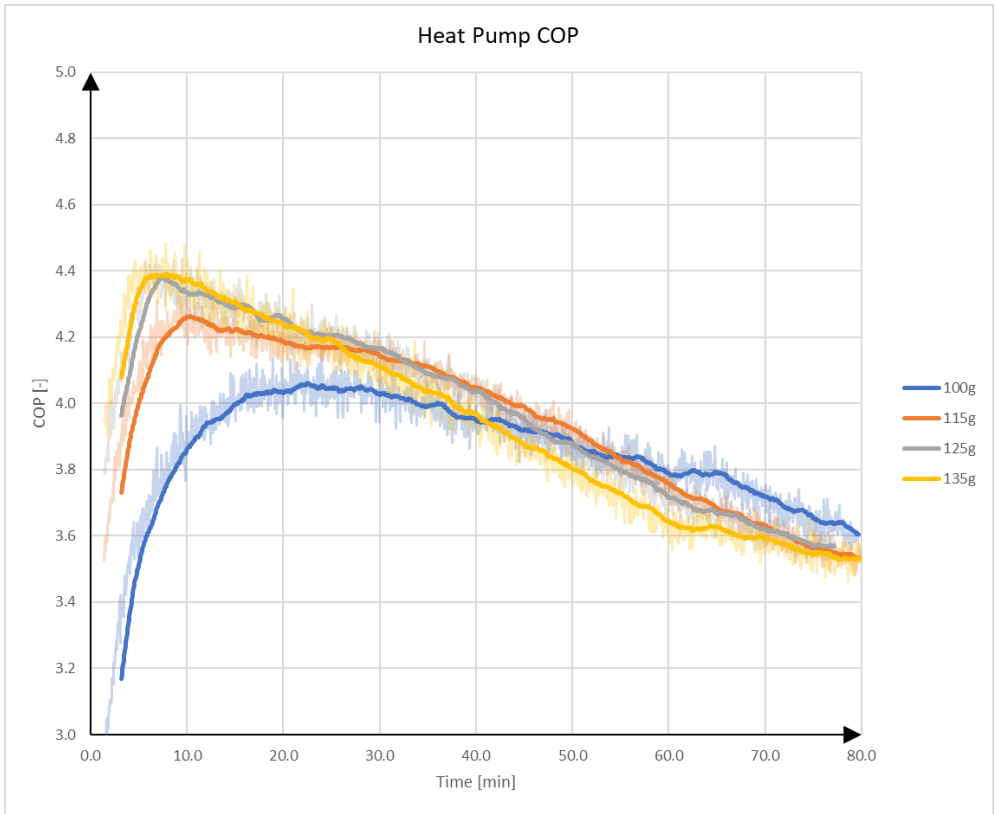


Figure 41 - Average Heat Pump COP at different R290 charge levels

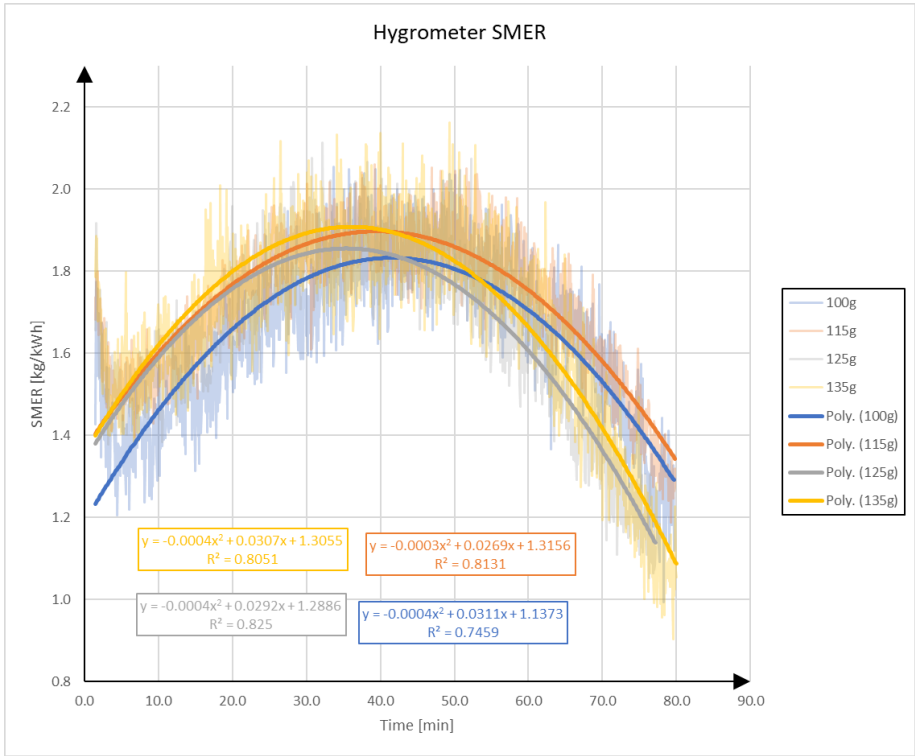


Figure 42 - Average SMER at different R290 charge levels based on hygrometer values

Refrigerant charge is found to influence the pressure ratio, degree of subcooling and degree of overheating. As an initial approach to capillary tube optimization, optimizing the degree of overheating provides significant increase in performance and is presumably the most important factor regarding compressor lifetime. Subcooling is dependent on overheating in the sense that increased charge limits overheating and increases subcooling. As discussed earlier, overheating is the most important parameter, thus leaving subcooling to be optimized by heat exchanger dimensioning.

Charge influences the pressure ratio especially at the initial stages of the drying cycle. Though, most of the time the effect of refrigerant charge on pressure ratio is to marginal to be a used as criteria for optimization. Subsequent to obtaining unarmful operation conditions for the compressor by adequate overheating, overall system performance in terms of COP and SMER is the parameters that are relevant for charge optimization.

4.2.6 Capillary tube accommodation

The original capillary tube designed for the R134a system is 78.5cm long with an internal diameter of 1.00mm. To investigate the effect of capillary tube accommodation, capillary tube lengths of 42.0 cm and 120.0 cm is tested, keeping the internal diameter constant at 1.0mm. Capillary tube length of 120.0 cm was calculated to be ideal for the system, based on the Wolf and Pate 2002 correlation. To elucidate the effect of optimal capillary tube sizing, the tube was first shortened to 42 cm. Due to time limitations and excessive wear on the compressor, only one experiment was run on the 42.0 cm tube. The system was charged with 115g R290 for this experiment.

A series of experiments were performed on the 120.0 cm capillary tube. Charged levels were set at 115g, 135g and 150g. The best performance was achieved at 150g charge, initializing repetitive experiments at this charge to verify results. Due to the safety regulations in IEC 60335-2-89:2010 and laboratory regulations, exceeding 150g charge were not permitted. Figure 43 shows performance parameters of the first experiment on each charge level.

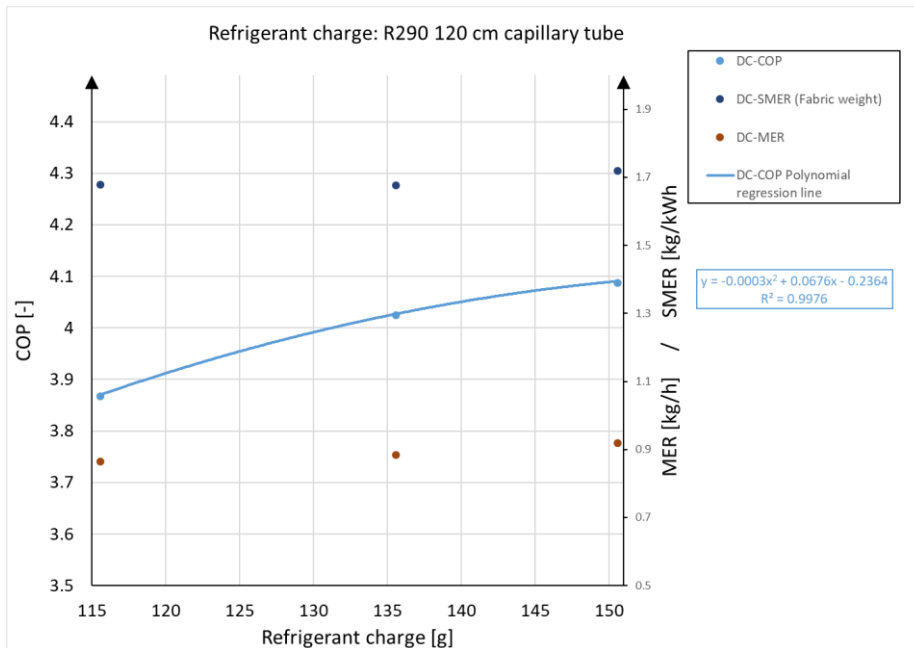


Figure 43 - Initial experiment performance of R290 at 120 cm capillary tube and increasing refrigerant charge

At 115g charge excessive overheating (≈ 20 K) at the evaporator outlet were detected. The DC-COP at this charge were calculated to be lower than what was obtained at 125g charge with the original capillary tube. To obtain adequate overheating, the charge was increased by 20g R290, providing a total charge of 135g. At 135g, overheating during the first two-thirds of the drying cycle were measured to be higher than desired. The DC-COP increased significantly, exceeding what was obtained using the original capillary tube. Increasing the charge to the maximum limit of 150g R290 yielded ideal superheating throughout the main parts of the experiments. Overheating throughout the drying cycle is plotted in Figure 44. To ensure comparability with the single experiments performed at 115g and 135g charge levels, only data from the first experiment at 150g charge is plotted.

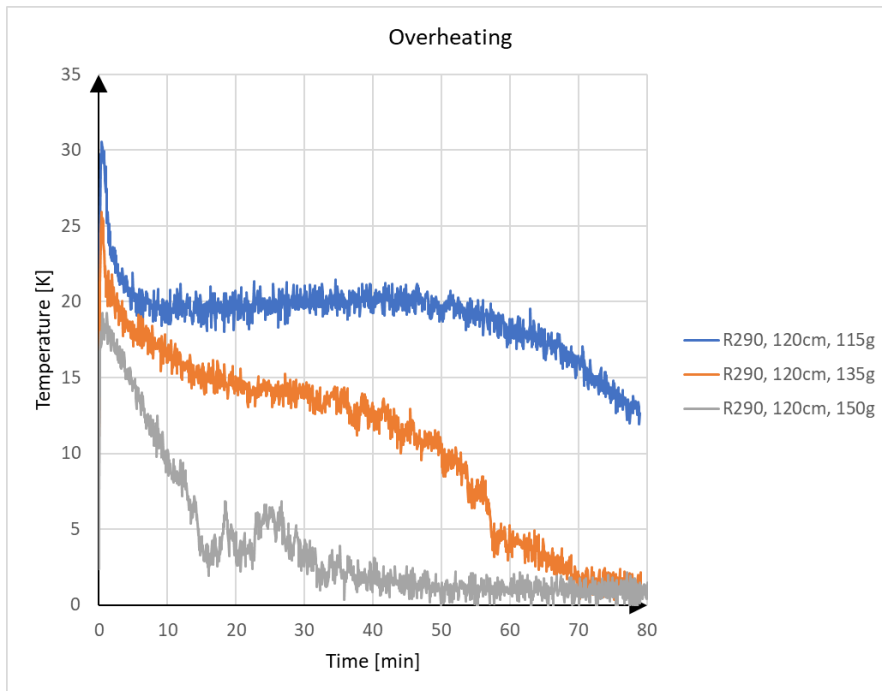


Figure 44 - Overheating at the evaporator outlet at different charge levels

The pressure ratio at different charges and capillary tube lengths are seen in Figure 45. At 42cm capillary tube length and 115g charge, as well as 120cm capillary tube length and 115g – 135g charge levels, not enough experiments on each set of parameters were performed to produce the quality of measurements necessary to be presented in the following figures.

The pressure ratio of the R134a system is considerably higher than for the R134a system at similar capillary tube length. The average difference in pressure ratio is calculated to be 22%. By increasing the capillary tube length by 53% from 78.5cm to 120cm and increasing the R290 charge level by 11% from 135g to 150g, the average pressure ratio increased by 8.5%. As seen in Figure 45 increase in charge level causes the pressure ratio to decline, while increase in capillary tube length causes the pressure ratio to increase.

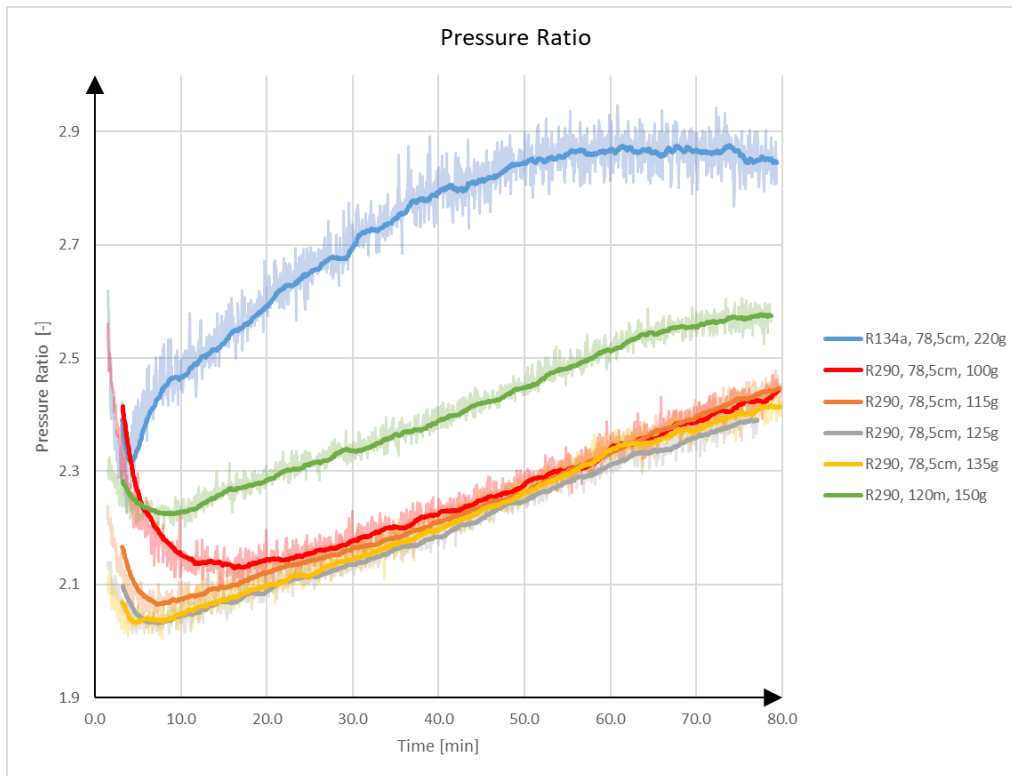


Figure 45 - Measured pressure ratio across the compressor

As discussed in section 4.2.3, compressor efficiency increased throughout the R290 drying cycle. A strong correlation was found between the pressure ratio and compressor efficiency. Figure 46 shows how compressor efficiency continues to increase following the increase in pressure ratio caused by capillary tube replacement. However, the results do not indicate that maximum compressor efficiency is obtained, suggesting that further increase in capillary tube length may improve compressor efficiency thus improving system performance.

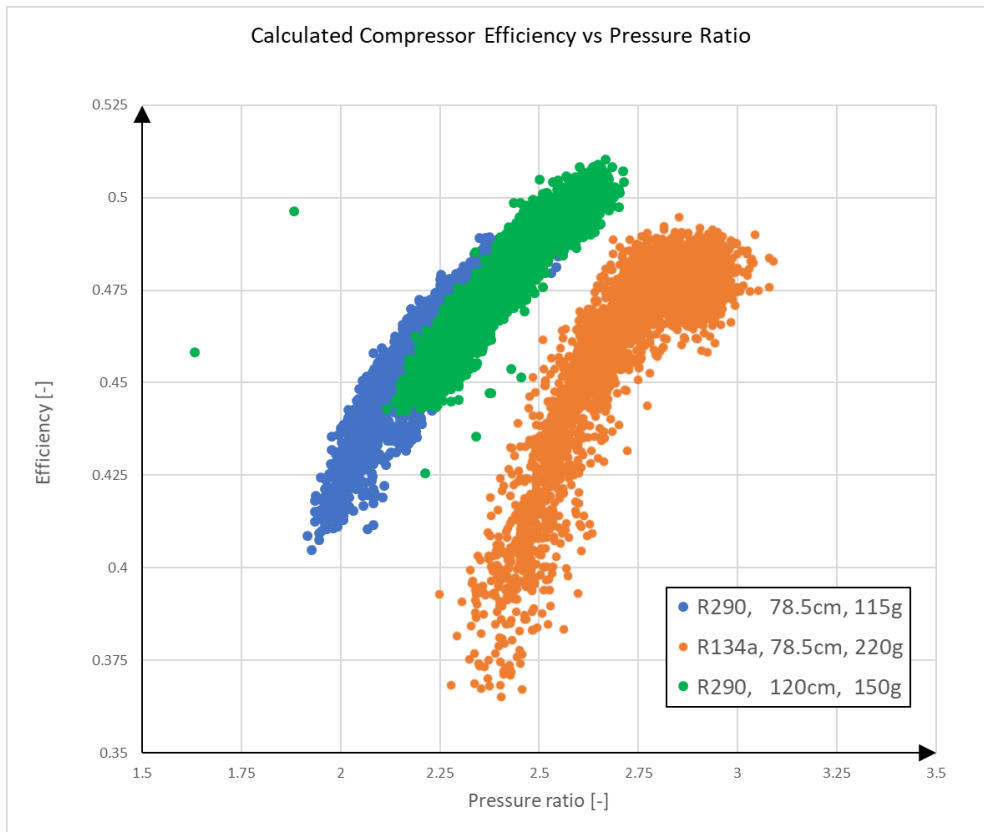


Figure 46 - Calculated compressor efficiency vs Pressure ratio

COP development throughout the drying cycle at 120 cm capillary tube and 150g R290 charge is seen in Figure 47. COP at 78.5cm capillary tube and different charge levels are included for comparison. During the main part of the experiments the COP at the mentioned conditions are superior to COP while using the original 78.5cm capillary tube. Improved compressor efficiency has a direct effect on the COP of the heat pump, suggesting that improved COP may be obtained by obtaining optimal pressure ratio throughout main parts of the experiment. Compensating for the improved compressor efficiency, R134a and R290 COP are in the same range.

Figure 48 shows SMER based on hygrometer reading at the same conditions as in Figure 47. The SMER at 120 cm capillary tube does not show considerably different characteristics compared to SMER before capillary tube replacement. Attention is brought to the fact that about 2/5 of the energy consumption for the SMER calculation is the energy used to power the drum fan and rotate the drum.

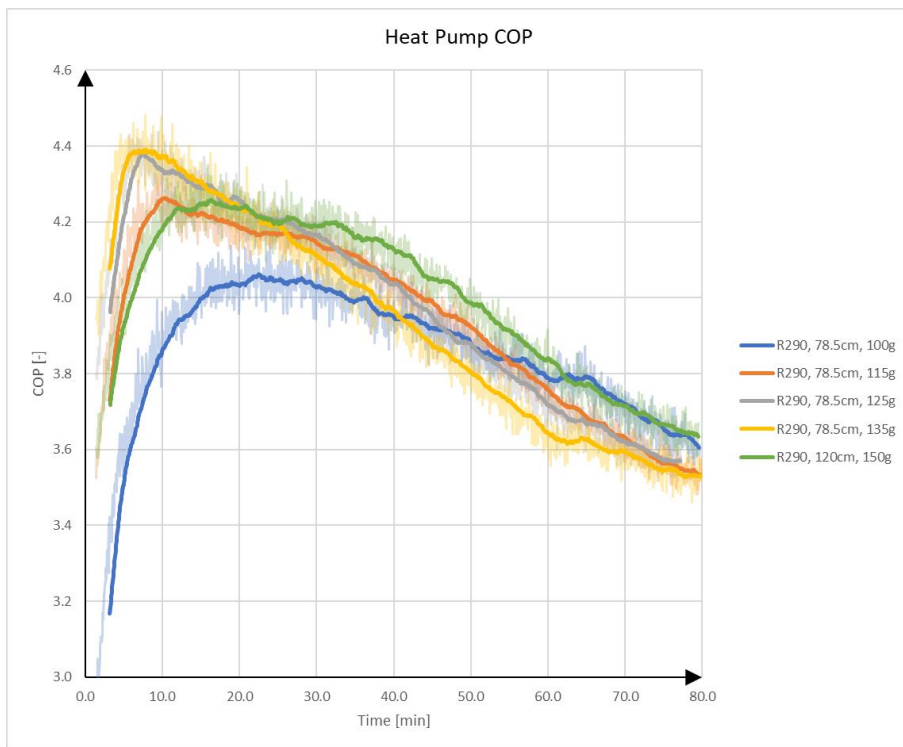


Figure 47 - Calculated average Heat pump COP, including 120cm capillary tube at 150g charge

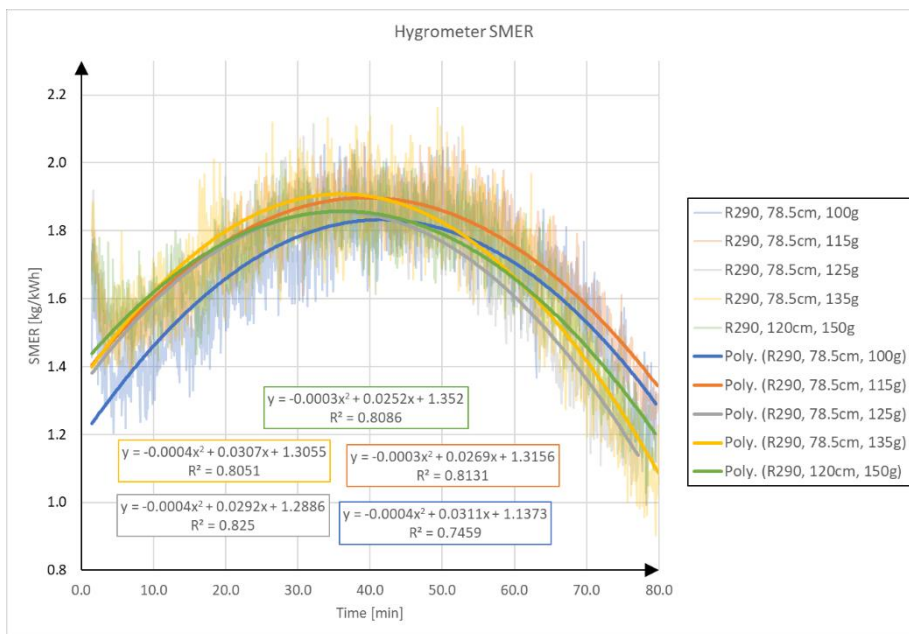


Figure 48 – Average SMER based on hygrometer readings, including 120cm capillary tube at 150g charge

4.2.7 Overall performance

The average performance of the dryer, expressed as DC-COP, DC-SMER and DC-MER is expressed in Table 12. It shows that the highest DC-COP value were obtained while charged with R290, after the capillary tube were replaced. The increase in average DC-COP were 6%, while the increase before replacing the capillary tube were 3%. Statistically it was not found difference between the DC-COP while charged with R134a versus R290 before capillary tube replacement ($P > 0.05$). The increase in DC-COP after capillary tube replacement were found to be statistically significant ($P < 0.05$).

Table 13 - Overall system performance

Refrigerant charge	Capillary tube length [cm]	DC-COP [-]	DC-SMER (fabric weight) [kg/kWh]	DC-MER (fabric weight) [kg/kWh]
R134a, 220g	78.5	3.80	1.69	0.914
R290, 100g	78.5	3.88	1.68	0.887
R290, 115g	78.5	3.93	1.71	0.896
R290, 125g	78.5	3.96	1.67	0.892
R290, 135g	78.5	3.92	1.69	0.911
R290, 150g	120	4.03	1.70	0.912

Although higher average DC-SMER were obtained using R290 than R134a, the difference and amount of data is not large enough to statistically conclude that SMER has increased.

When comparing drying performance, the maximum drying rate in the case of 134a is higher, due to the higher drying temperature when compared to R290. As the drying process of R134a occurs in the right part of the IX-diagram in Figure 23 on page 51, it is more efficient compared to the drying process of R290 seen in the middle of the IX-diagram in Figure 24 on page 52. The increased efficiency of drying on the right side of the IX-diagram due to the nature of air-water vapor mixture influences the SMER. Though significantly higher DC-COP is calculated for the R290 system, the temperature is not high enough to provide significantly higher DC-SMER and DC-MER.

4.3 Reliability and assumptions

Though verified and calibrated, all measurements are prone to errors caused by uncertainty of the instrumentation as well as influence by the ambient and non-homogenous flows and conditions. The highest level of reliability in this study are achieved by weighing of the fabric, as the only uncertainty of the weighing is the uncertainty of the scale. Therefore there should be attached great importance to results based on weighing of the fabric.

Assumptions have had to be made according to the compressors volumetric efficiency (clearance volume) and deceleration of the electric motor. These parameters in combination with the compressor displacement and synchronous speed are used to calculate the refrigerant volume flow, and in turn the refrigerant mass flow.

Throughout the initial phase of the experiments unsteady behavior is observed. Since study of transient behavior at startup is not a prioritized part of this study, the first one to five minutes of data from experiments are normally excluded from the presented figures. Volatile transient behavior increases the required amplitude of the figure axis, obscuring important trends throughout the main parts of the experiments. The observed transient behavior does not fit to the applied regression equations, diminishing the scientific value of combining the transient data with the main experimental data.

Though not prioritized in this study, the possible energy efficiency and wear rate improvements from the study of transient behavior should not be neglected. Measures such as introducing an electric heater to shorten the duration of transient behavior or improve conditions may be reasonable.

4.3.1 COP calculation

COP are calculated based on pressure and temperature measurements. There are two pressure transmitters installed in the system, on each side of the compressor. This means that pressure drop across each component and between most of the thermistors is not measured. Installation of additional pressure transmitters would require additional taps to be soldered to the system, possibly affecting comparability to the original system. The decision has been made not to install additional pressure transmitters, and to neglect pressure loss in heat exchangers and tubing.

As for the temperature transmitters the temperature is measured on the outside of the tubes. Though the transmitters are insulated from the ambient, readings at excessively high and low temperatures are likely to be somewhat affected by ambient temperature. This is indicated by the lack of superheating at the compressor outlet. Importantly, efforts have been made to maintain the same level of errors and ambient influence throughout all experiments. This ensures comparability of measurements and calculations on the original and rebuild system.

4.3.2 SMER calculation

Calculation of SMER from hygrometer values is based on multiplying the measured humidity of the air by the airstream. As no part of the airstream may be assumed to be laminar, the airflow needs to be calculated to be used to calculate SMER from hygrometer values. An equivalent airflow is therefore calculated by comparing the difference in measured air humidity across the drum to moisture evaporation measured by weighing of the fabric. As this calculation does not account for air leaks, bypass air etc., the equivalent airstream may only be used for calculations based on the same hygrometers readings.

As the hygrometer readings are susceptible to errors caused by air leaks, bypass air etc., the SMER calculated from fabric weight should be the values used for evaluation of the total efficiency of the system. As weighing during experiments affects results, the SMER calculated from hygrometer values provides the best possible intermittent data.

Collection and weighing of the condensed water shows a large amount of escaped water from the system. Leakage in the range of 20 – 40% of the initial water content has been observed, indicating significant air exchange rates to the ambient. Some effect is observed by the sealing of air leaks and attention to details while assembling the drum dryer.

4.4 Comparison between R134a and R290

Even though heat exchangers, fan and drum sizing are not optimized for R290 duty, R290 on average outperforms R134a on both COP and SMER. Statistically, only COP increase may be concluded. The experimental results does not suggest any deterioration of performance parameters subsequent to implementation of R290 in the drum dryer.

5 Further work and improvements

A considerable amount of data has been collected during this study. More than half a million data points has been collected and processed to create a solid basis for conclusions. The most prominent limitation regarding testing of different parameters is the need for cooling of the system between experiments. This need limits the amount of experiments to one experiment per day. Forced cooling of the system by use of fans has been tested but are not found improve cooling sufficiently to increase experiment frequency.

By measuring the compressor surface temperature as well as air temperature surrounding the compressor, a valid estimate for compressor heat loss may be calculated. In turn, this allows for the calculation of overheating of the refrigerant between the compressor inlet and cylinder inlet, improving the foundation for charge optimization. Alternatively, a literature review on the subject may be performed, providing the necessary statistical data.

Applying a test regime of selected capillary tube lengths and charges, allows for the ideal combination of capillary tube length and charge may be calculated by statistical regression analysis of the collected data. It is suggested to develop a simulation model prior to selecting the parameters of the test regime. By applying the simulation model, improved quality in the selection of parameters may be obtained.

Prolonging the period of time where the maximum COP and SMER is obtained improves energy efficiency. Introducing an electric heater to the heat pump circuit appears to possibly improve drying rates and energy efficiency during warm up. Introduction of the heater may be performed by coiling a resistor around the refrigerant tube. Insulation against the ambient is important to ensure that the added heat is transferred to the refrigerant.

To improve the understanding of air leaks and their influence on drying performance, investigation of air leaks and heat rejection is relevant. Application of thermography may serve as an initial suggestion to the qualities and rates of air that is exchanged. It is suggested that the sealing of air leaks combined with improved insulation of the drum dryer may drastically

improve SMER. It seems that the HPDD is built as a conventional condensing drum dryer, only replacing the condensing unit and air heater with a heat pump. Carefully redesigning the complete HPDD taking into account the importance of retaining the air in a closed loop may reduce energy consumption and improve drying rates.

The results indicate that optimizing the condenser and evaporator sizing to fit operation with R290 may improve efficiency by reducing pressure loss. Simulation of different heat exchanger designs using e.g. HXsim may be beneficial. The reduction in COP due to reduced subcooling must be taken into account.

A summarized list of tasks proposed for further work on this topic follows. The order may be treated as a guideline to priority ranking

- Development and verification of a simulation model to simulate different parameters and control regimes
- Capillary tube optimization
- Heat exchanger optimization
- Investigate the nature of air leaks and their effect on system performance
- Introduction of an electrical heater in order to obtain high COP and SMER rates at earlier stages of drying

6 Conclusion

Energy efficiency is key to achieving the reduction in greenhouse gas emissions needed to preserve the Earth's climate. Unfortunately, the positive effect of energy efficiency may be diminished by the use of climate affecting chemicals such as HFC refrigerants. By maintaining and improving energy efficiency while implementing environmental and climate friendly refrigerants, a substantial refinement towards substantial heating and refrigeration may be obtained.

R290 is well-suited to substitute R134a in heat pump assisted drum dryers. Providing compressor replacement implementation of R290 can be done without diminishing COP or SMER values, thus achieving the same level of energy efficiency as systems utilizing R134a.

By proper replacement of the capillary tube, improvement of the R290 heat pump COP may be obtained, releasing additional potential for energy efficiency improvement. 6% improvement in COP was obtained during experiments.

The combination of maintained energy efficiency and a tremendous reduction in the refrigerants global warming potential provides a significant decrease in the environmental impact of the drum dryer.

The results of this study indicate that the drawbacks of implementing R290 as refrigerant in heat pump assisted drum dryers are limited to the flammability of R290. For applications where the risk of ignition is not impending, applying R290 is an obvious choice.

References

1. Goldberg, M., *Heat pump closed loop drying*. 1986, Google Patents.
2. Greenpeace, *HFOs: the new generation of F-gases*. 2016.
3. Hane Marit Dalen, B.M.L., *Formålsfordeling av husholdningenes elektrisitetsforbruk i 2006 - Utvikling over tid 1990 - 2006* 2009, Statistics Norway.
4. Braun, J.E., P.K. Bansal, and E.A. Groll, *Energy efficiency analysis of air cycle heat pump dryers*. International Journal of Refrigeration, 2002. **25**(7): p. 954-965.
5. *Code of Federal Regulations - PART 430 - ENERGY CONSERVATION PROGRAM FOR CONSUMER PRODUCTS - Title 10 -Energy - CHAPTER II -DEPARTMENT OF ENERGY. SUBCHAPTER D -ENERGY CONSERVATION*, U.S.D.o. Energy, Editor. 2017: Government Publishing office [US].
6. Association of Home Appliance Manufacturers, W., DC (2009), *Household Tumble Type Clothes Dryers*, in *HLD-1-2009*.
7. TeGrotenhuis, W., *Clothes Dryer Automatic Termination Sensor Evaluation - Volume 1: Characterization of Energy Use in Residential Clothes Dryers* 2014, Pacific Northwest National Laboratory.
8. TeGrotenhuis, W., et al., *Modeling and design of a high efficiency hybrid heat pump clothes dryer*. Applied Thermal Engineering, 2017. **124**: p. 170-177.
9. Patel, V.K., et al., *Experimental evaluation and thermodynamic system modeling of thermoelectric heat pump clothes dryer*. Applied Energy, 2018. **217**: p. 221-232.
10. Gluesenkamp, K., *Thermoelectric Clothes Dryer - 2016 Building Technologies Office Peer Review*. 2016, Oak Ridge National Laboratory.
11. Gopalnarayanan, S. and R. Radermacher, *Heat-pump assisted dryer using refrigerant mixtures -- Batch mode drying*. Conference: American Society of Heating, Refrigerating and Air-Conditioning Engineers (ASHRAE) winter meeting, Philadelphia, PA (United States), 24-28 Feb 1997; Other Information: PBD: 1997; Related Information: Is Part Of ASHRAE transactions: Technical and symposium papers, 1997. Volume 103, Part 1; PB: 1136 p. 1997: American Society of Heating, Refrigerating and Air-Conditioning Engineers, Inc., Atlanta, GA (United States). Medium: X; Size: pp. 888-898.
12. Stene, J. *Lecture series TEP4260 at Norwegian University of Science and Technology (NTNU)*. 2017.
13. Ciconkov, R., *Refrigerants: There is still no vision for sustainable solutions*. International Journal of Refrigeration, 2018. **86**: p. 441-448.
14. Elnan, Å., *Development of new heat pump cloth drum dryer with CO₂ as working fluid*, in *Department of Energy and Process Engineering*. 2011, Norwegian University of Science and Technology.
15. Akre-Aas, J., *HFO kuldemedier*. 2016.
16. Ravikumar, T.S. and D. Mohan Lal, *On-road performance analysis of R134a/R600a/R290 refrigerant mixture in an automobile air-conditioning system with mineral oil as lubricant*. Energy Conversion and Management, 2009. **50**(8): p. 1891-1901.
17. Tashtoush, B., M. Tahat, and M.A. Shudeifat, *Experimental study of new refrigerant mixtures to replace R12 in domestic refrigerators*. Applied Thermal Engineering, 2002. **22**(5): p. 495-506.
18. AGA, *SIKKERHETSDATABLAD Tetraflourethan (R134a)*.
19. *Montreal Protocol on Substances that Deplete the Ozone Layer (with annex). Concluded at Montreal on 16 September 1987*, U.N.-T. Series, Editor. 1989, United Nations: Montreal.

20. *REGULATION (EU) No 517/2014 OF THE EUROPEAN PARLIAMENT AND OF THE COUNCIL of 16 April 2014 on fluorinated greenhouse gases and repealing Regulation (EC) No 842/2006*, in 842/2006, T.E.P.A.T.C.O.T.E. UNION, Editor. 2014: Official Journal of the European Union.
21. *Propan*, in *Store norske leksikon*. 2009.
22. *R290 Refrigerant Grade Propane - High quality natural refrigerant*. 2017/09/12]; Available from: https://www.lindeus.com/internet.lg.lg.usa/en/images/Linde%20R290%20Refrigerant%20Grade%20Propane138_11493.pdf?v=.
23. *Danfoss - Practical Application of Refrigerants R 600a and R 290 in Small Hermetic Systems - Application Guideline*. 2009.
24. *NS-EN ISO 11114-1:2012 Gas cylinders - Compatibility of cylinder and valve materials with gas contents - Part 1: Metallic materials*.
25. Aylward, G.H., *SI chemical data / Gordon Aylward and Tristan Findlay*, ed. T.J.V. Findlay. 2007, Milton, Qld: John Wiley & Sons Australia.
26. Calm, J.M. and G. Hourahan, *Refrigerant data update*. Hpac Engineering, 2007. **79**(1): p. 50-64.
27. AFROX, *MATERIAL SAFETY DATA SHEET (MSDS) R134A*. 2011.
28. NATIONAL REFRIGERANTS, I., *Safety Data Shet - R290 PROPANE*. 2015.
29. SECOP. *Natural Refrigerants - Hydrocarbons – Isobutane (R600a) and Propane (R290)*. 2017/10/04]; Available from: <https://www.secop.com/solutions/natural-refrigerants/>.
30. Bellomare, F. and S. Minetto, *Experimental Analysis of Hydrocarbons as Drop-in Replacement in Household Heat Pump Tumble Dryers*. Energy Procedia, 2015. **81**: p. 1212-1221.
31. Minetto, S., *Compressor used for HC experiments*, E. Storslett, Editor.
32. Sánchez, D., et al., *Energy performance evaluation of R1234yf, R1234ze(E), R600a, R290 and R152a as low-GWP R134a alternatives*. International Journal of Refrigeration, 2017. **74**(Supplement C): p. 269-282.
33. Tecumseh, *Guidelines for the utilization of R600a and R290*. 2011.
34. *Tecumseh Technical Bulletin - Hydrocarbons*.
35. *SECOP Application guideline - Practical application of refrigerants R600a and R290 in small hermetic systems*. 2011.
36. *NEK IEC 60335-2-89:2010 Husehold and similar electrical appliances - Safety - Part 2-89: Particular requireents for commercial refrigerating appliances with an incorporated or remote refrigerant unit og compressor*, N. IEC, Editor. 2010.
37. McLaughlin, C. *Hydrocarbon limit likely to move to 500 grams by 2018*. 08/12/2016 08/09/2017]; Available from: <http://hydrocarbons21.com/articles/7322/hydrocarbon-limit-likely-to-move-to-500-grams-by-2018>.
38. Secop. *N-series in Detail*. [cited 2017 10/23]; Available from: <https://www.secop.com/products/product-portfolio/serie/n-series/>.
39. IPU & Department of Mechanical Engineering - Technical University of Denmark, *CoolPack*. 2000 - 2012.
40. Bhandari, B., *Handbook of Industrial Drying, Fourth Edition Edited by A. S. Mujumdar*. Drying Technology, 2015. **33**(1): p. 128-129.
41. Kian Jon, C. and C. Siaw Kiang, *Heat Pump Drying Systems*, in *Handbook of Industrial Drying, Third Edition*. 2006, CRC Press.

42. *Bosch Spare Part Finder Detail Page - Tumble dryer WTW86298SN/20*. 11/07/2017]; Available from: <http://www.bosch-home.co.uk/customer-service/care-protection-and-parts/WTW86298SN/20#/TabsTogglebox=spare-section-3/Togglebox=tb0538/>.
43. Lee, T., *Compressor oil*, E. Storslett, Editor. 2018.
44. SUNON, *SUNON Specification for apporval - DP203A 2123LST.GN*. 2005.
45. Rechi Precision Co. LTD. *Rotary Compressor*. 10/31/2017]; Available from: <http://www.rechi.com/en/webProductsEN.do?method=getCompressor>.
46. *Pump Water pump 230V, 26W, 50Hz*. 11/07/2017]; Available from: <http://www.bosch-home.co.uk/store/00145388>.
47. Donna, *Bosch Q&A*, E. Storslett, Editor. 2017.
48. Eriksen, J., *VS: Kontakt kundeservice Bosch12.09.2017 - esps@stud.ntnu.no [InteractionID:2e0761c9-1c12-4dd1-850c-9753386e77ee]*, E. Storslett, Editor. 2017.
49. Bansal, P., A. Mohabir, and W. Miller, *A novel method to determine air leakage in heat pump clothes dryers*. *Energy*, 2016. **96**: p. 1-7.
50. VAISALA, *Vaisala HUMICAP Humidity and Temperature Transmitter Series HMT330 User's Guide*. 2013.
51. VAISALA *Humidity Conversation Formulas - Calculation formulas for humidity*. 2013.
52. Nellis, G. and S.A. Klein, *Heat Transfer*. 2009: Cambridge University Press.
53. *NS-EN ISO 11114-2:2013 - Gas cylinders -Compatibility of cylinder and valve materials with gas contents -Part 2: Non-metallic materials*.

List of figures

Figure 1 - Illustration of a conventional electric drum drying cycle. Figure created by TeGrotenhuis et.al. [8]	5
Figure 2 - Conventional air vented dryer	6
Figure 3 - Conventional condensing dryer	6
Figure 4 - Thermoelectric dryer	7
Figure 5 - Air cycle heat pump dryer	7
Figure 6 - Heat pump drum dryer.....	8
Figure 7 - System schematic for a vacuum heat pump assisted drum dryer system	9
Figure 8 - Hybrid heat pump dryer including electric heater	12
Figure 9 - Secop compressors: evaporation pressures. Figure created by Secop[38].....	20
Figure 10 - I-x diagram / Psychrometric chart	22
Figure 11 - Exploded drawing [42]	25
Figure 12 - Experimental rig	32
Figure 13 - Printout of the LabVIEW Block Diagram	36
Figure 14 – Instrumentation	38
Figure 15 - Initial sensor placement	39
Figure 16 - Repositioning of T10/H10, T5 and T7.....	40
Figure 17 - T11/H11 position.....	40
Figure 18 - T9/H9 position.....	40
Figure 19 - Pressure transmitters connections before rebuild	40
Figure 20 - Sensor positions and transmitter connections after rebuild	41
Figure 21 – Flow chart: LMTD calculation	44
Figure 22 – Flow chart: COP _H and compressor efficiency calculation	46
Figure 23 - IX Diagram with plots for drying with R134a at 220g charge	51
Figure 24 - IX diagram with plots for drying with R290 at 115g charge.....	52
Figure 25 – Moisture ratio at 220g R134a and 115g R290 charge.....	53
Figure 26 - LMTD heat exchangers at 220g R134a and 115g R290 charge	54
Figure 27 - R134a Air cycle Relative Humidity and Temperature at 220g charge.....	56
Figure 28 - R290 Air cycle Relative Humidity and Temperature at 115g charge.....	56
Figure 29 - Condensation and evaporation temperature at 220g R134a and 115g R290 charge	57
Figure 30 - R134a heat pump cycle average thermistor temperatures at 220g charge.....	59
Figure 31 - R290 Heat pump cycle average thermistor temperatures at 115g charge.....	60
Figure 32 - Subcooling at the condenser outlet and overheating at the evaporator outlet at 220g R134a and 115g R290 charge.....	61
Figure 33 - Evaporator pressure loss at 220g R134a and 115g R290 charge.....	62
Figure 34 – Calculated Heat Pump COP at 220g R134a and 115g R290 charge.....	63
Figure 35 - Calculated Compressor Efficiency vs Suction pressure at 220g R134a and 115g R290 charge	64
Figure 36 - Calculated Compressor Efficiency vs Pressure Ratio at 220g R134a and 115g R290 charge	65
Figure 37 - Calculated Compressor Efficiency at 220g R134a and 115g R290 charge	67
Figure 38 - Specific moisture extraction rate (SMER) calculated from hygrometers at 220g R134a and 115g R290 charge.....	69
Figure 39 - Moisture extraction rate calculated from hygrometers at 220g R134a and 115g R290 charge	70
Figure 40 - Optimal R290 charge.....	71

Figure 41 - Average Heat Pump COP at different R290 charge levels	72
Figure 42 - Average SMER at different R290 charge levels based on hygrometer values	72
Figure 43 - Initial experiment performance of R290 at 120 cm capillary tube and increasing refrigerant charge.....	74
Figure 44 - Overheating at the evaporator outlet at different charge levels.....	75
Figure 45 - Measured pressure ratio across the compressor.....	76
Figure 46 - Calculated compressor efficiency vs Pressure ratio.....	77
Figure 47 - Calculated average Heat pump COP, including 120cm capillary tube at 150g charge	78
Figure 48 – Average SMER based on hygrometer readings, including 120cm capillary tube at 150g charge	78

List of tables

Table 1- Overview of relevant design parameters derived from literature [4]	4
Table 2 - Materials compatibility with R290 [23].....	15
Table 3 - Chemical Properties of refrigerants R134a and R290[25, 26]	16
Table 4 - Specifics heats of water at 1.01 bara [39]	23
Table 5 - Pipe diameter	26
Table 6 - Rated input power of the drum dryer’s original main components.....	27
Table 7 - Design specifications	28
Table 8 - Tecumseh AE4430U-FZ1A specifications	29
Table 9 - Standardized procedure.....	33
Table 10 - Constants for Equation 8.....	43
Table 11 - Valid experiments	49
Table 12 - Compressor efficiency correlation factors	65
Table 13 - Overall system performance	79

Appendix

A large quantity of sensor data is logged and processed as a part of this thesis. Due to the vast amount of data points, the logs are not applicable for analog representation. Therefore, appendix D-A to D-D only exist in digital format. This is also the case for the LabView VI. If you wish to obtain these appendixes, please contact the author.

Printed appendixes: Appendix A: Materials compatibility of propane
 Appendix B: List of experiments
 Appendix C: Data Sheet: Rechi 39E073B
 Appendix D: Data Sheet: Tecumseh AE4430U-FZ1A
 Appendix E: Risk Assessment

Digital appendixes: Appendix D-A: Excel: Experiments log (.zip)
 Appendix D-B: LabVIEW VI: LabVIEW Tørketrommel 2018
 Appendix D-C: Risk Assessment Report
 Appendix D-D: Excel: Processed logs (.zip)

APPENDIX A: MATERIALS COMPATIBILITY OF PROPANE

Materials compatibility of propane according to NS-EN ISO 11114-2:2013 [53]

	Name	Compatibility recommendation
Plastics	Polytetrafluoroethylene (PTFE)	- Acceptable
	Polyimide (PI)	- Acceptable
	Polychlorotrifluoroethylene (PCTFE)	- Acceptable
	Polyvinylidene fluoride (PVDF)	- Acceptable
	Polyamide (PA)	- Acceptable
	Polypropylene (PP)	- Acceptable
	Polyoxymethylene (POM)	- Acceptable
	Polyetheretherketone (PEEK)	- Acceptable
	Polypropylene sulphide (PPS)	- Acceptable
	Polyvinyl chloride (PVC)	- Not acceptable for use under all normal service conditions - Swelling
Elastomers	Butyl rubber (IIR)	- Not acceptable for use under all normal service conditions - Swelling
	Nitrile rubber (NBR)	- Acceptable
	Chloroprene rubber (CR)	- Not acceptable for use under all normal service conditions - Swelling
	Fluorocarbon rubber (FKM)	- Acceptable
	Methyl-vinyl-silicone rubber (VMQ)	- Not acceptable for use under all normal service conditions - Swelling - Change of mechanical properties
	Ethylene propylene diene monomer (EPDM)	- Not acceptable for use under all normal service conditions - Swelling - Change of mechanical properties
	Methyl-fluoro-silicone rubber (FVMQ)	- Not acceptable for use under all normal service conditions - Swelling
	Polyacrylate rubber (ACM)	- Acceptable
	Polyurethane rubber (PUR)	- Not acceptable for use under all normal service conditions - Swelling
Fluid lubricant	Hydrocarbon (HC)	- Not acceptable for use under all normal service conditions - Weight loss
	Fluorocarbon (FC)	- Acceptable
Solid lubricant	Molybdenum disulfide (MoS ₂)	- Acceptable

APPENDIX B: LIST OF EXPERIMENTS

All experiments performed as part of the master thesis is listed in this appendix. The table displays the date, reference code/file name, refrigerant and comments. Experiments included in Table 11 is highlighted in grey, and the number referring to Table 11 is stated in the first column. In cases where the length of the experiment deviates from the standard setups, the length of the experiment is stated together with the setup defining the other parameters of the experiment.

The reference code/file name is used when processing experiments logs. It is a unique code for each experiment applied as the name of the file containing the original experiments log. It is used as a reference code when processing experimental data and can be used to track the calculations preceding the data presented in the thesis.

R. nr	Date	Ref. code / file name	System	Comments
	02/02/2018	02022018-1	R134a	Setup 1 – 66 minutes (LabView failure)
	02/05/2018	05022018-1	R134a	Setup 1
	02/06/2018	06022018-1	R134a	Setup 1
	02/07/2018	07022018-1	R134a	Setup 1 - 180 minutes Over-drying experiment
	02/14/2018	-----	-----	Repositioning of sensors: H1/T9, H2/T10 and T5. Sealing of air leaks
1	02/15/2018	15022018-1	R134a	Setup 1
	02/16/2018	16022018-1	R134a	Setup 1 – 60 minutes
2	02/16/2018	16022018-2	R134a	Setup 2
	02/19/2018	19022018-1	R134a	Setup 1 – 180 minutes
3	02/20/2018	20022018-1	R134a	Setup 2
4	02/20/2018	20022018-2	R134a	Setup 2
5	02/22/2018	22022018-1	R134a	Setup 3
6	03/05/2018	05032018-1	R134a	Setup 4.
	03/19/2018	-----	-----	Installation and calibration of pressure sensors P1 and P2. System recharged with 220g R134a.
7	03/19/2018	19032018-1	R134a	Setup 1
8	03/20/2018	20032018-1	R134a	Setup 1
9	03/21/2018	21032018-1	R134a	Setup 1
	03/22/2018	22032018-1	R134A	Setup 4, 105 minutes
	04/09/2018	-----	----	Insulation of compressor
	04/09/2018	09042018-1	R134a	Setup 1
	04/17/2018	-----	----	System rebuild – R290 Charge: 100g
10	04/18/2018	18042918-1	R290	Setup 1
	04/19/2018	-----	----	Charge increased by 15g R290 New charge: 115g
11	04/19/2018	19042018-1	R290	Setup 1
12	04/20/2018	20042018-1	R290	Setup 1
13	04/23/2018	23042018-1	R290	Setup 1
	04/24/2018	24042018-1	R290	Setup 2 Logging failed shortly after start
14	04/25/2018	25042018-1	R290	Setup 2
15	04/25/2018	25042018-2	R290	Setup 2
16	04/26/2018	26042018-1	R290	Setup 2
17	04/27/2018	27042018-1	R290	Setup 4
18	04/30/2018	30042018-1	R290	Setup 1, 120 min
	05/08/2018	-----	----	Charge increased by 10g R290 New charge: 125g
19	05/08/2018	08052018-1	R290	Setup 1
	05/08/2018	-----	----	Charge increased by 10g R290 New charge: 135g
20	05/09/2018	09052018-1	R290	Setup 1

	05/09/2018	09052018-2	R290	Setup 1 Results rejected due to elevated temperatures at startup
21	05/10/2018	10052018-1	R290	Setup 1
22	05/11/2018	11052018-1	R290	Setup 1
	05/11/2018	-----	----	Charge decreased by 10g R290 New charge: 125g
23	05/12/2018	12052018-1	R290	Setup 1
24	05/13/2018	13052018-1	R290	Setup 1
25	05/14/2018	14052018-1	R290	Setup 1
	05/15/2018	-----	----	Charge decreased by 10g R290 New charge: 115g
26	05/15/2018	15052018-1	R290	Setup 1
27	05/16/2018	16052018-1	R290	Setup 1
	05/15/2018	-----	----	Charge decreased by 15g R290 New charge: 100g
28	05/18/2018	18052018-1	R290	Setup 1
29	05/22/2018	22052018-1	R290	Setup 1
	05/23/2018	-----	----	Capillary tube replacement – New capillary tube: D=1.00mm L = 42cm Charge: 115g R290
30	05/24/2018	24052018-1	R290	Setup 1
	05/25/2018	-----	----	Capillary tube replacement – New capillary tube: D=1.00mm L = 120 cm Charge: 115g R290
31	05/26/2018	26052018-1	R290	Setup 1
	05/26/2018	-----	----	Charge increased by 20g R290 New charge: 135g
32	05/27/2018	27052018-1	R290	Setup 1
	05/28/2018	-----	----	Charge increased by 15g R290 New charge: 150g
33	05/28/2018	28052018-1	R290	Setup 1
34	05/29/2018	29052018-1	R290	Setup 1
35	05/30/2018	30052018-1	R290	Setup 1
36	05/31/2018	31052018-1	R290	Setup 1
37	06/01/2018	01062018-1	R290	Setup 1

APPENDIX C: DATA SHEET: RECHI 39E073B

瑞智精密股份有限公司

Constant-Speed -- General Air-Conditioner / Dehumidifier

R134a -- 1φ 220-240V / 50Hz

Model	Disp. (c/drev)	Capacitor (μF)	Capacitor (VAC)	Cooling Capacity (Btu/h)	Capacity (W)	Input Power (W)	EER (Btu/h.W)	COP (W/W)	Testing Condition	Safety Recognition					
										C-UL	VPC	TUV	CCC	VDE	Others
39E073B	7.5	12	330	2875	840	300	09.58	2.80	ASHRAE/T	X	X	◎	◎	◎	◎

APPENDIX D: DATA SHEET: TECUMSEH AE4430U-FZ1A



Technical Data Sheet

3/21/2018

Model: AE4430U-FZ1A (AE4430U-FZ)

Product Description

Type: Reciprocating
Application: HBP - High Back Pressure
Refrigerant: R-290
Voltage/Frequency: 220-240V ~ 50Hz
Version: N/A

Product Specifications

Performance

Condition	Test Voltage	Refrigeration Capacity			Input Power		Efficiency			EVAP TEMP	COND TEMP	AMBIENT TEMP	RETURN GAS	LIQUID TEMP
		Btu/h	kcal/h	W	W	Btu/Wh	kcal/Wh	W/W						
ASHRAE	220V ~ 50HZ	2700	680	791	315	8.57	2.16	2.51	7.2°C (45°F)	54°C (130°F)	35°C (95°F)	35°C (95°F)	46°C (115°F)	

General

Evaporating Temp. Range: -15°C to 15°C (5°F to 59°F)
Motor Torque: High Start Torque (HST)
Compressor Cooling: Fan

Mechanical

Weight: 10
Weight Unit of Measure: KG
Displacement (cc): 6.12
Oil Type: Polyolester
Viscosity (cSt): 32
Oil Charge (cc): 284.9

Electrical

Voltage Range (50 Hz): 198-253
Voltage Range (60 Hz): N/A
Locked Rotor Amps (LRA): 11
Rated Load Amps (RLA 50 Hz): 1.88
Rated Load Amps (RLA 60 Hz): 0
Max. Continuous Current (MCC in Amps): 0
Motor Resistance (Ohm) - Main: 10.09
Motor Resistance (Ohm) - Start: 33.84
Motor Type: CSIR
Overload Type: N/A
Relay Type: N/A

Agency Approval

CE Listed, GOST RUSSIA Listed, GOST UKRAINE Listed, VDE Listed

APPENDIX E: RISK ASSESSMENT

NTNU	Hazardous activity identification process			Prepared by	Number	Date
				HSE section	HMSRV/2901E	09.01.2013
HSE				Approved by		Replaces
				The Rector		01.12.2008
						

Unit: Department of Energy and Process Engineering

Date: **January, 2018**

Line manager: Terese Løvås

Participants in the identification process (including their function): Espen Storslett (Student)

Short description of the main activity/main process: Master project for student Espen Storslett.

Project title: Experimental investigation of a heat pump assisted drum drying system using propane (R290) as working fluid

Is the project work purely theoretical? (YES/NO): NO Answer "YES" implies that supervisor is assured that no activities

requiring risk assessment are involved in the work. If YES, briefly describe the activities below. The risk assessment form need not be filled out.

ID nr.	Activity/process	Responsible person	Existing documentation	Existing safety measures	Laws, regulations etc.	Comment
1	Laboratory Work	Espen Storslett	Risk Assessment Report	According to Risk Assessment Report	-	Risk assessment for laboratory work is done in preparation for the project.

NTNU		Prepared by	Number	Date
		HSE section	HMSRFV2803E	04.02.2011
HSE/KS		Approved by		Replaces
		The Rector		01.12.2008
				

Risk assessment

Unit: Department of Energy and Process Engineering

Date: January, 2018

Line manager: Terese Løvås

Participants in the identification process (including their function): Espen Storslett (Student)

Short description of the main activity/main process: Master project for student Espen Storslett.

Project title: Experimental investigation of a heat pump assisted drum drying system using propane (R290) as working fluid

Activity from the identification process form	Potential undestrate incident/strain	Likelihood: (1-5)	Consequence:			Risk Value (human)	Comments/status Suggested measures
			Human (A-E)	Environment (A-E)	Economy/material (A-E)		
#1	Lab accident	1	B	A	A	B1	Acceptable risk

Likelihood, e.g.:

1. Minimal
2. Low
3. Medium
4. High
5. Very high

Consequence, e.g.:

- A. Safe
- B. Relatively safe
- C. Dangerous
- D. Critical
- E. Very critical

Risk value (each one to be estimated separately):

- Human = Likelihood x Human Consequence
 Environmental = Likelihood x Environmental consequence
 Financial/material = Likelihood x Consequence for Economy/material

NTNU		Prepared by	Number	Date	
		HSE section	HMSRV2603E	04.02.2011	
		Approved by		Replaces	
HSE/IKS		The Rector		01.12.2008	

Risk assessment

Potential undesirable incident/strain

Identify possible incidents and conditions that may lead to situations that pose a hazard to people, the environment and any materiel/equipment involved.

Criteria for the assessment of likelihood and consequence in relation to fieldwork

Each activity is assessed according to a worst-case scenario. Likelihood and consequence are to be assessed separately for each potential undesirable incident. Before starting on the quantification, the participants should agree what they understand by the assessment criteria:

Likelihood

Minimal 1	Low 2	Medium 3	High 4	Very high 5
Once every 50 years or less	Once every 10 years or less	Once a year or less	Once a month or less	Once a week

Consequence

Grading	Human	Environment	Financial/material
E Very critical	May produce fatality/ies	Very prolonged, non-reversible damage	Shutdown of work >1 year.
D Critical	Permanent injury, may produce serious serious health damage/sickness	Prolonged damage: Long recovery time.	Shutdown of work 0.5-1 year.
C Dangerous	Serious personal injury	Minor damage: Long recovery time	Shutdown of work < 1 month
B Relatively safe	Injury that requires medical treatment	Minor damage: Short recovery time	Shutdown of work < 1week
A Safe	Injury that requires first aid	Insignificant damage: Short recovery time	Shutdown of work < 1day

The unit makes its own decision as to whether opting to fill in or not consequences for economy/materiel, for example if the unit is going to use particularly valuable equipment. It is up to the individual unit to choose the assessment criteria for this column.

Risk = Likelihood x Consequence

Please calculate the risk value for "Human", "Environment" and, if chosen, "Economy/materiel", separately.

About the column "Comments/status, suggested preventative and corrective measures":

Measures can impact on both likelihood and consequences. Prioritise measures that can prevent the incident from occurring. In other words, likelihood-reducing measures are to be prioritised above greater emergency preparedness, i.e.: consequence-reducing measures.

NTNU		Risk matrix	prepared by	Number	Date
	HSE/KS		HSE Section	HMSRV/2804	8 March 2010
			approved by	Page	Replaces
			Rector	4 of 4	9 February 2010
					

MATRIX FOR RISK ASSESSMENTS at NTNU

CONSEQUENCE					
Extremely serious	E1	E2	E3	E4	E5
Serious	D1	D2	D3	D4	D5
Moderate	C1	C2	C3	C4	C5
Minor	B1	B2	B3	B4	B5
Not significant	A1	A2	A3	A4	A5
	Very low	Low	Medium	High	Very high
LIKELIHOOD					

Principle for acceptance criteria. Explanation of the colours used in the risk matrix.

Colour	Description
Red	Unacceptable risk. Measures must be taken to reduce the risk.
Yellow	Assessment range. Measures must be considered.
Green	Acceptable risk. Measures can be considered based on other considerations.